MONASH University

PEPTIDE HYDROGELS FOR THE TREATMENT OF

NEURODEGENERATIVE DISEASES

Julian Charles Ratcliffe

BEng (Hons. 2A)

A thesis submitted for the degree of *Doctor of Philosophy* at

Monash University in March 2018

Department of Materials Science and Engineering

Copyright notice

Abstract

This project involved the development of a self-assembling peptide hydrogel system, capable of delivering a neurotrophic signal to the central nervous system in a spatially and temporally controlled manner. Neurotrophins are a promising approach to the treatment of Parkinson's disease and other neurodegenerative conditions, through this project, it was hoped that progress toward a treatment of the condition would be made.

Initially hydrogels were loaded with a small molecule brain derived neurotrophic factor (BDNF) mimetic, to see if it was possible to use the hydrogel as a reservoir of the drug, and achieve a prolonged release effect. When this proved unsuccessful, focus changed to developing a novel hydrogel, which contained a BDNF derived sequence. The intention being to create a hydrogel which was intrinsically neurotrophic. Through this work, a new method of Fmoc hydrogel preparation was developed, in which carbon dioxide was diffused into the peptide solution in order to adjust pH and trigger gelation.

The second part of this project involved investigating co-assembly of the BDNF derived Fmoc self-assembling peptide developed earlier, with published Fmoc peptides containing additional biofunctional motifs. The resulting hydrogels contained both BDNF and fibronectin derived sequences. Some blended gels were found to be biocompatible, and were tested for their ability to activate the TrkB receptor in vitro. One blended peptide hydrogel was found to be both biocompatible, and capable of phosphorylating TrkB.

The third part to this work involved the development of another BDNF derived self-assembling peptide hydrogel, this time based on the self-complementary method of self-assembly. The resulting hydrogel was biocompatible, and capable of activating TrkB in vitro.

In the final part of the project the Fmoc BDNF derived peptide hydrogel blend which showed the highest activity with TrkB was then tested in vivo to characterise the inflammatory response to the hydrogel following injection into the brain. It was

found that the blended hydrogel induced a similar inflammatory response to a PBS only control, and is therefore a suitable material for this application.

Declaration

This thesis contains no material which has been accepted for the award of any other degree or diploma at any university or equivalent institution and that, to the best of my knowledge and belief, this thesis contains no material previously published or written by another person, except where due reference is made in the text of the thesis.

Signature: …………………………

Print Name: Julian Ratcliffe

Date: 27/03/2018

PART B: Suggested Declaration for Thesis

[This declaration to be completed for each conjointly authored publication and to be placed at the
start of the thesis.]

Monash University

Declaration for Thesis

Declaration by candidate

The nature and extent of my contribution to the work was the following:

Nature of contribution	Extent of contribution (%)
Experimental design and conduct, data processing, manuscript writing	

The following co-authors contributed to the work. If co-authors are students at Monash University, the extent of their contribution in percentage terms must be stated:

| Name	Nature of contribution	Extent of contribution (%) for student co-authors only
Kun Zhou	Chapter 6 – Experiment design, and performed in vivo surgeries.	N/A
Juliet Taylor	Chapter 4-5 – prepared primary cells for treatment	N/A
Peter Crack	Chapter 4-5, manuscript correction	N/A
David Finklestein	Chapter 6 – Manuscript correction	N/A
James Gardiner	Manuscript correction	N/A
John Forsythe	Assistance in planning, experiment design and Manuscript correction	N/A

The undersigned hereby certify that the above declaration correctly reflects the nature and extent of the candidate's and co-authors' contributions to this work*.

Candidate's Signature		Date 27/03/2018

Main Supervisor's Signature		Date 27/03/2018
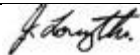
Acknowledgements

I would like to thank my supervisors Associate Professor John Forsythe and Dr James Gardiner, for their continued encouragement. Your support helped me to chase my ideas, and truly make this project my own.

To Kun Zhou, who has been a reassuring partner in this research from start to finish. Your assistance with all aspects of the project, from cell work to characterisation methods, has been greatly appreciated.

James Carthew and Karla Contreras, your assistance with my many biological questions was invaluable.

I would like to thank the entire Forsythe biomaterials group, particularly past members, Dr Sepideh Mothamed and Dr Andrew Rodda for their support and friendship throughout the project. Your suggestions and assistance helped me get over the line.

Associate Professor Peter Crack and Associate Professor David Finklestein (Melbourne University), your assistance at the end of the project cannot be overstated. The positivity and support offered by you and your groups was fantastic.

I would also like to thank Lynne Waddington, Jacinta White and Malisja DeVries at CSIRO for their encouragement, and faith in me, especially at the later stages of the project.

Finally, I would like to thank Jessie Ratcliffe, without your support and understanding, I would never have made it this far.

Contents

List of abbreviations

ALS	Amyotrophic lateral sclerosis
BBB	Blood brain barrier
BDNF	Brain derived neurotrophic factor
BSA	Bovine serum albumin
CNS	Central nervous system
CO2	Carbon dioxide
CryoTEM	Cryogenic transmission electron microscopy
DBS	Deep brain stimulation
DIPEA	Diisopropylethylamine
DMEM	Dulbecco's modified eagle medium
DMF	N,N-dimethyl formamide
ECM	Extracellular matrix
FCS	Foetal calf serum
FL	Full length
Fmoc	Fluorenylmethyloxycarbonyl
GDL	Glucono-δ-lactone
GDNF	Glial cell-line derived neurotrophic factor
GFAP	Glial fibrillary acidic protein
GFRα	GDNF family receptor α
HFIP	Hexafluoroisopropanol
HOBt	Hydroxybenzotriazole
HPLC	High pressure liquic chromatography
HRP	Horseraddish peroxidase
L-dopa	Levodopa
LM22A-4	N,N',N''-tris(2-hydroxyethyl)-1,3,5-benzenetricarboxamide
MAPK	Mitogen-activated protein kinase
MPTP	1-methyl-4-phenyl-1,2,3,6-tetrahydropyridine
MTS	3-(4,5-dimethylthiazol-2-yl)-5-(3-carboxymethoxyphenyl)-2-(4-sulfophenyl)-2H-tetrazolium
NGF	Nerve growth factor
NT-3	Neurotrophin 3
NT-4	Neurotrophin 4
p75ntr	p75 neurotrophin receptor
PBS	Phoosphate buffered saline
PD	Parkinsin's disease
PI3K	Phosphatidylinositol 3-kinase
PLC-γ	Phospholipase C-γ
pTrkB	Phosphorylated tropomyosin receptor kinase B
QSBB	Queen Square Brain Bank
RIPA	Radioimmunoprecipitation assay
SAP	Self-assembling peptide
SN	Substantia nigra
TEM	Transmission electron microscopy
TH	Tyrosine hydroxylase
TIPS	Triisopropylsilane
Trk	Tropomyosin receptor kinase

List of amino acids and abbreviations

Amino Acid	3 letter	1 letter	Amino Acid	3 letter	1 letter
Alanine	Ala	A	Leucine	Leu	L
Arginine	Arg	R	Methionine	Met	M
Aspartic Acid	Asp	D	Phenylalanine	Phe	F
Cysteine	Cys	C	Proline	Pro	P
Glutamic Acid	Glu	E	Serine	Ser	S
Glutamine	Gln	Q	Threonine	Thr	T
Glycine	Gly	G	Tryptophan	Trp	W
Histidine	His	H	Tyrosine	Tyr	Y
Isoleucine	Ile	I	Valine	Val	V

Chapter 1 Literature Review

Neurodegenerative diseases are an increasing burden on the world's healthcare systems, as incidence of these conditions increases with our aging population. There are several diseases that share a similar neurodegenerative origin, all of which may benefit from an appropriate regenerative material. However, for practical reasons this project has focused on only one of these conditions, Parkinson's disease. In this chapter, the incidence, pathology, and treatment of the disease are discussed

An overview of current clinical strategies is provided, including dopamine treatment – levodopa, deep brain stimulation (DBS), and neurosurgical methods. Treatment strategies still under investigation are also discussed here. Biomaterial and neurotrophic treatment strategies are investigated as an alternative to the symptomatic therapies currently available. Neurotrophins are of interest, particularly BDNF and GDNF, as they have the potential to halt or reverse the progression of neurodegeneration, and studies regarding their use in Parkinson's disease treatment have been promising.

Subsequent discussion will outline the use of hydrogels in potential therapies. Hydrogels are a class of material being widely researched with respect to its potential use in the central nervous system[1]–[4]. The combination of favourable mechanical properties, evasion of non-specific binding and ease of diffusion through the material makes them attractive. Different types of hydrogels are outlined here. These are, chemically crosslinked hydrogels – such as PEG, gelatin and other organic systems, as well as macromolecular hydrogels, which form hydrogels through weaker bonds – hydrogen bonding, and hydrophobic interactions. Particular emphasis is placed on the use of peptides in hydrogel construction. Hydrogels made from peptides are an attractive option for biological applications, as they are degradable and it is relatively simple to incorporate bioactive ligands into their design.

1.1 Parkinson 's disease

Parkinson's disease (PD) currently affects 16/10,000 people in Western European populations [5] and is becoming increasing common with an ageing population[6]. In the United States alone, 59000 cases are diagnosed each year[7]. It is characterised by a combination of motor and non-motor symptoms which worsen as the disease progresses. While common perception of PD is associated with tremor, only 50% of patients with PD will present this symptom[8]. Other common symptoms present in PD patients are bradykinesia (slowness of movement), rigidity and postural instability. Less frequent symptoms include orofacial dyskinesias[7] (involuntary facial movements) as well as several non-motor symptoms, the most common of which is pain[8]. Not all symptoms may be present in all patients[9], making accurate diagnosis difficult. Typically, symptoms don't appear until 50% to 80% of dopaminergic neurons have already died[10]. Another confounding factor in the correct diagnosis of PD is that there are several diseases which mimic some or all of the symptoms, but have a different underlying cause[8]. The variety of symptoms caused by PD can lead to unnecessary or inappropriate referrals before a correct diagnosis is reached[8], [11]. Sometimes an entirely inaccurate diagnosis results. This places further strain on the patient and healthcare system. While early diagnosis is difficult, due to the progressive nature of the disease, identification becomes easier as the disease progresses, as symptoms will increase.

Diagnosis of PD is based upon the Queen Square Brain Bank (QSBB) criteria, originally developed in 1988[12]. The method has been improved upon since then, and by 2001, the diagnosis accuracy had climbed to 90%[13]. There is therefore a greater chance of accurate diagnosis at earlier stages of the disease. The goal of successful treatment of Parkinson's disease relies on early and accurate detection. If a method of stopping the degeneration at a point is developed, early intervention will leave patients in far better condition. In addition, if regeneration is achieved, it may only be partial, so an earlier starting point for treatment will surely lead to better outcomes.

The primary pathological event causing Parkinson's disease is the loss of dopaminergic neurons within the substantia nigra (SN) and the resulting depletion of dopamine in the striatum[5], [8]. This is often characterised by a decrease in tyrosine hydroxylase (TH) positive cells. Secondary to this is the presence of Lewy Bodies – insoluble cytoplasmic inclusions of alpha-synuclein[14]. These inclusions may also be present in the condition dementia with Lewy bodies[8]. Both of these effects are irreversible and progress with time, leading to reduced quality of life for patients.

Current therapies for Parkinson's disease are capable of treating the symptomatic effects of the disease only[15]–[17] and do nothing to stop or slow the progressive loss of SN neurons. Since its development in 1968[18] Levodopa (L-3,4-dihydroxyphenylalanine or L-dopa) has remained the most used and most effective treatment for Parkinson's disease. Levodopa is an orally available dopamine precursor. A small percentage of which is capable of crossing the blood brain barrier and reaching the striatum. The levodopa is converted into dopamine by the enzyme aromatic L-amino-acid decarboxylase in the brain[19] as illustrated in Figure 1.1. This effectively replaces the dopamine lost through the degeneration of neurons in the SN. However, dopamine isn't unique to this region of the brain, so the remaining dose, which is transported throughout the body, can act upon the cardiovascular system, kidneys, digestive system and pancreas. This overflow of exogenous dopamine can have adverse side-effects such as peripheral neuropathy[20] for the patient. Balancing the treatment in order to achieve relief of symptoms, while introducing minimal side-effects, is a process that takes time, and can be very specific to the individual.
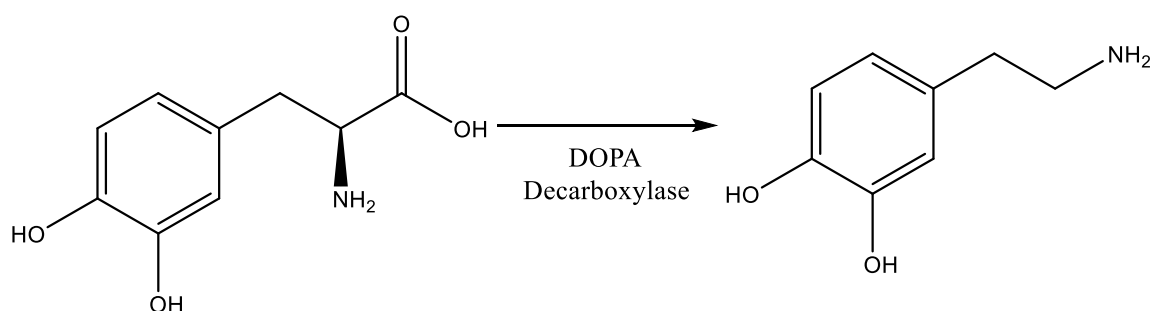
Figure 1.1: The reaction of levodopa being converted to dopamine

Pharmacotherapy of Parkinson's disease allows for significant improvement of motor symptoms, and provides greater mobility and function in daily life[21]. Treatment with levodopa is associated with the "on-off" phenomenon. This is a switch between mobility and immobility, usually as an end of dose "wearing off" which is reasonably predictable[22]. Less commonly, there can be sudden unpredictable fluctuations of motor function[23]. Current treatments focus on the restoration of dopamine, either through a pro-dopamine drug, or a dopamine receptor agonist. As the disease progresses, the endogenous dopamine production continues to drop, benefits decrease, and patients steadily become more reliant on dopamine replacement. Effective management of the disease is difficult. The goal with management of Parkinson's disease is to balance clinical efficacy while minimising adverse effects.

Since its introduction, levodopa has remained the most used medication in treating the motor symptoms of Parkinson's disease[21]. Dopamine is typically ionised at physiological pH, and is unable to cross the blood brain barrier(BBB). Levodopa however, is able to cross the BBB through interaction with L-type amino acid transporter 1[24], and therefore functions as an orally available treatment. Once in the brain levodopa is metabolised to dopamine. Levodopa is also metabolised to dopamine in the gut, and typically 30% of a dose will enter systemic circulation[21]. In order to counter these effects, levodopa is often administered alongside carbidopa, a peripheral dopamine decarboxylase inhibitor, which can't cross the BBB, resulting in less dopamine conversion outside the brain, which helps to reduce the peripheral side effects of levodopa[23], [25]. This combined drug approach approximately triples levodopa's bioavailability in the brain, leading to reduced dose requirements, and fewer adverse effects. Adverse effects caused by levodopa/carbidopa products include nausea, vomiting, postural hypotension, sedation, vivid dreams, dizziness, and confusion among others. Because of the predominantly elderly nature of Parkinson's disease patients, the risk of falls is a serious problem. Levodopa induced orthostatic hypotension, which occurs in up to 20% of patients contributes to the observed motor symptoms[21].

Another treatment option is the use of dopamine receptor agonists. These drugs can be used alone, or in conjunction with levodopa/carbidopa. They function through direct activation of dopamine receptors in the caudate-putamen region of the brain, and enhance the function of dopamine. As a monotherapy they function best in the early stages of Parkinson's disease. There are two classes of dopamine agonist, the ergot and non-ergot classes. Ergot dopamine agonists are nonspecific, and able to interact with D_1 and D_2 dopamine receptors, as well as serotonin and adrenergic receptors. They are infrequently used for treatment of Parkinson's disease, as their non-selective nature means negative side-effects are common[26]. Non-ergot dopamine agonists are specific to the D_2 and D_3 receptors, and have demonstrated clinical efficacy, and good safety and tolerability. The non-ergot class dopaminergic agonist oral formulations absorb readily through the gastrointestinal tract, and can readily cross the blood brain barrier. No conversion to an active state is required, and they have a much longer half-life than levodopa, requiring less frequent doses.

Ablative neurosurgical treatment for Parkinson's disease can be beneficial for patients who do not receive sufficient relief of symptoms from pharmacotherapy. With the development of advanced procedures, namely MRI-guided and stereotactic technologies, surgical procedures have become a more attractive option[27]. Common targets for neurosurgery are the thalamus, globus pallidus and subthalamic nucleus[28]. Thalamotomy can effectively treat greater than 85% of patients who experience debilitating tremors, as well as some degree of rigidity. It has no effect on akinesia or bradykinesia however[29]. Clearly, as PD presents itself differently in patients, it is necessary to tailor the target to the symptoms of the patient.

Deep brain stimulation (DBS) involves the use of electrodes to stimulate specific regions of the brain. It is able to achieve comparable or better outcomes compared to ablative surgery, with fewer side effects and no tissue damage. It has taken the place of ablative neurosurgery in the majority of cases, with neurosurgery now only used if DBS is not possible[28]. The most common target of DBS is the subthalamic nucleus. DBS of the subthalamic nucleus is able to achieve an improvement in all symptoms of PD, and can reduce the need for levodopa pharmacotherapy[30], [31]. This has the

added benefit of reducing possible dyskinesia induced by levodopa therapy[32]. The thalamus and globus pallidus are also possible targets[30]. With stimulation of the globus pallidus, an improvement in all PD symptoms, including an increased "on phase" duration can be obtained[30]. More generally, DBS is a much more flexible treatment, as the treatment can be tailored to the individual, with the ability to adjust the stimulation parameters as needed. During the optimisation process, of stimulation, side effects can be experienced. More troubling is the possible spread of stimulation, leading to neighbouring regions of the brain being stimulated. Effects on cognition[33], [34] behaviour[31] and mood[35] have been reported.

While levodopa pharmacotherapy and DBS have managed to improve quality of life for the majority of PD patients, they are still only able to reduce the symptoms of the disease. They do nothing to address the continued degradation of the dopaminergic cells. Therefore, new therapies are required. One goal of a new therapy is to protect dopaminergic neurons form further degeneration, as it would be possible to halt the progression of the disease, meaning quality of life could be maintained. Ideally a new therapy will be capable of regenerating or replacing the lost dopaminergic cells. This would enable reversal of the pathology of the disease, and thus lead to functional recovery. If this effect was sustained, a cure for Parkinson's disease may be possible.

1.1.1 Neurotrophins as a therapy

Neurotrophins are proteins which perform several important roles in the development and maintenance of the nervous system, as well as key roles in normal brain function and synaptic plasticity[36]. Additionally, neurotrophins have several functions outside the nervous system. Non-brain areas of activity include the immune system[37], kidney, ovaries and testis[38], [39]. There are multiple classes of neurotrophin that have been identified. The first of these is the neurotrophic factors, consisting of nerve growth factor (NGF), brain derived neurotrophic factor (BDNF), neurotrophin 3 (NT-3), and neurotrophin 4 (NT-4). All of the neurotrophic factors bind specifically to a tropomyosin receptor kinase (Trk), with NGF binding to TrkA, BDNF binds to TrkB, NT-3 uniquely can bind to both TrkB and TrkC, and NT-4 binds to TrkB[40]. All bind with lower affinity to the common receptor p75 neurotrophin

receptor (p75ntr). The other class of particular interest is the glial cell-line derived neurotrophic factor family. The glial cell-line derived neurotrophic factor family, all share the Ret protein receptors, which are highly expressed in the SN[41]–[43]. Ret receptors require association with a GDNF family receptor α (GFRα) in order to function *in vivo*[44].

1.1.1.1 BDNF

Brain derived neurotrophic factor, or BDNF, was the second neurotrophic factor to be discovered[45]. It functions both within the central nervous system, and in the peripheral nervous system and other tissues had been explored. BDNF acts through both the specific TrkB receptor, and the p75ntr receptor, which is used by all of the neurotrophin family. BDNF exists in 2 stages, proBDNF and mature BDNF, both of which are functional, and have distinct functions. ProBDNF has been found to be proapoptotic in cells expressing both p75ntr and sortilin[46]. Cleavage of proBDNF produces mature BDNF[47]. Mature BDNF is important in early development of the nervous system, and continues to function throughout adult life[48]. BDNF functions as a neurotrophin, having roles in neural cell survival[49], differentiation[50], proliferation[51], learning[52] and synaptic plasticity[53].

BDNF is distributed throughout the central and peripheral nervous system. The role of BDNF varies depending on the balance of mature to proBDNF, the concentration of each, the tissue, as well as the receptor(s) involved[46], [54]. Binding of BDNF to the TrkB receptor causes homodimerisation, followed by phosphorylation of the intracellular domain.

Within the central nervous system (CNS), three known TrkB isoforms exist which are able to bind to BDNF. These are full length (FL) TrkB, and the truncated, T1 and T2 isoforms. The T1 and T2 isoforms have the same extracellular and transmembrane domain as the full length protein, but lack cytoplasmic tyrosine kinase domains[55]. All isoforms are present in neural cells and perform differing roles.
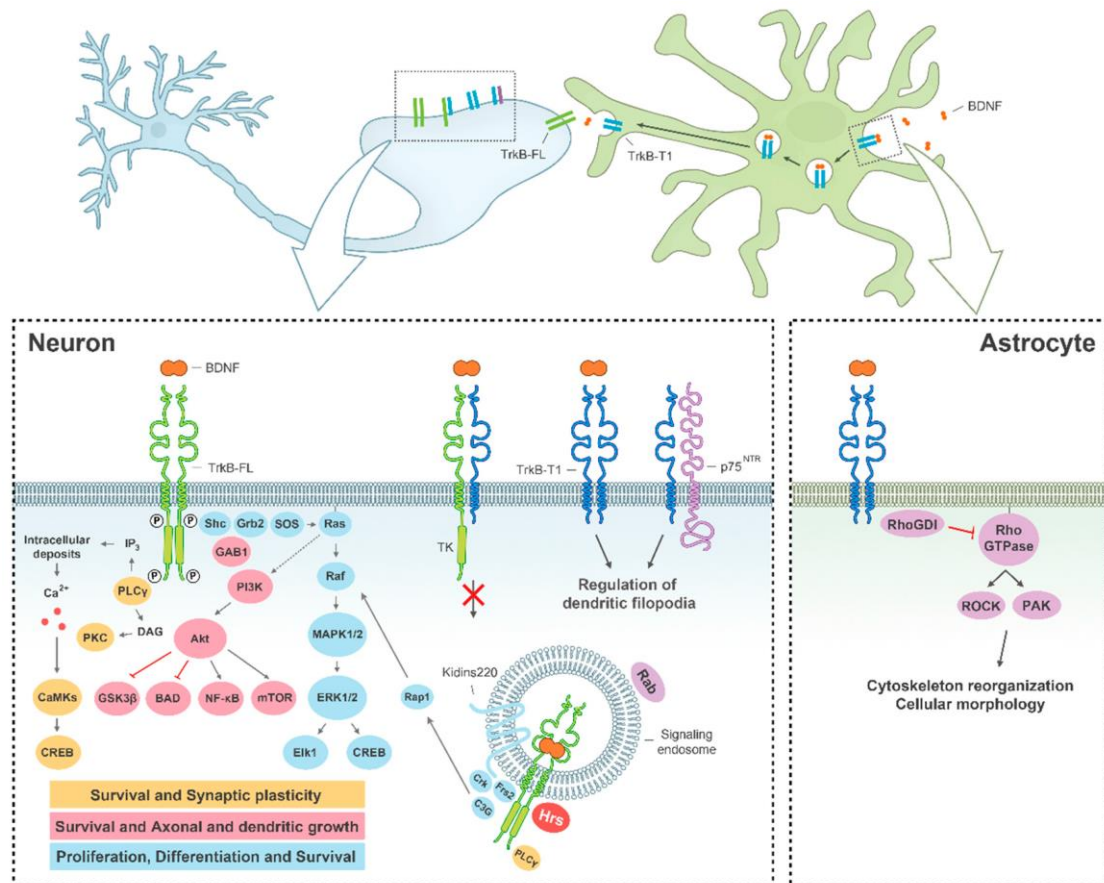
Figure 1.2: In the CNS, binding of BDNF to TrkB-FL induces dimerization of the receptor, and phosphorylation of the cytoplasmic domain. This leads to activation of the PI3K, PLC-γ and MAPK pathways, shown here in pink, yellow and blue respectively. These pathways perform many functions, including proliferation, neuroprotection, differentiation and neural growth. Phosphorylation sites on TrkB-FL are indicated "P". Internalisation of dimerised TrkB-FL can continue to function within endosomes. TrkB-T1 doesn't activate the three main pathways associated with BDNF function, and can form heterodimers with TrkB-FL, blocking its function. TrkB-T1 regulates the concentration of BDNF, and induces dendritic elongation. Reproduced from open access article, MDPI[56].

BDNF binding to the full length TrkB receptor leads to auto-phosphorylation of tyrosine domains in the cytoplasmic domain of the protein. This in turn leads to the activation of both the mitogen-activated protein kinase (MAPK) and phosphatidylinositol 3-kinase (PI3K)/AKT pathways[57], as well as the phospholipase C-γ (PLC-γ)/PKC pathway[58], [59], AMPK/ACC[60] and NFκB pathway[61][62]. Activation of the PI3K/AKT signalling cascade results in survival[63] and proliferation of neuronal cells. Activation of MAPK triggers many cellular processes, including growth[64] and protection of neural cells, differentiation and the release of neurotransmitters[57], [61].

The truncated TrkB receptor has a very different cytoplasmic domain, lacking the tyrosine kinase domain[65][66], and therefore is unable to activate the same

pathways as the full length receptor[66]. Despite these differences, a study in which neural stem cells were isolated from the subventricular zone, showed that these cells contained predominantly truncated TrkB, and that when treated with BDNF, the AKT, ERK-1/2, and STAT-3 pathways are all activated[51].

By competing for BDNF, and forming heterodimers with full length TrkB, TrkB T1 can behave as the dominant isoform[66]. Increased TrkB T1 expression surrounding injuries can limit BDNF availability, preventing axonal regeneration[67]. TrkB T1 is also able to induce neurite outgrowth, stimulate intracellular signalling and modify cytoskeletal structures[68]. The role of the different TrkB receptors on dendritic growth also vary, with TrkB T1 minimising proximal branching of dendrites, and promoting elongation of dendrites, while full length TrkB promotes proximal dendritic branching and inhibited dendritic elongation These two isoforms inhibit each other's function[69].

Both TrkB and p75ntr are expressed in the striatum and SN[70], [71]. Studies have indicated that BDNF can support the survival of nigral dopaminergic neurons[72]. It has also been shown that BDNF signalling via TrkB plays an important role in the aging brain on the survival of nigrostriatal dopaminergic neurons[65]. Reduced levels of BDNF have been linked to many neurodegenerative conditions, including Alzheimer's disease[73], [74], Parkinson's disease[75]–[77], Huntington's disease[78] and amyotrophic lateral sclerosis (ALS)[79]. BDNF also has important function with respect to motor function in the adult brain, and decreased BDNF has been linked with dysfunction of the motor system.

BDNF is therefore a promising option for the treatment of neurodegeneration in Parkinson's disease. It has been shown to be a neurotrophic factor for dopaminergic neurons, leading to greater survival of TH positive cells in primary cultures[72], and reduced BDNF has been linked to incidence of Parkinson's disease[80]. *In vivo* studies have shown that BDNF infusion is capable of reducing cells loss, and improved reinervation in models of Parkinson's disease[81]. Other studies showed that blocking of BDNF signalling in the SN during development leads to increased cell death in the SN, indicating that BDNF has an important role in the development

of this region of the brain[82]. In a study of early Parkinson's disease, the PI3K/Akt pathway and MAPK pathway were shown to inhibit the apoptotic pathway, and offer a potential endogenous neuroprotective mechanism[83].

1.1.1.2 GDNF

The GDNF family of receptors have generated significant interest as a potential target for the treatment of neurodegenerative diseases, and particularly Parkinson's disease. Studies *in vitro* and *in vivo* have demonstrated the ability of GDNF to improve survival and differentiation of neurons[82], [84], [85]. The GDNF group factors GDNF, neurturin and presephin have been found to have beneficial effects on dopaminergic neurons[86]–[89]. While artemin is found to be more beneficial in dorsal root ganglion sensory neuronal populations[90][91]. The use of implanted micropumps for the delivery of GDNF to the brains of patients with Parkinson's disease has been trialled[84], [92], [93]. Sufficiently high doses significantly improved patient performance on the Unified Parkinson's Disease Rating Scale, with general improvements in motor function and quality of life being observed.

GDNF has been found to be a more potent and specific neurotrophin for dopaminergic neuronal populations than BDNF[94]. BDNF has the potential benefit however of targeting motor and non-motor pathologies[53].

1.1.1.3 Neurotrophin mimetics offer advantages over full proteins

A challenge in the use of neurotrophic factors as a therapy is effective delivery to the central nervous system. A recent review[48] outlined that a successful neurotrophin therapy must be capable of delivering a controlled dose of the neurotrophin over a potentially very controlled time scale with great spatial precision. BDNF is a moderately sized, charged protein, and therefore minimal amounts are capable of crossing the blood brain barrier[95]–[97]. Studies in which BDNF was delivered intravenously or intrathecaly resulted in very little penetration of the protein into the brain and parenchyma beyond superficial layers[98]. Another issue with these delivery methods is the half-life of BDNF of only half an hour[99]. Many solutions have been proposed to overcome this shortfall. Implantation of a micropump which can continuously deliver BDNF into the brain has been tested[100]. Micropump

growth factor delivery however carries risks, with low flow rates not providing efficacious dose levels, and higher flow rates resulting in potential tissue damage[101]. Less invasive methods investigated the use of viral vectors to deliver recombinant BDNF *in vivo* have been investigated[97], as has the use of hydrogels[102], which carry a high concentration of the protein, release it over a prolonged period, and protect it from degradation. As these gels are able to be delivered though an injection, they are minimally invasive, while being capable of providing both the physical and chemical cues necessary to support neurons, and improve survival, growth and proliferation.

The development of small molecule mimetics has provided an alternative to full protein BDNF. These small molecules (most less than 1kDa compared to 14kDa) have a longer half-life, better pharmacokinetic properties, and some can cross the blood brain barrier without difficulty[103]. Additionally, small synthetic molecules are far easier and cheaper to synthesise and purify than a full protein, making commercialisation of any potential therapy much simpler.

Table 1.1: BDNF Mimetics and TrkB agonists

Name	MW (Da)	Effective Concentration	References
Natural Products			
Deoxygedunin	466.57	5mg/kg	[104]–[106]
7,8-dihydroxyflavone	254.24	5mg/kg , 10-250nM	[103], [107]–[114]
4'-dimethylamino-7,8-dihydroxyflavone	297.31	1mg/kg, 10nM	[115]–[118]
Peptides			
cyclo[dPAKKR]	580.6	10nM	[96], [119]–[121]
TDP6	2412.0	10nM	[121], [122]
Ac-Ser-Lys-Lys-Arg-CONH2	558.36	0.05-10µM	[123]
Ac-Ile-Lys-Arg-Gly- CONH2	513.34	0.1-10µM	[123]
B_{AG}	1775	600-6000nM	[124], [125]
Synthetic			
LM22A-4	339.34	0.5-500nM	[126]–[129]
N-Acetylserotonin	218.25	100nM	[130]
Amitriptyline	277.40	10-250nM	[131]

1.1.1.4 Natural BDNF mimetics

Several neurotrophic natural products have been identified. A review covering a wide range of these can be found elsewhere[132]. Of these, deoxygedunin and 7,8-dihydroxyflavone are both capable of stimulating the TrkB receptor *in vivo.* Both have been thoroughly investigated as a BDNF mimetic. The structure of these molecules is shown in Figure 1.3.

Both deoxygedunin and 7,8-dihydroxyflavone have been found to bind to TrkB both *in vivo* and *in vitro*, in a BDNF independent manner. Pre-treatment with deoxygedunin before artificially inducing a parkinsonian condition via 1-methyl-4-phenyl-1,2,3,6-tetrahydropyridine (MPTP) treatment, reduces the observed toxicity to TH positive cells[103], [106]. This illustrates the potential of BDNF mimicking small molecules in the treatment of the disease.
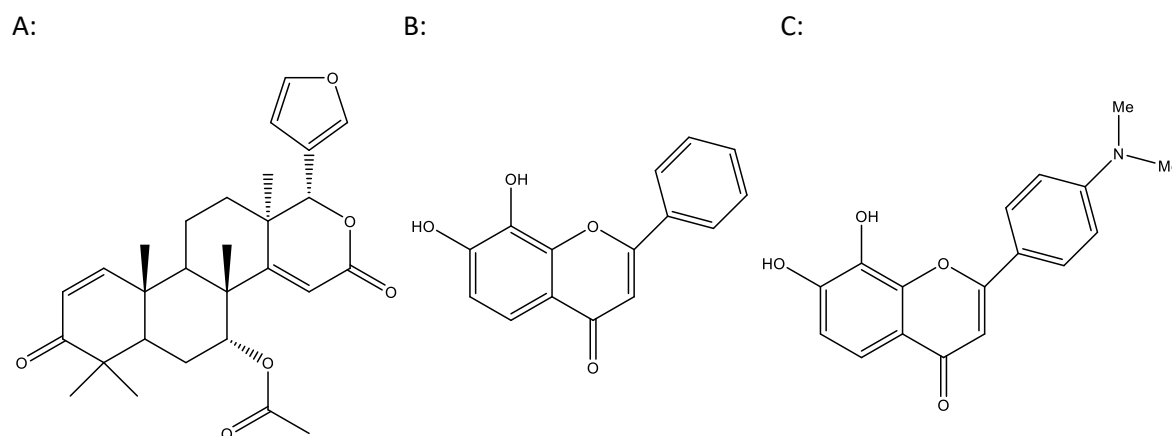
Figure 1.3: Neurotrophic natural products, A: deoxygedunin B: 7,8-dihydroxyflavone and C: 4'-dimethylamino-7,8-dihydroxyflavone.

The synthetic derivative of 7,8-dihydroxyflavone, 4'-dimethylamino-7,8-dihydroxyflavone (Figure 1.3) has been shown to be more effective in activating TrkB *in vivo*[115], displaying greater potency at lower concentrations, as well as a longer-lived stimulatory effect. Following peripheral administration of both 7,8-dihydroxyflavone at 5mg/kg/day and its synthetic derivative 4'-dimethylamino-7,8-dihydroxyflavone at 1mg/kg/day, both induced significant TrkB phosphorylation, resulting in improved motor performance of Huntington's disease mice[116].

1.1.1.5 Synthetic BDNF mimetics

The ligand N,N',N"-tris(2-hydroxyethyl)-1,3,5-benzenetricarboxamide (LM22A-4) is a promising water soluble synthetic BDNF mimetic, which has been found to act through TrkB as a partial agonist[133]. The structure of LM22A-4 is shown in Figure 1.4A. It was discovered through computational modelling of loop 2 subregion b of the full BDNF protein. Its function has been verified both *in vivo*[128], [129] and *in vitro*[126]. In mouse models of Rett syndrome, one study found that chronic administration of LM22A-4 increased TrkB signalling, resulting in improvements in resting breathing frequency[128], while another found that acute treatment led to a reversal of Rett syndrome associated breathing difficulties[129]. In a mouse model of Huntington's disease it was found to improve motor ability, prevent striatal inflammation, and to reduce huntingtin aggregates in the striatum and cortex[134].
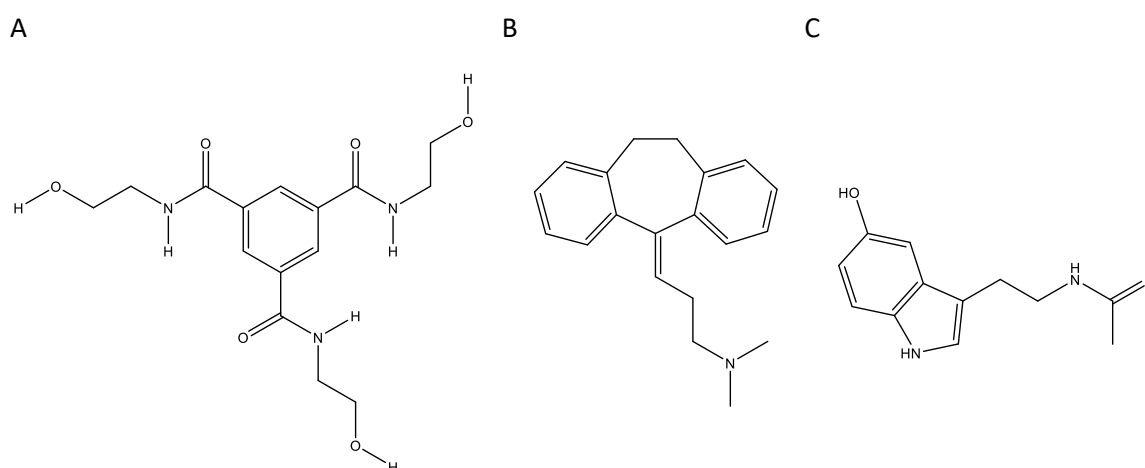
Figure 1.4: The chemical structures of synthetic BDNF mimetics A: LM22A-4, B: amitriptyline and C: N-acetylserotonin.

Amitriptyline, an antidepressant drug, induces phosphorylation of both TrkA and TrkB[131]. Its structure is shown in Figure 1.4B. When cells were pre-treated with anti-NGF and anti-BDNF before treatment with amitriptyline, phosphorylation of TrkA and TrkB were still activated, showing that amitriptyline stimulates these receptors independently of their native neurotrophins. A more recent study using fibroblast expressing catalytic TrkB receptors and E18 rat primary hippocampal and cortical neuronal cultures found that, while BDNF was able to activate Trkb, amitriptyline was unable to do so in either case[135]. Another study found it to act as a TrkB inhibitor[125]. The activity of amitriptyline on the TrkA and TrkB receptors is still under investigation.

N-acetylserotonin, a melatonin precursor has been identified as a TrkB agonist, in primary hippocampal and cortical cultures[130]. The structure of N-acetylserotonin is shown in Figure 1.4C. *In vitro* analysis showed that N-acetylserotonin activates TrkB, but not TrkA or TrkC in a dose-dependent manner, while *in vivo* analysis showed that N-acetylserotonin is able to cross both the blood-brain barrier and the blood-retinal barrier[136]. Another *in vivo* analysis of N-acetylserotonin activity supports its ability to act directly through the TrkB receptor, while melatonin was found to increase mature BDNF concentrations in the hippocampus[137].

1.1.1.6 Peptide based BDNF mimetics

An initial attempt to create a peptide mimetic of BDNF loop 2, produced an antagonist[138]. Further work on this peptide involved synthesising bicyclic and tricyclic dimers of this sequence, intended to mimic a pair of solvent exposed loops. Three of the bicyclic peptides showed improved neuronal survival in primary cultures of embryonic chick dorsal root ganglion sensory neurons, 30% as effectively as BDNF. The tricyclic dimer, called TDP6, showed both greater survival and potency compared to the bicyclic versions, with an EC_{50} of only 11pM[122]. TDP6 functioned as a partial agonist, phosphorylating TrkB on its own, but competing with BDNF, and inhibiting the function of the full protein. Primary cultures of oligodendrocytes demonstrated the ability of TDP6 to promote meylination in a TrkB dependent manner[121].

A BDNF mimetic for the p75ntr receptor was developed from a tripeptide located on loop 4 of BDNF. This peptide, cyclo[dPAKKR] was resistant to proteolysis, and exhibited good neural survival *in vitro*[119]. Subsequent development on this system led to the development of several synthetic derivatives of cyclo[dPAKKR], the most potent of which was the longest-chain fatty alkyl amide-substituted pentapeptide[96]. Further studies have verified that cyclo[dPAKKR] acts through p75ntr, and has neurotrophic effect *in vivo*[121], [139].

Taking the SRRGE motif from NT-4, which was identified as a functional region of the protein, a constrained cyclic peptide, N-Ac-CSRRGEC-NH2 was synthesised, and found to be an antagonist of TrkB. It was possible to then synthesise a cyclised dimer

of this, N-Ac-C<u>SRRGE</u>LAAS<u>RRGE</u>LC-NH2 (B$_{AG}$), which was found to be as effective at promoting neurite outgrowth as NT-4 and BDNF *in vitro*[124].

Five tetrapeptide fragments from BDNF were identified as potential candidates as a TrkB agonist. Two of these, IKRG and SKKR, both retained a partial agonist function *in vitro*[123]. These peptides have been shown to be neuroprotective, as well as upregulating both TrkB and BDNF in primary hippocampal cell cultures. This function can be blocked by treating cells with the TrkB inhibitor K252a. Unlike the other peptide TrkB agonists which have been developed, these still possess agonistic function in a linear form.

1.1.2 Mimetics, direct or indirect signalling?

Many of these BDNF mimetics are reported as TrkB agonists *in vivo*, while there is less evidence of their function *in vitro*. Recently, a comprehensive complementary analysis of BDNF and other neurotrophins, alongside the published compounds, LN22A-4, 7,8-DHF, Deoxygedunin, DMAQ-B1 Amitriptyline and Deprenyl was conducted, investigating their ability to activate TrkB, and several downstream pathways *in vitro* [140]. The work involved a HEK cell line, transfected with TrkB, CHO K1 and SH-SY5Y cell lines, and primary cortical neurons. A wide panel of assays were conducted, concluding that none of the compounds tested demonstrated significant activation of TrkB, with DMAQ-B1 alone briefly inducing a small amount of ERK and AKT activity. This thorough investigation of the *in vitro* activity of these compounds alongside BDNF highlights that the action of the mimetics *in vivo* may be different to *in vitro*. Other studies have reported the failure of some of these widely reported molecules to activate TrkB [125], [135], or perform as expected with respect to cell survival[125].

1.2 Cell Scaffolds

Cells within the central nervous system are exposed to a complex 3D microenvironment[141], [142]. Physically, cells interact with the extracellular matrix(ECM), which presents a range of nanostructures to cells, often in a complex hierarchical arrangement[143], [144]. Cells are sensitive to both the morphology and mechanical properties of the ECM. Additionally, cells interact with the plasma membranes of the neighbouring cells. These factors, combined with biochemical cues, help a cell know when to grow, multiply, differentiate or die[145]. In order to successfully treat a neurodegenerative disease, a combinatorial approach, in which an appropriate physical support is provided to cells, in addition to a drug, will allow greater control over the microenvironment offered to cells. This in turn will improve the chances of developing a successful treatment[146].

Neural tissue engineering scaffolds which mimic elements of the *in vivo* microenvironment are being developed, which have shown benefit in neural cell proliferation, migration and differentiation of cells during the repair process. Two methods of scaffold fabrication are receiving attention, the 'top-down' approach of electrospinning[147]–[149], and the 'bottom-up' method of self-assembly[150]–[154]. Both methods allow the production of a fibrous network, with a broad range of feature sizes achievable depending on the method used. This allows for a material or method to be selected to match specific ECM environments.

Self-assembled systems are an attractive approach for the development of a neural scaffold, as the nanofibrous structure of these materials resembles some elements of the native ECM. Of the available self-assembling materials, peptide based self-assembling systems are extremely versatile and useful. This is due in part to the 20 natural amino acids and many other synthetic derivatives available for synthesis, and the biocompatibility and biodegradability that is intrinsic to these systems. Peptide amphiphiles[155], [156], aromatic peptide amphiphiles[157]–[159] and self-complementary peptides[160]–[162] are three of the more common categories of self-assembling peptide under investigation. Peptide amphiphiles involve a peptide sequence conjugated to a long hydrophobic organic tail, which frequently results in

the formation of micelles or nanofibers. Aromatic peptide amphiphiles are usually short sequences, up to 8 amino acids, with an aromatic functionalisation such as fluorenylmethyloxycarbonyl (Fmoc)[158], [163], [164] or napthaline[165]–[167] used to induce self-assembly into a nanofibrous network through π stacking. Self-complementary peptides, such as the commercially available RADA system[168] utilise alternating hydrophobic and hydrophilic amino acids which stack to form nanofibrous hydrogels.

β peptides are an interesting candidate for neural scaffolding, as they offer many of the same advantages as conventional peptide based systems, but with significantly greater stability *in vivo*[169], [170], which may be important when long term structural support of tissue is required.

In order to offer the best chances of successful treatment, the use of a physical scaffold, which can be used to deliver a drug in addition of providing an appropriate physical environment for cell growth and survival, is desirable.

1.2.1 Gel scaffolds for neural applications

Hydrogels are materials with solid-like behaviour, composed of a crosslinked organic, or tangled nanofibrous network providing physical support, which swell to hold several times their own weight in water[171]. They are an attractive class of material for use in biological systems, as the mechanical properties are in the range of many soft tissues. Due to the high water content, they can be effectively used as a drug reservoir, leading to controlled release of a therapeutic agent[165], [172], [173]. There are two main categories of hydrogel – 1) chemically crosslinked hydrogels, in which covalent bonds are responsible for the bulk properties of the gel, and 2) physical hydrogels, which are held together by weaker secondary bonds, such as π-π stacking, hydrogen bonding and hydrophobic interactions.

Many physical hydrogels are reversible[174][175], meaning they can respond to stimuli, and can be switched between the gel and liquid state. Many physical hydrogels are also injectable[2], [176] – as the secondary bonds that break at high shear can reform once the stress is removed, allowing them to flow, then re-form as a gel.

1.2.2 Fmoc self-assembling peptides

Short peptides capped with planar aromatic molecules, such as Fmoc have shown flexibility in both mechanical properties of the gel, and cellular response *in vitro*. Fmoc Leu-Asp was first reported as a self-assembling gel in 1995[177]. This work detailed the use of a thermal switch to trigger gelation of the peptide into a hydrogel at concentrations as low as 1 wt%. Since then, Fmoc peptides have been explored for applications in cell culture[178]–[183] and drug delivery[184].

Table 1.2: Self-assembling peptide hydrogels with neural applications.

Peptide	Origin of sequence	Storage Modulus	Gelation concentration	References
VTAVV	α-synuclein	Unknown	6 mg/ml	[3]
VTVVA	α-synuclein	Unknown	6 mg/ml	[3]
VYAVA	α-synuclein	20-100 Pa	6 mg/ml	[3]
VHAVA	α-synuclein	20-900 Pa	Unknown	[3]
VHVVA	α-synuclein	Unknown	Unknown	[3]
FRGDF	Fibronectin and integrins	10 kPa	10-20 mg/ml	[185], [186]
DIKVAV	Laminin	10-25 kPa	20 mg/ml	[185][187][1]
DDIKVAV	Laminin	1–30 kPa	10-20 mg/ml	[102][187][188]
DYIGSRF	Laminin	200 Pa	Unknown	[185]

Fmoc peptide hydrogels self-assemble into an anti-parallel β-sheet structure, with π-π stacking of the Fmoc moieties[189], [190], and other secondary bonding dependent upon the specific peptide sequence. Due to the hydrophobic nature of the peptides, they are typically insoluble at physiological pH in aqueous solutions. Fmoc self-assembling peptides which have been developed for use in neural applications are shown in Table 1.2.

1.2.3 Gelation methods

The solvent switch method of Fmoc hydrogel formation involves first dissolving the peptide at high concentration in good solvent, then diluting this in a poor solvent for the peptide, leading to gelation. With the Fmoc-Phe-Phe system, hydrogels have been formed by diluting peptide in hexafluoroisopropanol (HFIP) with water[181], and

from DMSO into PBS[183]. The amount of residual DMSO in the hydrogel was reported to influence the mechanical properties.

Several enzymatic methods have been developed for the formation of hydrogels from Fmoc peptides. These involve a pre-peptide in solution, which is converted by an enzymatic process into a gel-forming peptide. Several dipeptides have been developed which use a phosphorylated tyrosine residue in the pre-peptide, with a phosphatase enzyme being used to dephosphorylate the peptides and trigger gelation[159], [191]–[193].

The pH switch method of hydrogel preparation originally involved dissolving the hydrogel at high pH (phosphate buffered saline (PBS) and NaOH or similar) with a hydrogel forming when pH was reduced again, using HCl. The rate of gelation however is very rapid, meaning the gels formed were often inhomogeneous, and mechanical properties and appearance were sometimes inconsistent. Adams et al developed a protocol for the use of Glucono-δ-lactone (GDL) as an alternative means of reducing the pH of the solutions to trigger gelation[194]. This works through the gradual hydrolysis of GDL into gluconic acid, causing a gradual homogenous reduction of pH in the solution, resulting in much more reproducible hydrogels. This method had been adopted by several research groups now, and is widely investigated[167], [184], [195], [196]. There is some evidence indicating that this method, for some hydrogels at least leads to less entanglements of nanofibers, and a weaker hydrogel[196].

A variation to the pH switching method involving the use of gaseous carbon dioxide (CO_2) was developed, in which a thin layer (50nm) of Fmoc-Phe-Phe was gelled on the surface of 'liquid marbles'[197]. The use of a gaseous phase to gel the surface meant homogenous gelation across samples, without mechanical disturbance of the structures. Liquid marbles were placed in a petri dish, which was itself placed in another dish, which contained dry ice, leading to a high CO_2 environment. This CO_2 then dissolved into the liquid phase, forming carbonic acid, and triggering self-assembly. This method is yet to be applied to the production of bulk hydrogels.

A temperature switching method of Fmoc hydrogel formation has also been developed, which involves raising the temperature of the solvent to allow sufficient solubility of the peptides, then upon cooling the solution, a hydrogel is formed[177], [198].

1.2.3.1 Macromolecular structure/modelling

Libraries of peptides have been developed, in order to build an understanding of the relationship between the peptide structure, and resulting properties, in an attempt to build a set of rules for the development of new hydrogels[174], [178]. A careful balance of hydrophobicity and sufficient ionisable moieties is required for hydrogel formation. Figure 1.5 shows the Fmoc-FF-OH peptide, which strongly self-assembles, due to the Fmoc group on the N terminal, with the Phe residues providing additional π-π stacking, and the carboxylic acid on the C terminal allowing for ionisation at high pH, and therefore solubility in an aqueous solution. If the peptide is too hydrophilic, it may simply remain in solution, and if too hydrophobic, it may not dissolve in the first place, or precipitate from solution before forming fibres, and self-assembling.
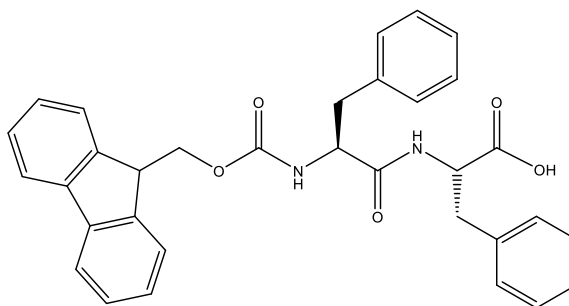
Figure 1.5: The chemical structure of Fmoc-Phe-Phe-OH.

Fmoc peptide hydrogels are commonly investigated through a range of microscopy, mechanical and spectroscopic methods. Mechanical characterisation is generally in the form of rheological testing, where a time course is used to determine gelation time, and peak stiffness. Frequency sweeps can be used to determine the gel shear modulus and the glassy modulus of the hydrogel[199], [200]. Strain sweeps are used to find the linear viscoelastic region of the material[200]. Many of these hydrogels are described as shear thinning, or self-healing, due to their ability to flow under high shear forces, and return to a gel state once this force is removed. A recent investigation utilising a confocal-rheometer assembly has demonstrated that the

fracture and re-healing of hydrogels may not be a homogenous phenomenon, with the shear forces and therefore fracture and healing being localised, while the bulk of the hydrogel experiences significantly less force[201].

FTIR can be used to provide information relating to the secondary bonding found within the hydrogel. Peaks at 1630 cm^{-1} and a shoulder at 1690 cm^{-1} are often cited as evidence of an anti-parallel β-sheet structure[3], [202]–[204] although the peak at 1690 cm^{-1} has now been attributed to the adsorption of the stacked carbamate group, rather than the antiparallel β -sheet secondary structure[205], [206] which means these peptides are self-assembling into parallel as opposed to anti-parallel β-sheets. A peak at 1641-1650 cm^{-1} can indicate a random-coil structure[207][206]. And a broad peak at 1590 cm^{-1} for dipeptide gels indicates that some c-terminal carboxylic acid groups remain deprotonated[206], [208], [209].

Due to the chiral nature of beta-sheets, circular dichroism can also be used to probe the structure of the hydrogel, with characteristic CD signals between 200 and 220 nm and 270 and 310 nm[165], [210]–[212]. The fibres that Fmoc peptides form tend to be on the nanometer scale, so TEM methods are highly applicable. Drying a hydrogel onto a grid, and staining using a negative stain, such a uranyl acetate or phosphotungstic acid is a common, and simple approach[203]. AFM is another frequently used method[3], [186]. Both of these methods require dehydration of the sample, so the structures, and arrangement of the fibres may not be a truly accurate representation of what exists in the hydrated state. CryoTEM avoids the issues associated with drying the sample and has been shown to be an effective method of imaging these systems[213], although due to the poor contrast available, combining this with one of the previous methods is ideal.

Detailed structural analyses have been conducted on a number of Fmoc peptide systems. A model of Fmoc-Phe-Phe was developed[203] which was based upon measurements taken with circular dichromism and FT-IR analysis suggested an anti-parallel β-sheet structure, with the fluorenyl rings in a π-π stacked arrangement. The model derived from these measurements is shown in Figure 1.6, and was in agreement with measurements of the hydrogel by WAXS and TEM. A model of a

hybrid hydrogel, containing both Fmoc-Phe-Phe and Fmoc-Arg-Gly-Asp was developed, based off TEM images showing 3nm fibres, and using the previously established model[180]. This structure was verified by CD and FTIR spectra. Similar structures have been proposed for many Fmoc self-assembling peptides [136], [137]. There is however some evidence of a parallel model for these peptide hydrogels[214]–[216], and at this time, both can be suggested by the available data[214]. Until higher resolution structural analyses are available, such as solid state NMR, or crystallographic analysis, the true confirmation of these structures cannot be confirmed.
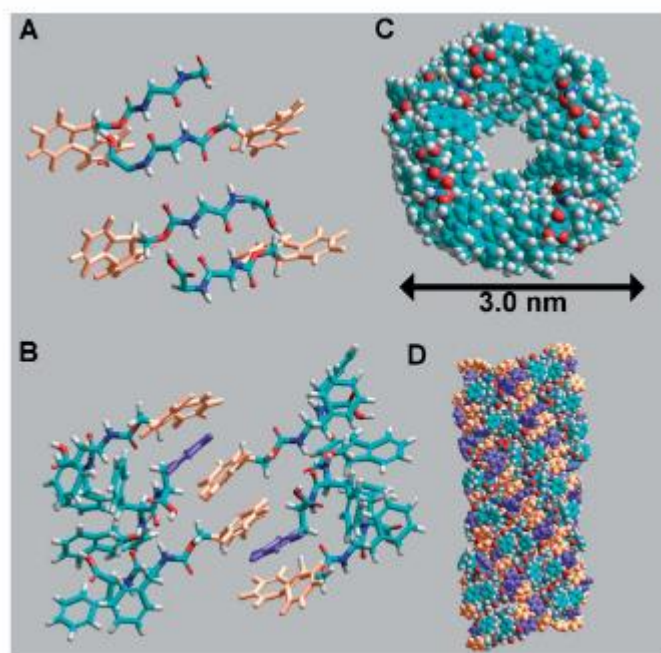
Figure 1.6 A commonly cited structure of Fmoc self-assembling peptides is that of the anti-parallel β-sheet (A), in the case of Fmoc-FF phenyl rings interleave themselves with the fmoc groups (B). Due to the chirality of the system, there is an offset between each sheet, which results in a cylindrical structure (C and D). Fmoc groups are coloured orange, and phenyl groups are coloured purple to highlight their arrangement in the resulting structure. Reproduced with permission from Wiley [203]

1.2.3.2 Functional Fmoc peptides

While many Fmoc peptides are biocompatible, and structurally mimic extracellular matrix environments, they are limited in their application. While the fibrous macromolecular structure of these hydrogels is similar to the extracellular environment, most have no biological functionality. Many biologically active small peptides exist. One of the benefits of using a peptide based material system, is that it is possible to build a material that contains biofunctional peptide motifs in its

structure. When designing an Fmoc self-assembling peptide system, the length, as well as the hydrophobicity are very important to the self-assembly behaviour of these peptides. It is therefore highly unlikely that the addition of a functional short peptide to the end of an existing Fmoc self-assembling peptide with result in a functional self-assembling hydrogel. Most functionalised self-assembling Fmoc hydrogels are the result of careful selection of additional residues to control the hydrophobicity and pKa of the peptide. Phe is the hydrophobic amino acid most used for modifying self-assembly, as it can add to the π-π stacking nature of the peptides, and Fmoc-Phe-Phe is already known to self-assemble. Asp is commonly used if the peptide is too hydrophobic, or if gelation only occurs at very high pH values[187]. The goal when modifying the solubility of the peptides like this is to make a sequence that is minimally soluble at pH7.4, but can be dissolved at higher pH. If successful, upon reducing the pH back toward neutral, the peptides will self-assemble into a fibrous structure, which entangles and forms a self-supporting hydrogel. The cell adhesive ligands, RGD, IKVAV and YIGSR have all been used in surface functionalisation in biomaterials. These peptides have all been modified, through the addition of the Fmoc moiety to the C terminal, and the addition of Phe or Asp residues to the peptide, in order to adjust the peptide's hydrophobicity and pKa. The resulting peptide hydrogels, Fmoc-FRGDF-OH[196], Fmoc-DIKVAV-OH[187] and Fmoc-DYIGSRF-OH[217] are all capable of self-assembly at physiological pH, and have been tested *in vivo*.

Blended Fmoc hydrogels have been investigated, as they allow for optimising mechanical properties, as well as incorporating biological or chemical functionalisation. Blends of Fmoc-Phe-Phe with Fmoc- Lys, Fmoc-Ser and Fmoc-Glu were investigated for the chemical functionality provided by the different side groups[179]. The resulting hydrogels were self-supporting, and exhibited elastic moduli from 502Pa up to 21.2 kPa at 25°C and 20mmol l^{-1}. All gel blends support the growth of bovine chondrocytes, with Fmoc-Phe-Phe/Ser and Fmoc-Phe-Phe/Glu blends additionally supporting the growth of human dermal fibroblasts. Co-assembly of Fmoc-Phe-Phe with Fmoc-Arg-Gly-Asp led to improved cell adheasion and spreading on the blended hydrogel compared to Fmoc-Phe-Phe alone, indicating

that the RGD motif is bioavailable in this co-assembled hydrogel system.[207]. Fmoc-Phe-Phe blended 1:1 with Fmoc-Phe-Gly or Fmoc-β-(2-naphthyl)-alanine were investigated[218]. The peptide Fmoc-Phe-Gly alone was not able to form a self-supporting hydrogel, but when blended 1:1 with Fmoc-Phe-Phe, a clear stable hydrogel resulted, showing that through co-gelation, incorporation of non-ideal gelators which possess a desired chemical or biological functionalisation may be achieved[218]. Blends of Fmoc-Gly-Gly with Fmoc-Phe-Phe are also more stable than either peptide hydrogel alone, due to their increased fluorenyl interactions[178].

1.2.3.3 Self-complementary peptide systems

The self-complementary peptide sequence EAK16 (Ala-Glu-Ala-Glu-Ala-Lys-Ala-Lys)$_2$ originates in the yeast protein zuotin and was first published as self-assembling hydrogel in 1993[219]. This was followed up by RAD16 (Arg-Ala-Arg-Ala-Asp-Ala-Asp-Ala)$_2$ in 1995[160] which is a systematically modified version of the EAK16 sequence. After some more investigation, the sequence RAD16-I was developed, and is now commercially available under the name PuraMatrix by Corning. PuraMatrix has been applied to spinal cord[168] and peripheral nerve[220] regeneration, following seeding the hydrogel with Schwann cells. It has also been used in a system for growing primary neural cells in low serum conditions without the need for feeder cells for two months[221]. Modified versions of this peptide have been developed, in which functional peptides derived from laminin I (YIGSR, RYVVLPR, PDSGR)[222], [223] and collagen IV (TAGSCLRKFSTM)[222] fibronectin (RGD/RGDS)[224], and a 2-unit RGD binding sequence (PRGDSGYRGDS) [223] have all been studied. The functionalised peptides generally improved cell adhesion, growth and survival when compared to the unmodified RADA sequence. Co-assembly of these functionalised peptides with RAD16 significantly affects the mechanical properties of the hydrogel[222], meaning they can be blended with each other in order to control the density of functional motifs, and/or mechanical properties.

With the intention of creating a system with more consistent mechanical properties both with and without modification, a new self-complementary peptide was developed by Collier and Messersmith[225] called Q11 (Ac-QQKFQFQFEQQ-Am).

The 11 amino acid peptide self-assembled into a fibrillar network which they then crosslink enzymatically. They further investigated this system, synthesising functionalised versions of the peptide containing either IKVAV or the RGDS sequence, and co-assembling these with the base peptide[226]. The resulting hydrogels were better able to support HUVEC cell spreading, growth and attachment compared to the base Q11 hydrogel alone, while maintaining consistent mechanical properties.

Two octa-peptides FEKII (FEFEFKFK) and FEFKFEFK were published in 2007 as self-assembling peptide hydrogels. Since the discovery of these octa-peptides, several variants have been explored, with a double length variant FEKII18 (FEFEFKFK-GG-FKFKFEFE) which effectively crosslinks the structure[227]. The double length peptide will self-assemble alone, or can be co-assembled with the single length FEKII peptide, leading to significantly stiffer hydrogels. Another variant made was histidine functionalised (HHHHHHFEFEFKFK). This peptide was also capable of independent self-assembly, but was primarily made to investigate the co-assembly of these systems[228]. The histidine functionalised peptide was blended into the base sequence at a 1:9 ratio and stained using nickel nitrilotriacetic acid (Ni-NTA) nanogold. TEM analysis showed that the co-assembled structure had a fibre diameter greater than either of the peptides alone – suspected to be caused by π stacking of the histidine groups leading to two fibres associating. The nanogold had an average spacing of 21nm, and was present along either side of the fibres. This spacing suggested one in 44 peptides within the fibres was substituted with a functionalised peptide. This peptide has also been used to make a double temperature-sensitive polymer-peptide conjugate[229] in which the peptide was conjugated to a poly(N-isopropylacrylamide) polymer. The resulting hydrogel system exhibits a lower critical solution temperature phase transition at 30°C and a gel melting transition at 75°C, with both transitions being fully reversible.

The peptide, H-Phe-Glu-Phe-Gln-Phe-Lys-OH (MBG-1) self assembles into a stable hydrogel at 37°C, at 1% w/w in a 50% water/PBS solution[162]. Variations to the system were investigated, with altered amino acids sequences, N and C terminal

functionalisations explored[176]. Of these, H- Phe-Glu-Phe-Gln-Phe-Lys-NH$_2$ and the all D amino acid variant, H-phe-glu-phe-gln-phe-lys-NH$_2$ were investigated with respect to their stability *in vivo*. Predictably, the D-version demonstrated no observable degradation in human plasma. Release of morphine from the scaffold was investigated, and a gradual release over 3 days was observed which seemed to be independent of the drug concentration, indicating an interaction between the drug and peptide. The L-amino acid peptide was biocompatible to 24 hours *in vitro*, while the D-amino acid hydrogel showed decreased cell viability. *In vivo* injections of the all-L hydrogel loaded with morphine showed a significantly increased duration of nociceptive efficacy compared to a simple injection of morphine only, with a measurable effect remaining at 24 hours *in vivo*. A follow up study has shown this family of peptides is able to sustain a nociceptive effect for up to 4 days from a single injection[172].

1.2.3.4 The significance of chirality on self-assembly

The use of D amino acids in peptide hydrogels enables greater proteolytic stability of the system[230], while still enabling ease of synthesis, and many of the other benefits of peptide hydrogels.

Table 1.3: Hydrogel forming uncapped heterochiral tripeptides.

Peptide	G′
^{D}VFF	10 kPa
^{D}FFV	10 kPa
^{D}LFF	20 kPa

The three tripeptides in Table 1.3 were developed without any capping groups and are all capable of self-assembling into rigid hydrogels following a pH switch[231], [232]. These peptides all have a change in chirality for the N-terminal amino acid in the sequence. Compared to their all L counterparts, these peptides under TEM and AFM microscopy are all composed of long nanofibers, which are responsible for gelation. The D amino acid at the N terminal of the peptide enables self-assembly into an extended 3D molecular structure, with a phenylalanine zipper between

adjacent β-sheets[233]. This structural model is supported by CD, FTIR and XRD data.

These hydrogels have been shown to encapsulate rhodamine[173], as a model aromatic drug, and later ciprofloxacin[231], which showed an initial burst release, to approximately 30% of the drug content, then a much slower controlled release profile. Demonstrating their potential as a drug delivery system for hydrophobic, planar drug molecules.

The effect of altered chirality on other self-assembling systems has been investigated, with all D variants of the EAK16 self-assembling peptide still forming a hydrogel[230], [234], but variants with hetero-chirality (Alternating L and D amino acids) only able to form smaller aggregates, instead of the nanofibers required for gelation of the system[235].

1.3 Overview of this work

Currently, there is a lack of any therapy for neurodegenerative diseases capable of going beyond offering symptomatic relief. In order to begin addressing this deficit in treatment options, this project has focused on the development of a system capable of delivering a neurotrophic signalling molecule to the central nervous system in a spatially and temporally controlled manner. The objective being to enable targeted neuroprotection, and potentially recovery of the affected area. To date, hydrogels have been used to encapsulate full BDNF protein[102] and provide prolonged release, which goes some way to achieving this goal, but the use of small molecule mimetics enables the specific activation of the TrkB and not the p75ntr receptor, and better stability of the drug in vivo.

The materials investigated in this work combine published functional short peptides, and what is known about Fmoc-based and self-complementary peptides, to form new hydrogels containing a BDNF derived motif. The co-assembly of these novel peptides with existing, published materials is investigated in order to achieve the best combination of mechanical properties, and chemical signalling for use in the central nervous system.

1.1 References

[1]   F. L. Maclean, Y. Wang, R. Walker, M. K. Horne, R. J. Williams, and D. R. Nisbet, "Reducing Astrocytic Scarring after Traumatic Brain Injury with a Multifaceted Anti-Inflammatory Hydrogel System," *ACS Biomater. Sci. Eng.*, vol. 3, no. 10, pp. 2542–2549, Oct. 2017.

[2]   S. Motamed, M. P. Del Borgo, K. Kulkarni, N. Habila, K. Zhou, P. Perlmutter, J. S. Forsythe, and M. I. Aguilar, "A self-assembling β-peptide hydrogel for neural tissue engineering," *Soft Matter*, vol. 12, no. 8, pp. 2243–2246, 2016.

[3]   S. Das, K. Zhou, D. Ghosh, N. N. Jha, P. K. Singh, R. S. Jacob, C. C. Bernard, D. I. Finkelstein, J. S. Forsythe, and S. K. Maji, "Implantable amyloid hydrogels for promoting stem cell differentiation to neurons," *Nat. Publ. Gr.*, vol. 8, 2016.

[4]   T. Nakaji-Hirabayashi, K. Kato, and H. Iwata, "In vivo study on the survival of neural stem cells transplanted into the rat brain with a collagen hydrogel that incorporates laminin-derived polypeptides," *Bioconjug. Chem.*, vol. 24, no. 11, pp. 1798–1804, 2013.

[5]   C. A. Davie, "A review of Parkinson's disease," *British Medical Bulletin*, vol. 86, no. 1. pp. 109–127, 2008.

[6]   T. Pringsheim, N. Jette, A. Frolkis, and T. D. L. Steeves, "The prevalence of Parkinson's disease: A systematic review and meta-analysis," *Movement Disorders*, vol. 29, no. 13. pp. 1583–1590, 2014.

[7]   K. A. Kitchen Andren, N. M. Gabel, J. Stelmokas, A. M. Rich, and L. A. Bieliauskas, "Population Base Rates and Disease Course of Common Psychiatric and Neurodegenerative Disorders," *Neuropsychol. Rev.*, vol. 27, no. 3, pp. 284–301, Sep. 2017.

[8]   K. Ali and H. R. Morris, "Parkinson's disease: chameleons and mimics.," *Pract. Neurol.*, pp. 1–23, 2014.

[9]   J. Andrew, S. Blankson, and A. J. Lees, "Clinicopathologic Study of 100 Cases of Parkinson's Disease," 2016.

[10] G. DeMaagd and A. Philip, "Parkinson's Disease and Its Management: Part 1: Disease Entity, Risk Factors, Pathophysiology, Clinical Presentation, and Diagnosis.," *P T*, vol. 40, no. 8, pp. 504–32, Aug. 2015.

[11] S. S. O'Sullivan, D. R. Williams, D. A. Gallagher, L. A. Massey, L. Silveira-Moriyama, and A. J. Lees, "Nonmotor symptoms as presenting complaints in Parkinson's disease: A clinicopathological study," *Mov. Disord.*, vol. 23, no. 1, pp. 101–106, Jan. 2008.

[12] W. R. G. Gibb and A. J. Lees, "The relevance of the Lewy body to the pathogenesis of ideopathic Parkinson's disease," *J. Neurol. Neurosurgery, Psychiatry*, vol. 51, pp. 745–752, 1988.

[13] A. J. Hughes, S. E. Daniel, and A. J. Lees, "Improved accuracy of clinical diagnosis of Lewy body Parkinson's disease," *Neurology*, vol. 57, no. 8, pp. 1497–1499, Oct. 2001.

[14] T. F. Outeiro, E. Kontopoulos, S. M. Altmann, I. Kufareva, K. E. Strathearn, A. M. Amore, C. B. Volk, M. M. Maxwell, J.-C. Rochet, P. J. McLean, A. B. Young, R. Abagyan, M. B. Feany, B. T. Hyman, and A. G. Kazantsev, "Sirtuin 2 Inhibitors Rescue -Synuclein-Mediated Toxicity in Models of Parkinson's Disease," *Science (80-.).*, vol. 317, no. 5837, pp. 516–519, Jul. 2007.

[15] P. Hickey, "Available and emerging treatments for Parkinson ' s disease : a review," pp. 241–254, 2011.

[16] C. L. Tomlinson, R. Stowe, S. Patel, C. Rick, R. Gray, and C. E. Clarke, "Systematic Review of Levodopa Dose Equivalency Reporting in Parkinson ' s Disease," vol. 25, no. 15, pp. 2649–2685, 2010.

[17] S. Fahn, D. Oakes, I. Shoulson, K. Kieburtz, A. Rudolph, A. Lang, C. W. Olanow, C. Tanner, K. Marek, and Parkinson Study Group, "Levodopa and the Progression of Parkinson's Disease," *N. Engl. J. Med.*, vol. 351, no. 24, pp. 2498–2508, 2004.

[18] G. C. Cotzias, P. S. Papavasiliou, and R. Gellene, "Modification of

Parkinsonism — Chronic Treatment with L-Dopa," *N. Engl. J. Med.*, vol. 280, no. 7, pp. 337–345, Feb. 1969.

[19] A. Lopez, A. Muñoz, M. . Guerra, and J. . Labandeira-Garcia, "Mechanisms of the effects of exogenous levodopa on the dopamine-denervated striatum," *Neuroscience*, vol. 103, no. 3, pp. 639–651, Mar. 2001.

[20] T. Müller, T. van Laar, D. R. Cornblath, P. Odin, F. Klostermann, F. J. Grandas, G. Ebersbach, P. P. Urban, F. Valldeoriola, and A. Antonini, "Peripheral neuropathy in Parkinson's disease: Levodopa exposure and implications for duodenal delivery," *Parkinsonism Relat. Disord.*, vol. 19, no. 5, pp. 501–507, May 2013.

[21] G. DeMaagd and A. Philip, "Part 2: Introduction to the Pharmacotherapy of Parkinson's Disease, With a Focus on the Use of Dopaminergic Agents.," *P T*, vol. 40, no. 9, pp. 590–600, Sep. 2015.

[22] R. Bhidayasiri and D. Tarsy, "Parkinson's Disease: 'On-Off' Phenomenon," in *Movement Disorders: A Video Atlas*, Totowa, NJ: Humana Press, 2012, pp. 14–15.

[23] M. Contin and P. Martinelli, "Pharmacokinetics of levodopa," *J. Neurol.*, vol. 257, no. S2, pp. 253–261, Nov. 2010.

[24] E. M. del Amo, A. Urtti, and M. Yliperttula, "Pharmacokinetic role of L-type amino acid transporters LAT1 and LAT2," *Eur. J. Pharm. Sci.*, vol. 35, no. 3, pp. 161–174, Oct. 2008.

[25] J. G. Nutt, W. R. Woodward, and J. L. Anderson, "The effect of carbidopa on the pharmacokinetics of intravenously administered levodopa: The mechanism of action in the treatment of parkinsonism," *Ann. Neurol.*, vol. 18, no. 5, pp. 537–543, Nov. 1985.

[26] Y. Smith, T. Wichmann, S. A. Factor, and M. R. DeLong, "Parkinson's disease therapeutics: new developments and challenges since the introduction of levodopa.," *Neuropsychopharmacology*, vol. 37, no. 1, pp. 213–46, Jan. 2012.

[27] P. R. Schuurman and D. A. Bosch, "Surgical considerations in movement

disorders: deep brain stimulation, ablation and transplantation," in *Operative Neuromodulation: Volume 2: Neural Networks Surgery*, D. E. Sakas and B. A. Simpson, Eds. Vienna: Springer Vienna, 2007, pp. 119–125.

[28] P. R. Schuurman, D. A. Bosch, P. M. M. Bossuyt, G. J. Bonsel, E. J. W. van Someren, R. M. A. de Bie, M. P. Merkus, and J. D. Speelman, "A Comparison of Continuous Thalamic Stimulation and Thalamotomy for Suppression of Severe Tremor," *N. Engl. J. Med.*, vol. 342, no. 7, pp. 461–468, Feb. 2000.

[29] Yoshishige Nagaseki, Tohru Shibazaki, Tatsuo Hirai, Yasuhiro Kawashima, Masafumi Hirato, Hirochiyo Wada, Mizuho Miyazaki, and Chihiro Ohye, "Long-term follow-up results of selective VIM-thalamotomy," *J. Neurosurg.*, vol. 65, no. 3, pp. 296–302, 1986.

[30] J. Obeso, C. Olanow, M. Rodriguez-Oroz, P. Krack, R. Kumar, and A. Lang, "Deep-Brain Stimulation of the Subthalamic Nucleus or the Pars Interna of the Globus Pallidus in Parkinson's Disease," *N. Engl. J. Med.*, vol. 345, no. 13, pp. 956–963, Sep. 2001.

[31] J. L. Houeto, V. Mesnage, L. Mallet, B. Pillon, M. Gargiulo, du M. ST, B. AM, B. Pidoux, D. Dormont, P. Cornu, and Y. Agid, "Behavioural disorders, Parkinson's disease and subthalamic stimulation," *J. Neurol. Neurosurg. Psychiatry*, vol. 72, pp. 701–707, 2002.

[32] P. Limousin, P. Krack, P. Pollak, A. Benazzouz, C. Ardouin, D. Hoffmann, and A.-L. Benabid, "Electrical Stimulation of the Subthalamic Nucleus in Advanced Parkinson's Disease," *N. Engl. J. Med.*, vol. 339, no. 16, pp. 1105–1111, Oct. 1998.

[33] H. M. M. Smeding, R. A. J. Esselink, B. Schmand, M. Koning-Haanstra, I. Nijhuis, E. M. Wijnalda, and J. D. Speelman, "Unilateral pallidotomy versus bilateral subthalamic nucleus stimulation in PD," *J. Neurol.*, vol. 252, no. 2, pp. 176–182, Feb. 2005.

[34] J. C. Rothlind, R. W. Cockshott, P. a Starr, and W. J. Marks, "Neuropsychological performance following staged bilateral pallidal or subthalamic nucleus deep brain stimulation for Parkinson's disease.," *J. Int.*

Neuropsychol. Soc., vol. 13, no. 1, pp. 68–79, Jan. 2007.

[35] A. Berney, F. Vingerhoets, A. Perrin, P. Guex, J.-G. Villemure, P. R. Burkhard, C. Benkelfat, and J. Ghika, "Effect on mood of subthalamic DBS for Parkinson's disease A consecutive series of 24 patients," *Neurology*, vol. 59, no. 9, p. 1427 LP-1429, Nov. 2002.

[36] L. Aron and R. Klein, "Repairing the parkinsonian brain with neurotrophic factors," *Trends Neurosci.*, vol. 34, no. 2, pp. 88–100, 2011.

[37] R. Linker, R. Gold, and F. Luhder, "Function of Neurotrophic Factors Beyond the Nervous System: Inflammation and Autoimmune Demyelination," *Crit. Rev. Immunol.*, vol. 29, no. 1, pp. 43–68, 2009.

[38] K. Seidla, A. Buchberger, and C. Erck, "Expression of Nerve Growth Factor and Neurotrophin Receptors in Testicular Cells Suggest Novel Roles for Neurotrophins Outside the Nervous System," *Reprod. Fertil. Dev*, vol. 8, pp. 1075–87, 1996.

[39] M. Ceccanti, S. De Nicolò, R. Mancinelli, G. Chaldakov, V. Carito, M. Ceccanti, G. Laviola, P. Tirassa, and M. Fiore, "NGF and BDNF long-term variations in the thyroid, testis and adrenal glands of a mouse model of fetal alcohol spectrum disorders.," *Ann. Ist. Super. Sanita*, vol. 49, no. 4, pp. 383–90, 2013.

[40] R. N. Corporation, P. Alto, N. Survival, D. D. Development, N. Maturation, D. Development, P. Neuropathies, C. Impairment, O. Indications, B. Antagonists, and D. R. Agonists, "Neurotrophic factors," vol. 3, pp. 221–236, 2007.

[41] P. Durbec, C. V. Marcos-Gutierrez, C. Kilkenny, M. Grigoriou, K. Wartiowaara, P. Suvanto, D. Smith, B. Ponder, F. Costantini, M. Saarma, H. Sariola, and V. Pachnis, "GDNF signalling through the Ret receptor tyrosine kinase," *Nature*, vol. 381, no. 6585, pp. 789–793, Jun. 1996.

[42] M. Trupp, E. Arenas, M. Fainzilber, A.-S. Nilsson, B.-A. Sieber, M. Grigoriou, C. Kilkenny, E. Salazar-Grueso, V. Pachnis, U. Arumäe, H. Sariola, M. Saarma, and C. F. Ibáñez, "Functional receptor for GDNF encoded by the c-ret proto-

oncogene," *Nature*, vol. 381, no. 6585, pp. 785–789, Jun. 1996.

[43]   M. Trupp, N. Belluardo, H. Funakoshi, and C. F. Ibáñez, "Complementary and overlapping expression of glial cell line-derived neurotrophic factor (GDNF), c-ret proto-oncogene, and GDNF receptor-alpha indicates multiple mechanisms of trophic actions in the adult rat CNS.," *J. Neurosci.*, vol. 17, no. 10, pp. 3554–67, May 1997.

[44]   P. Naveilhan, C. Baudet, A. Mikaels, L. Shen, H. Westphal, and P. Ernfors, "Expression and regulation of GFRα3, a glial cell line-derived neurotrophic factor family receptor," *Proc. Natl. Acad. Sci.*, vol. 95, no. 3, pp. 1295–1300, Feb. 1998.

[45]   Y. A. Barde, D. Edgar, and H. Thoenen, "Purification of a new neurotrophic factor from mammalian brain.," *EMBO J.*, vol. 1, no. 5, pp. 549–553, 1982.

[46]   H. K. Teng, "ProBDNF Induces Neuronal Apoptosis via Activation of a Receptor Complex of p75NTR and Sortilin," *J. Neurosci.*, vol. 25, no. 22, pp. 5455–5463, Jun. 2005.

[47]   P. T. Pang, "Cleavage of proBDNF by tPA/Plasmin Is Essential for Long-Term Hippocampal Plasticity," *Science (80-.).*, vol. 306, no. 5695, pp. 487–491, Oct. 2004.

[48]   A. H. Nagahara and M. H. Tuszynski, "Potential therapeutic uses of BDNF in neurological and psychiatric disorders," *Nat. Rev. Drug Discov.*, vol. 10, no. 3, pp. 209–219, Mar. 2011.

[49]   L. N. Gillespie, G. M. Clark, P. F. Bartlett, and P. L. Marzella, "BDNF-induced survival of auditory neurons in vivo: Cessation of treatment leads to accelerated loss of survival effects," *J. Neurosci. Res.*, vol. 71, no. 6, pp. 785–790, Mar. 2003.

[50]   Y. Nishida, N. Adati, R. Ozawa, A. Maeda, Y. Sakaki, and T. Takeda, "Identification and classification of genes regulated by phosphatidylinositol 3-kinase- and TRKB-mediated signalling pathways during neuronal

differentiation in two subtypes of the human neuroblastoma cell line SH-SY5Y.," *BMC Res. Notes*, vol. 1, p. 95, 2008.

[51] O. Islam, T. X. Loo, and K. Heese, "Brain-Derived Neurotrophic Factor (BDNF) has Proliferative Effects on Neural Stem Cells through the Truncated TRK-B Receptor , MAP Kinase , AKT , and STAT-3 Signaling Pathways," vol. 3, pp. 42–53, 2009.

[52] D. C. Choi, S. L. Gourley, and K. J. Ressler, "Prelimbic BDNF and TrkB signaling regulates consolidation of both appetitive and aversive emotional learning," *Transl. Psychiatry*, vol. 2, no. 12, pp. e205-6, 2012.

[53] S. D. Kuipers and C. R. Bramham, "Brain-derived neurotrophic factor mechanisms and function in adult synaptic plasticity: New insights and implications for therapy," *Curr. Opin. Drug Discov. Dev.*, vol. 9, no. 5, pp. 580–586, 2006.

[54] N. H. Woo, H. K. Teng, C.-J. Siao, C. Chiaruttini, P. T. Pang, T. A. Milner, B. L. Hempstead, and B. Lu, "Activation of p75NTR by proBDNF facilitates hippocampal long-term depression," *Nat. Neurosci.*, vol. 8, no. 8, pp. 1069–1077, Aug. 2005.

[55] M. Barbacid, "The Trk family of neurotrophin receptors," *J. Neurobiol.*, vol. 25, no. 11, pp. 1386–1403, Nov. 1994.

[56] G. Tejeda and M. Díaz-Guerra, "Integral Characterization of Defective BDNF/TrkB Signalling in Neurological and Psychiatric Disorders Leads the Way to New Therapies," *Int. J. Mol. Sci.*, vol. 18, no. 12, p. 268, Jan. 2017.

[57] J. C. Arévalo and S. H. Wu, "Neurotrophin signaling: many exciting surprises!," *Cell. Mol. Life Sci.*, vol. 63, no. 13, pp. 1523–1537, Jul. 2006.

[58] E. J. Huang and L. F. Reichardt, "Trk Receptors: Roles in Neuronal Signal Transduction," *Annu. Rev. Biochem.*, vol. 72, no. 1, pp. 609–642, 2003.

[59] R. D. Groth and P. G. Mermelstein, "Brain-derived neurotrophic factor activation of NFAT (nuclear factor of activated T-cells)-dependent

transcription: a role for the transcription factor NFATc4 in neurotrophin-mediated gene expression.," *J. Neurosci.*, vol. 23, no. 22, pp. 8125–34, Sep. 2003.

[60] V. B. Matthews, M.-B. Åström, M. H. S. Chan, C. R. Bruce, K. S. Krabbe, O. Prelovsek, T. Åkerström, C. Yfanti, C. Broholm, O. H. Mortensen, M. Penkowa, P. Hojman, A. Zankari, M. J. Watt, H. Bruunsgaard, B. K. Pedersen, and M. A. Febbraio, "Brain-derived neurotrophic factor is produced by skeletal muscle cells in response to contraction and enhances fat oxidation via activation of AMP-activated protein kinase," *Diabetologia*, vol. 52, no. 7, pp. 1409–1418, Jul. 2009.

[61] V. K. Sandhya, R. Raju, R. Verma, J. Advani, R. Sharma, A. Radhakrishnan, V. Nanjappa, J. Narayana, B. L. Somani, K. K. Mukherjee, A. Pandey, R. Christopher, and T. S. K. Prasad, "A network map of BDNF/TRKB and BDNF/p75NTR signaling system," *J. Cell Commun. Signal.*, vol. 7, no. 4, pp. 301–307, Dec. 2013.

[62] M. A. Burke and M. Bothwell, "P75 neurotrophin receptor mediates neurotrophin activation of NF-kappa B and induction of iNOS expression in P19 neurons," *J. Neurobiol.*, vol. 55, no. 2, pp. 191–203, 2003.

[63] J. Ninkovic and M. Götz, "Signaling in adult neurogenesis: from stem cell niche to neuronal networks," *Curr. Opin. Neurobiol.*, vol. 17, no. 3, pp. 338–344, Jun. 2007.

[64] K. Obata and K. Noguchi, "BDNF in sensory neurons and chronic pain," *Neurosci. Res.*, vol. 55, no. 1, pp. 1–10, May 2006.

[65] M. Baydyuk, M. T. Nguyen, and B. Xu, "Chronic deprivation of TrkB signaling leads to selective late-onset nigrostriatal dopaminergic degeneration," *Exp. Neurol.*, vol. 228, no. 1, pp. 118–125, Mar. 2011.

[66] A. Haapasalo, I. Sipola, K. Larsson, K. E. O. Åkerman, P. Stoilov, S. Stamm, G. Wong, and E. Castrén, "Regulation of TRKB Surface Expression by Brain-derived Neurotrophic Factor and Truncated TRKB Isoforms," *J. Biol. Chem.*, vol. 277, no. 45, pp. 43160–43167, Nov. 2002.

[67]   R. H. Fryer, D. R. Kaplan, and L. F. Kromer, "Truncated trkB receptors on nonneuronal cells inhibit BDNF-induced neurite outgrowth in vitro.," *Exp. Neurol.*, vol. 148, no. 2, pp. 616–627, 1997.

[68]   B. M. Fenner, "Truncated TrkB: Beyond a dominant negative receptor," *Cytokine Growth Factor Rev.*, vol. 23, no. 1–2, pp. 15–24, Feb. 2012.

[69]   D. C. Lo and T. A. Yacoubian, "Truncated and full-length TrkB receptors regulate distinct modes of dendritic growth," *Nat. Neurosci.*, vol. 3, no. 4, pp. 342–349, Apr. 2000.

[70]   Q. Yan, R. . Rosenfeld, C. . Matheson, N. Hawkins, O. . Lopez, L. Bennett, and A. . Welcher, "Expression of brain-derived neurotrophic factor protein in the adult rat central nervous system," *Neuroscience*, vol. 78, no. 2, pp. 431–448, Mar. 1997.

[71]   S. Marco, A. M. Canudas, J. M. Canals, N. Gavaldà, E. Pérez-Navarro, and J. Alberch, "Excitatory Amino Acids Differentially Regulate the Expression of GDNF, Neurturin, and Their Receptors in the Adult Rat Striatum," *Exp. Neurol.*, vol. 174, no. 2, pp. 243–252, Apr. 2002.

[72]   C. Hyman, M. Hofer, Y.-A. Barde, M. Juhasz, G. D. Yancopoulos, S. P. Squinto, and R. M. Lindsay, "BDNF is a neurotrophic factor for dopaminergic neurons of the substantia nigra," *Nature*, vol. 350, no. 6315, pp. 230–232, Mar. 1991.

[73]   H. S. Phillips, J. M. Hains, M. Armanini, G. R. Laramee, S. A. Johnson, and J. W. Winslow, "BDNF mRNA is decreased in the hippocampus of individuals with Alzheimer's disease," *Neuron*, vol. 7, no. 5, pp. 695–702, 1991.

[74]   I. Ferrer, C. Marín, M. J. Rey, T. Ribalta, E. Goutan, R. Blanco, E. Tolosa, and E. Martí, "BDNF and full-length and truncated TrkB expression in Alzheimer disease. Implications in therapeutic strategies.," *J. Neuropathol. Exp. Neurol.*, vol. 58, no. 7, pp. 729–39, Jul. 1999.

[75]   P. Scalzo, A. Kümmer, T. L. Bretas, F. Cardoso, and A. L. Teixeira, "Serum levels of brain-derived neurotrophic factor correlate with motor impairment in

Parkinson's disease," *J. Neurol.*, vol. 257, no. 4, pp. 540–545, Apr. 2010.

[76]   Z. C. Baquet, P. C. Bickford, and K. R. Jones, "Brain-Derived Neurotrophic Factor Is Required for the Establishment of the Proper Number of Dopaminergic Neurons in the Substantia Nigra Pars Compacta," *J. Neurosci.*, vol. 25, no. 26, pp. 6251–6259, Jun. 2005.

[77]   D. W. Howells, M. J. Porritt, J. Y. F. Wong, P. E. Batchelor, R. Kalnins, A. J. Hughes, and G. A. Donnan, "Reduced BDNF mRNA Expression in the Parkinson's Disease Substantia Nigra," *Exp. Neurol.*, vol. 166, no. 1, pp. 127–135, Nov. 2000.

[78]   C. Zuccato, M. Marullo, P. Conforti, M. E. MacDonald, M. Tartari, and E. Cattaneo, "Systematic Assessment of BDNF and Its Receptor Levels in Human Cortices Affected by Huntington's Disease," *Brain Pathol.*, vol. 18, no. 2, pp. 225–238, Dec. 2007.

[79]   T. Nishio, N. Sunohara, and S. Furukawa, "Neutrophin switching in spinal motoneurons of amyotrophic lateral sclerosis.," *Neuroreport*, vol. 9, no. 7, pp. 1661–5, May 1998.

[80]   Y. He, X. Zhang, and W. Yung, "Role of BDNF in Central Motor Structures and Motor Diseases," 2013.

[81]   T. Tsukahara, M. Takeda, S. Shimohama, O. Ohara, and N. Hashimoto, "Effects of brain-derived neurotrophic factor on 1-methyl-4-phenyl-1,2,3,6-tetrahydropyridine-induced parkinsonism in monkeys.," *Neurosurgery*, vol. 37, no. 4, pp. 733-9; discussion 739-41, Oct. 1995.

[82]   T. F. Oo, D. M. Marchionini, O. Yarygina, P. D. O'Leary, R. A. Hughes, N. Kholodilov, and R. E. Burke, "Brain-derived neurotrophic factor regulates early postnatal developmental cell death of dopamine neurons of the substantia nigra in vivo," *Mol. Cell. Neurosci.*, vol. 41, no. 4, pp. 440–447, Jul. 2009.

[83]   N.-P. Lui, L.-W. Chen, W.-H. Yung, Y.-S. Chan, and K. K.-L. Yung, "Endogenous Repair by the Activation of Cell Survival Signalling Cascades

during the Early Stages of Rat Parkinsonism," *PLoS One*, vol. 7, no. 12, p. e51294, Dec. 2012.

[84] S. S. Gill, N. K. Patel, G. R. Hotton, K. O'Sullivan, R. McCarter, M. Bunnage, D. J. Brooks, C. N. Svendsen, and P. Heywood, "Direct brain infusion of glial cell line–derived neurotrophic factor in Parkinson disease," *Nat. Med.*, vol. 9, no. 5, pp. 589–595, May 2003.

[85] K. F. Bruggeman, R. J. Williams, and D. R. Nisbet, "Dynamic and Responsive Growth Factor Delivery from Electrospun and Hydrogel Tissue Engineering Materials," *Adv. Healthc. Mater.*, vol. 1700836, p. 1700836, 2017.

[86] J. Milbrandt, F. J. De Sauvage, T. J. Fahrner, R. H. Baloh, M. L. Leitner, M. G. Tansey, P. A. Lampe, R. O. Heuckeroth, P. T. Kotzbauer, and K. S. Simburger, "Persephin, a Novel Neurotrophic Factor Related to GDNF and Neurturin ventral midbrain dopaminergic neurons in vitro (Lin et al," *Neuron*, vol. 20, pp. 245–253, 1998.

[87] B. A. Horger, M. C. Nishimura, M. P. Armanini, L. C. Wang, K. T. Poulsen, C. Rosenblad, D. Kirik, B. Moffat, L. Simmons, E. Johnson, J. Milbrandt, A. Rosenthal, A. Bjorklund, R. A. Vandlen, M. A. Hynes, and H. S. Phillips, "Neurturin exerts potent actions on survival and function of midbrain dopaminergic neurons.," *J. Neurosci.*, vol. 18, no. 13, pp. 4929–37, Jul. 1998.

[88] A. Planken, *Role of Gdnf and Its Cross-Talk With Other Growth Factors in the Dopaminergic System*. 2012.

[89] M. M. Bespalov and M. Saarma, "GDNF family receptor complexes are emerging drug targets," *Trends Pharmacol. Sci.*, vol. 28, no. 2, pp. 68–74, 2007.

[90] R. H. Baloh, M. G. Tansey, P. A. Lampe, T. J. Fahrner, H. Enomoto, K. S. Simburger, M. L. Leitner, T. Araki, E. M. Johnson, and J. Milbrandt, "Artemin, a Novel Member of the GDNF Ligand Family, Supports Peripheral and Central Neurons and Signals through the GFRα3–RET Receptor Complex," *Neuron*, vol. 21, no. 6, pp. 1291–1302, Dec. 1998.

[91] L. R. Gardell, R. Wang, C. Ehrenfels, M. H. Ossipov, A. J. Rossomando, S. Miller, C. Buckley, A. K. Cai, A. Tse, S. F. Foley, B. Gong, L. Walus, P. Carmillo, D. Worley, C. Huang, T. Engber, B. Pepinsky, R. L. Cate, T. W. Vanderah, J. Lai, D. W. Y. Sah, and F. Porreca, "Multiple actions of systemic artemin in experimental neuropathy," *Nat. Med.*, vol. 9, no. 11, pp. 1383–1389, Nov. 2003.

[92] N. K. Patel, M. Bunnage, P. Plaha, C. N. Svendsen, P. Heywood, and S. S. Gill, "Intraputamenal infusion of glial cell line-derived neurotrophic factor in PD: A two-year outcome study," *Ann. Neurol.*, vol. 57, no. 2, pp. 298–302, Feb. 2005.

[93] J. T. Slevin, G. a Gerhardt, C. D. Smith, D. M. Gash, R. Kryscio, and B. Young, "Improvement of bilateral motor functions in patients with Parkinson disease through the unilateral intraputaminal infusion of glial cell line-derived neurotrophic factor.," *J. Neurosurg.*, vol. 102, no. 2, pp. 216–22, 2005.

[94] A. Models, "Gene Therapeutic Strategies for Neuroprotection: Implications for Parkinson's Disease," *Cell*, vol. 68, no. 144, pp. 58–68, 1997.

[95] R. D. Price, S. a. Milne, J. Sharkey, and N. Matsuoka, "Advances in small molecules promoting neurotrophic function," *Pharmacol. Ther.*, vol. 115, no. 2, pp. 292–306, 2007.

[96] J. M. Fletcher and R. A. Hughes, "Modified low molecular weight cyclic peptides as mimetics of BDNF with improved potency, proteolytic stability and transmembrane passage in vitro," *Bioorganic Med. Chem.*, vol. 17, no. 7, pp. 2695–2702, 2009.

[97] W. M. Pardridge, Y. S. Kang, and J. L. Buciak, "Transport of Human Recombinant Brain-Derived Neurotrophic Factor (BDNF) Through the Rat Blood−Brain Barrier in Vivo Using Vector-Mediated Peptide Drug Delivery," *Pharmaceutical Research: An Official Journal of the American Association of Pharmaceutical Scientists*, vol. 11, no. 5. pp. 738–746, 1994.

[98] D. P. Ankeny, D. M. McTigue, Z. Guan, Q. Yan, O. Kinstler, B. T. Stokes, and L. B. Jakeman, "Pegylated Brain-Derived Neurotrophic Factor Shows Improved Distribution into the Spinal Cord and Stimulates Locomotor Activity and

Morphological Changes after Injury," *Exp. Neurol.*, vol. 170, no. 1, pp. 85–100, Jul. 2001.

[99] Q. Han, W. Sun, H. Lin, W. Zhao, Y. Gao, Y. Zhao, B. Chen, Z. Xiao, W. Hu, Y. Li, B. Yang, and J. Dai, "Linear Ordered Collagen Scaffolds Loaded with Collagen-Binding Brain-Derived Neurotrophic Factor Improve the Recovery of Spinal Cord Injury in Rats," *Tissue Eng. Part A*, vol. 15, no. 10, pp. 2927–2935, Oct. 2009.

[100] C. Giampà, E. Montagna, C. Dato, M. A. B. Melone, G. Bernardi, and F. R. Fusco, "Systemic Delivery of Recombinant Brain Derived Neurotrophic Factor (BDNF) in the R6/2 Mouse Model of Huntington's Disease," *PLoS One*, vol. 8, no. 5, p. e64037, May 2013.

[101] A. E. Lang, S. Gill, N. K. Patel, A. Lozano, J. G. Nutt, R. Penn, D. J. Brooks, G. Hotton, E. Moro, P. Heywood, M. A. Brodsky, K. Burchiel, P. Kelly, A. Dalvi, B. Scott, M. Stacy, D. Turner, V. G. F. Wooten, W. J. Elias, E. R. Laws, V. Dhawan, A. J. Stoessl, J. Matcham, R. J. Coffey, and M. Traub, "Randomized controlled trial of intraputamenal glial cell line-derived neurotrophic factor infusion in Parkinson disease," *Ann. Neurol.*, vol. 59, no. 3, pp. 459–466, Mar. 2006.

[102] K. F. Bruggeman, A. L. Rodriguez, C. L. Parish, R. J. Williams, and D. R. Nisbet, "Temporally controlled release of multiple growth factors from a self-assembling peptide hydrogel," *Nanotechnology*, vol. 27, no. 38, p. 385102, Sep. 2016.

[103] S.-W. Jang, X. Liu, M. Yepes, K. R. Shepherd, G. W. Miller, Y. Liu, W. D. Wilson, G. Xiao, B. Blanchi, Y. E. Sun, and K. Ye, "A selective TrkB agonist with potent neurotrophic activities by 7,8-dihydroxyflavone," *Proc. Natl. Acad. Sci.*, vol. 107, no. 6, pp. 2687–2692, Feb. 2010.

[104] S. Jang, X. Liu, C. B. Chan, S. A. France, I. Sayeed, W. Tang, X. Lin, R. Andero, Q. Chang, K. J. Ressler, and K. Ye, "Deoxygedunin , a Natural Product with Potent Neurotrophic Activity in Mice," vol. 5, no. 7, 2010.

[105] A. W. English, K. Liu, J. M. Nicolini, A. M. Mulligan, and K. Ye, "Small-

molecule trkB agonists promote axon regeneration in cut peripheral nerves," *Proc. Natl. Acad. Sci.*, vol. 110, no. 40, pp. 16217–16222, 2013.

[106] S. Nie, Y. Xu, G. Chen, K. Ma, C. Han, Z. Guo, Z. Zhang, K. Ye, and X. Cao, "Small molecule TrkB agonist deoxygedunin protects nigrostriatal dopaminergic neurons from 6-OHDA and MPTP induced neurotoxicity in rodents," *Neuropharmacology*, vol. 99, pp. 448–458, 2015.

[107] N. A. Castello, M. H. Nguyen, J. D. Tran, D. Cheng, K. N. Green, and F. M. LaFerla, "7,8-dihydroxyflavone, a small molecule TrkB agonist, improves spatial memory and increases thin spine density in a mouse model of alzheimer disease-like neuronal loss," *PLoS One*, vol. 9, no. 3, pp. 17–19, 2014.

[108] E. Bollen, T. Vanmierlo, S. Akkerman, C. Wouters, H. M. W. Steinbusch, and J. Prickaerts, "7,8-Dihydroxyflavone improves memory consolidation processes in rats and mice," *Behav. Brain Res.*, vol. 257, pp. 8–12, 2013.

[109] C. Chen, X.-H. Li, S. Zhang, Y. Tu, Y.-M. Wang, and H.-T. Sun, "7,8-dihydroxyflavone ameliorates scopolamine-induced Alzheimer-like pathologic dysfunction.," *Rejuvenation Res.*, vol. 17, no. 3, pp. 249–54, 2014.

[110] L. Devi and M. Ohno, "7,8-Dihydroxyflavone, a Small-Molecule TrkB Agonist, Reverses Memory Deficits and BACE1 Elevation in a Mouse Model of Alzheimer's Disease," *Neuropsychopharmacology*, vol. 37, no. 2, pp. 434–444, 2012.

[111] R. Andero, N. Daviu, R. M. Escorihuela, R. Nadal, and A. Armario, "7,8-dihydroxyflavone, a TrkB receptor agonist, blocks long-term spatial memory impairment caused by immobilization stress in rats," *Hippocampus*, vol. 22, no. 3, pp. 399–408, 2012.

[112] O. T. Korkmaz, N. Aytan, I. Carreras, J.-K. Choi, N. W. Kowall, B. G. Jenkins, and A. Dedeoglu, "7,8-Dihydroxyflavone improves motor performance and enhances lower motor neuronal survival in a mouse model of amyotrophic lateral sclerosis.," *Neurosci. Lett.*, vol. 566, pp. 286–91, 2014.

[113] A. K. Apawu, F. K. Maina, J. R. Taylor, and T. a. Mathews, "Probing the ability of presynaptic tyrosine kinase receptors to regulate striatal dopamine dynamics," *ACS Chem. Neurosci.*, vol. 4, no. 5, pp. 895–904, 2013.

[114] R. a. Johnson, M. Lam, a. M. Punzo, H. Li, B. R. Lin, K. Ye, G. S. Mitchell, and Q. Chang, "7,8-dihydroxyflavone exhibits therapeutic efficacy in a mouse model of Rett syndrome," *J. Appl. Physiol.*, vol. 112, no. 5, pp. 704–710, 2012.

[115] X. Liu, C. Chan, S. Jang, S. Pradoldej, J. Huang, K. He, and L. H. Phun, "A Synthetic 7 , 8-Dihydroxyflavone Derivative Promotes Neurogenesis and Exhibits Potent Antidepressant Effect," pp. 8274–8286, 2010.

[116] M. Jiang, Q. Peng, X. Liu, J. Jin, Z. Hou, J. Zhang, S. Mori, C. A. Ross, K. Ye, and W. Duan, "Small-molecule TrKB receptor agonists improve motor function and extend survival in a mouse model of huntington's disease," *Hum. Mol. Genet.*, vol. 22, no. 12, pp. 2462–2470, 2013.

[117] C. Liu, C. B. Chan, and K. Ye, "7,8-dihydroxyflavone, a small molecular TrkB agonist, is useful for treating various BDNF-implicated human disorders," *Transl. Neurodegener.*, vol. 5, no. 1, p. 2, Dec. 2016.

[118] X. Liu, Q. Qi, G. Xiao, J. Li, H. R. Luo, and K. Ye, "O-Methylated Metabolite of 7,8-Dihydroxyflavone Activates TrkB Receptor and Displays Antidepressant Activity," *Pharmacology*, vol. 91, no. 3–4, pp. 185–200, 2013.

[119] J. M. Fletcher, C. J. Morton, R. A. Zwar, S. S. Murray, P. D. O'Leary, and R. A. Hughes, "Design of a Conformationally Defined and Proteolytically Stable Circular Mimetic of Brain-derived Neurotrophic Factor," *J. Biol. Chem.*, vol. 283, no. 48, pp. 33375–33383, Nov. 2008.

[120] A. J. Zhang, S. Khare, K. Gokulan, D. S. Linthicum, and K. Burgess, "Dimeric β-turn peptidomimetics as ligands for the neurotrophin receptor TrkC," *Bioorg. Med. Chem. Lett.*, vol. 11, no. 2, pp. 207–210, Jan. 2001.

[121] A. W. Wong, L. Giuffrida, R. Wood, H. Peckham, D. Gonsalvez, S. S. Murray, R. A. Hughes, and J. Xiao, "TDP6, a brain-derived neurotrophic factor-based

trkB peptide mimetic, promotes oligodendrocyte myelination," *Mol. Cell. Neurosci.*, vol. 63, pp. 132–140, Nov. 2014.

[122] P. D. O'Leary and R. a. Hughes, "Design of Potent Peptide Mimetics of Brain-derived Neurotrophic Factor," *J. Biol. Chem.*, vol. 278, no. 28, pp. 25738–25744, Jul. 2003.

[123] M. D. C. Cardenas-Aguayo, S. F. Kazim, I. Grundke-Iqbal, and K. Iqbal, "Neurogenic and Neurotrophic Effects of BDNF Peptides in Mouse Hippocampal Primary Neuronal Cell Cultures," *PLoS One*, vol. 8, no. 1, p. e53596, 2013.

[124] G. Williams, E.-J. Williams, P. Maison, M. N. Pangalos, F. S. Walsh, and P. Doherty, "Overcoming the Inhibitors of Myelin with a Novel Neurotrophin Strategy," *J. Biol. Chem.*, vol. 280, no. 7, pp. 5862–5869, Feb. 2005.

[125] D. Todd, I. Gowers, S. J. Dowler, M. D. Wall, G. McAllister, D. F. Fischer, S. Dijkstra, S. A. Fratantoni, R. van de Bospoort, J. Veenman-Koepke, G. Flynn, J. Arjomand, C. Dominguez, I. Munoz-Sanjuan, J. Wityak, and J. A. Bard, "A Monoclonal Antibody TrkB Receptor Agonist as a Potential Therapeutic for Huntington's Disease," *PLoS One*, vol. 9, no. 2, p. e87923, Feb. 2014.

[126] M. Kajiya, K. Takeshita, M. Kittaka, S. Matsuda, K. Ouhara, K. Takeda, T. Takata, M. Kitagawa, T. Fujita, H. Shiba, and H. Kurihara, "BDNF mimetic compound LM22A-4 regulates cementoblast differentiation via the TrkB-ERK/Akt signaling cascade," *Int. Immunopharmacol.*, vol. 19, no. 2, pp. 245–252, 2014.

[127] J. Han, J. Pollak, T. Yang, M. R. Siddiqui, K. P. Doyle, K. Taravosh-Lahn, E. Cekanaviciute, A. Han, J. Z. Goodman, B. Jones, D. Jing, S. M. Massa, F. M. Longo, and M. S. Buckwalter, "Delayed administration of a small molecule tropomyosin-related kinase B ligand promotes recovery after hypoxic-ischemic stroke," *Stroke*, vol. 43, no. 7, pp. 1918–1924, Jul. 2012.

[128] D. A. Schmid, T. Yang, M. Ogier, I. Adams, Y. Mirakhur, Q. Wang, S. M. Massa, F. M. Longo, and D. M. Katz, "A TrkB Small Molecule Partial Agonist

Rescues TrkB Phosphorylation Deficits and Improves Respiratory Function in a Mouse Model of Rett Syndrome," *J. Neurosci.*, vol. 32, no. 5, pp. 1803–1810, Feb. 2012.

[129] M. Kron, M. Lang, I. T. Adams, M. Sceniak, F. Longo, and D. M. Katz, "A BDNF loop-domain mimetic acutely reverses spontaneous apneas and respiratory abnormalities during behavioral arousal in a mouse model of Rett syndrome," *Dis. Model. Mech.*, vol. 7, no. 9, pp. 1047–1055, Sep. 2014.

[130] S.-W. Jang, X. Liu, S. Pradoldej, G. Tosini, Q. Chang, P. M. Iuvone, and K. Ye, "N-acetylserotonin activates TrkB receptor in a circadian rhythm," *Proc. Natl. Acad. Sci.*, vol. 107, no. 8, pp. 3876–3881, Feb. 2010.

[131] S. Jang, X. Liu, C.-B. Chan, D. Weinshenker, R. A. Hall, G. Xiao, and K. Ye, "The Antidepressant Amitriptyline is a TrkA and TrkB Receptor Agonist that Promotes TrkA/TrkB Heterodimerization and Has Potent Neurotrophic Activity," *Chem. Biol.*, vol. 16, no. 6, pp. 644–656, Jun. 2009.

[132] J. Xu, M. H. Lacoske, and E. a. Theodorakis, "Neurotrophic Natural Products: Chemistry and Biology," *Angew. Chemie - Int. Ed.*, vol. 53, no. 4, pp. 956–987, 2014.

[133] S. M. Massa, T. Yang, Y. Xie, J. Shi, M. Bilgen, J. N. Joyce, D. Nehama, J. Rajadas, and F. M. Longo, "Small molecule BDNF mimetics activate TrkB signaling and prevent neuronal degeneration in rodents," *J. Clin. Invest.*, vol. 120, no. 5, pp. 1774–1785, May 2010.

[134] D. A. Simmons, N. P. Belichenko, T. Yang, C. Condon, M. Monbureau, M. Shamloo, D. Jing, S. M. Massa, and F. M. Longo, "A Small Molecule TrkB Ligand Reduces Motor Impairment and Neuropathology in R6/2 and BACHD Mouse Models of Huntington's Disease," *J. Neurosci.*, vol. 33, no. 48, pp. 18712–18727, Nov. 2013.

[135] T. Rantamäki, L. Vesa, H. Antila, A. Di Lieto, P. Tammela, A. Schmitt, K.-P. Lesch, M. Rios, and E. Castrén, "Antidepressant Drugs Transactivate TrkB Neurotrophin Receptors in the Adult Rodent Brain Independently of BDNF

and Monoamine Transporter Blockade," *PLoS One*, vol. 6, no. 6, p. e20567, Jun. 2011.

[136] P. M. Iuvone, J. H. Boatright, G. Tosini, and K. Ye, "N-Acetylserotonin: Circadian Activation of the BDNF Receptor and Neuroprotection in the Retina and Brain," 2014, pp. 765–771.

[137] A. Choudhury, S. Singh, G. Palit, S. Shukla, and S. Ganguly, "Administration of N-acetylserotonin and melatonin alleviate chronic ketamine-induced behavioural phenotype accompanying BDNF-independent and dependent converging cytoprotective mechanisms in the hippocampus," *Behav. Brain Res.*, vol. 297, pp. 204–212, Jan. 2016.

[138] P. D. O'Leary and R. A. Hughes, "Structure-Activity Relationships of Conformationally Constrained Peptide Analogues of Loop 2 of Brain-Derived Neurotrophic Factor," *J. Neurochem.*, vol. 70, no. 4, pp. 1712–1721, Nov. 1998.

[139] J. Xiao, R. A. Hughes, J. Y. Lim, A. W. Wong, J. J. Ivanusic, A. H. Ferner, T. J. Kilpatrick, and S. S. Murray, "A small peptide mimetic of brain-derived neurotrophic factor promotes peripheral myelination," *J. Neurochem.*, vol. 125, no. 3, pp. 386–398, May 2013.

[140] U. Boltaev, Y. Meyer, F. Tolibzoda, T. Jacques, M. Gassaway, Q. Xu, F. Wagner, Y. Zhang, M. Palmer, E. Holson, and D. Sames, "Multiplex quantitative assays indicate a need for re-evaluating reported small-molecule TrkB agonists," *Sci. Signal.*, vol. 10, no. 493, p. eaal1670, Aug. 2017.

[141] J. T. S. Pettikiriarachchi, C. L. Parish, M. S. Shoichet, J. S. Forsythe, and D. R. Nisbet, "Biomaterials for Brain Tissue Engineering," *Aust. J. Chem.*, vol. 63, no. 8, p. 1143, 2010.

[142] F. J. O'Brien, "Biomaterials & scaffolds for tissue engineering," *Mater. Today*, vol. 14, no. 3, pp. 88–95, Mar. 2011.

[143] F. Rosso, A. Giordano, M. Barbarisi, and A. Barbarisi, "From Cell-ECM interactions to tissue engineering," *J. Cell. Physiol.*, vol. 199, no. 2, pp. 174–180,

May 2004.

[144] M. Martins-Green and M. J. Bissell, "Cell-ECM interactions in development," *Semin. Dev. Biol.*, vol. 6, no. 2, pp. 149–159, Apr. 1995.

[145] J. Barthes, H. Özçelik, M. Hindié, A. Ndreu-Halili, A. Hasan, and N. E. Vrana, "Cell Microenvironment Engineering and Monitoring for Tissue Engineering and Regenerative Medicine: The Recent Advances," *Biomed Res. Int.*, vol. 2014, no. i, pp. 1–18, 2014.

[146] R. G. Wylie, S. Ahsan, Y. Aizawa, K. L. Maxwell, C. M. Morshead, and M. S. Shoichet, "Spatially controlled simultaneous patterning of multiple growth factors in three-dimensional hydrogels," *Nat. Mater.*, vol. 10, no. 10, pp. 799–806, 2011.

[147] Y. N. Wu, F. Li, Y. Wu, W. Jia, P. Hannam, J. Qiao, and G. Li, "Formation of silica nanofibers with hierarchical structure via electrospinning," *Colloid Polym. Sci.*, vol. 289, no. 11, pp. 1253–1260, 2011.

[148] T. Pirzada, S. a Arvidson, C. D. Saquing, S. S. Shah, and S. a Khan, "Hybrid Silica − PVA Nanofibers via Sol − Gel Electrospinning," 2012.

[149] Q. P. Pham, U. Sharma, and A. G. Mikos, "Electrospinning of polymeric nanofibers for tissue engineering applications: a review.," *Tissue Eng.*, vol. 12, no. 5, pp. 1197–1211, 2006.

[150] J. Guo, H. Su, and Y. Zeng, "Reknitting the injured spinal cord by self-assembling peptide nanofiber scaffold," vol. 3, pp. 311–321, 2007.

[151] M. Reches and E. Gazit, "Molecular self-assembly of peptide nanostructures: mechanism of   association and potential uses," pp. 105–111, 2006.

[152] H. Cui, T. Muraoka, A. G. Cheetham, and S. I. Stupp, "Self-assembly of giant peptide nanobelts," *Nano Lett.*, vol. 9, no. 3, pp. 945–951, 2009.

[153] J. D. Hartgerink, E. Beniash, and S. I. Stupp, "Peptide-amphiphile nanofibers: A versatile scaffold for the preparation of self-assembling materials," *Proc. Natl.*

Acad. Sci., vol. 99, no. 8, pp. 5133–5138, Apr. 2002.

[154] J. Wang, K. Liu, R. Xing, X. Yan, N. D. Tsihlis, W. Jiang, Q. Jiang, J. M. Vercammen, V. S. Prakash, T. A. Pritts, S. I. Stupp, M. R. Kibbe, L. J. W. Shimon, F. Patolsky, and E. Gazit, "Peptide self-assembly: thermodynamics and kinetics," *Chem. Soc. Rev.*, vol. 45, no. 20, pp. 5589–5604, Oct. 2016.

[155] T. J. Moyer, H. Cui, and S. I. Stupp, "Tuning nanostructure dimensions with supramolecular twisting," *J. Phys. Chem. B*, vol. 117, no. 16, pp. 4604–4610, 2013.

[156] N. Stephanopoulos, J. H. Ortony, and S. I. Stupp, "Self-assembly for the synthesis of functional biomaterials," *Acta Mater.*, vol. 61, no. 3, pp. 912–930, 2013.

[157] S. Fleming and R. V Ulijn, "Design of nanostructures based on aromatic peptide amphiphiles.," *Chem Soc Rev*, vol. 8150, no. 43, pp. 8150–8177, 2014.

[158] S. Fleming, S. Debnath, P. W. J. M. Frederix, T. Tuttle, and R. V Ulijn, "Aromatic peptide amphiphiles: significance of the Fmoc moiety.," *Chem. Commun. {(Camb.)}*, vol. 49, no. 90, pp. 10587–10589, 2013.

[159] J. W. Sadownik, J. Leckie, and R. V Ulijn, "Micelle to fibre biocatalytic supramolecular transformation of an aromatic peptide amphiphilewz," *Chem. Commun*, vol. 47, pp. 728–730, 2011.

[160] S. Zhang, T. C. Holmes, C. M. DiPersio, R. O. Hynes, X. Su, and A. Rich, "Self-complementary oligopeptide matrices support mammalian cell attachment," *Biomaterials*, vol. 16, no. 18, pp. 1385–1393, 1995.

[161] T. C. Holmes, S. de Lacalle, X. Su, G. Liu, a Rich, and S. Zhang, "Extensive neurite outgrowth and active synapse formation on self-assembling peptide scaffolds.," *Proc. Natl. Acad. Sci. U. S. A.*, vol. 97, no. 12, pp. 6728–6733, 2000.

[162] M. Bibian, J. Mangelschots, J. Gardiner, L. Waddington, M. M. Diaz Acevedo, B. G. De Geest, B. Van Mele, A. Madder, R. Hoogenboom, and S. Ballet, "Rational design of a hexapeptide hydrogelator for controlled-release drug delivery," *J. Mater. Chem. B*, vol. 3, no. 5, pp. 759–765, 2015.

[163] B. Adhikari and A. Banerjee, "Short peptide based hydrogels: incorporation of graphene into the hydrogel," *Soft Matter*, vol. 7, no. 19, p. 9259, 2011.

[164] E. R. Draper, K. L. Morris, M. A. Little, J. Raeburn, C. Colquhoun, E. R. Cross, T. O. McDonald, L. C. Serpell, and D. J. Adams, "Hydrogels formed from Fmoc amino acids," *CrystEngComm*, vol. 17, no. 42, pp. 8047–8057, 2015.

[165] G. Liang, Z. Yang, R. Zhang, L. Li, Y. Fan, Y. Kuang, Y. Gao, T. Wang, W. W. Lu, and B. Xu, "Supramolecular Hydrogel of a D-Amino Acid Dipeptide for Controlled Drug Release in Vivo," *Langmuir*, vol. 25, no. 15, pp. 8419–8422, Aug. 2009.

[166] T. Li, M. Kalloudis, A. Z. Cardoso, D. J. Adams, and P. S. Clegg, "Drop-Casting Hydrogels at a Liquid Interface: The Case of Hydrophobic Dipeptides."

[167] L. Chen, K. Morris, A. Laybourn, D. Elias, M. R. Hicks, A. Rodger, L. Serpell, and D. J. Adams, "Self-Assembly Mechanism for a Naphthalene−Dipeptide Leading to Hydrogelation," *Langmuir*, vol. 26, no. 7, pp. 5232–5242, Apr. 2010.

[168] F. Moradi, M. Bahktiari, M. T. Joghataei, M. Nobakht, M. Soleimani, G. Hasanzadeh, A. Fallah, S. Zarbakhsh, L. B. Hejazian, M. Shirmohammadi, and F. Maleki, "BD PuraMatrix peptide hydrogel as a culture system for human fetal Schwann cells in spinal cord regeneration," *J. Neurosci. Res.*, vol. 90, no. 12, pp. 2335–2348, Dec. 2012.

[169] J. Mangelschots, M. Bibian, J. Gardiner, L. Waddington, Y. Van Wanseele, A. Van Eeckhaut, M. M. D. Acevedo, B. Van Mele, A. Madder, R. Hoogenboom, and S. Ballet, "Mixed α/β-Peptides as a Class of Short Amphipathic Peptide Hydrogelators with Enhanced Proteolytic Stability," *Biomacromolecules*, vol. 17, no. 2, pp. 437–445, Feb. 2016.

[170] K. Kulkarni, S. Motamed, N. Habila, P. Perlmutter, J. S. Forsythe, M.-I. Aguilar, and M. P. Del Borgo, "Orthogonal strategy for the synthesis of dual-functionalised β 3 -peptide based hydrogels," *Chem. Commun.*, vol. 52, no. 34, pp. 5844–5847, 2016.

[171] G. Yu, X. Yan, C. Han, and F. Huang, "Characterization of supramolecular gels," *Chem. Soc. Rev.*, vol. 42, no. 16, p. 6697, 2013.

[172] C. Martin, E. Oyen, Y. Van Wanseele, T. Ben Haddou, H. Schmidhammer, J. Andrade, L. Waddington, A. Van Eeckhaut, B. Van Mele, J. Gardiner, R. Hoogenboom, A. Madder, M. Spetea, and S. Ballet, "Injectable peptide-based hydrogel formulations for the extended in vivo release of opioids," *Mater. Today Chem.*, vol. 3, pp. 49–59, 2017.

[173] S. Marchesan, Y. Qu, L. J. Waddington, C. D. Easton, V. Glattauer, T. J. Lithgow, K. M. McLean, J. S. Forsythe, and P. G. Hartley, "Self-assembly of ciprofloxacin and a tripeptide into an antimicrobial nanostructured hydrogel," *Biomaterials*, vol. 34, no. 14, pp. 3678–3687, 2013.

[174] D. J. Adams, L. M. Mullen, M. Berta, L. Chen, and W. J. Frith, "Relationship between molecular structure, gelation behaviour and gel properties of Fmoc-dipeptides," *Soft Matter*, vol. 6, no. 9, p. 1971, 2010.

[175] Y. Loo, S. Zhang, and C. A. E. Hauser, "From short peptides to nanofibers to macromolecular assemblies in biomedicine," *Biotechnol. Adv.*, vol. 30, no. 3, pp. 593–603, May 2012.

[176] C. Martin, E. Oyen, J. Mangelschots, M. Bibian, T. Ben Haddou, J. Andrade, J. Gardiner, B. Van Mele, A. Madder, R. Hoogenboom, M. Spetea, and S. Ballet, "Injectable peptide hydrogels for controlled-release of opioids," *Med. Chem. Commun.*, vol. 7, no. 3, pp. 542–549, 2016.

[177] R. Vegners, I. Shestakova, I. Kalvinsh, R. M. Ezzell, and P. A. Janmey, "Use of a gel-forming dipeptide derivative as a carrier for antigen presentation," *J. Pept. Sci.*, vol. 1, no. 6, pp. 371–378, 1995.

[178] V. Jayawarna, M. Ali, T. a. Jowitt, A. F. Miller, A. Saiani, J. E. Gough, and R. V. Ulijn, "Nanostructured hydrogels for three-dimensional cell culture through self-assembly of fluorenylmethoxycarbonyl-dipeptides," *Adv. Mater.*, vol. 18, no. 5, pp. 611–614, Mar. 2006.

[179] V. Jayawarna, S. M. Richardson, A. R. Hirst, N. W. Hodson, A. Saiani, J. E. Gough, and R. V. Ulijn, "Introducing chemical functionality in Fmoc-peptide gels for cell culture," *Acta Biomater.*, vol. 5, no. 3, pp. 934–943, 2009.

[180] M. Zhou, A. M. Smith, A. K. Das, N. W. Hodson, R. F. Collins, R. V. Ulijn, and J. E. Gough, "Self-assembled peptide-based hydrogels as scaffolds for anchorage-dependent cells," *Biomaterials*, vol. 30, no. 13, pp. 2523–2530, 2009.

[181] A. Mahler, M. Reches, M. Rechter, S. Cohen, and E. Gazit, "Rigid, self-assembled hydrogel composed of a modified aromatic dipeptide," *Adv. Mater.*, vol. 18, no. 11, pp. 1365–1370, 2006.

[182] R. Orbach, L. Adler-Abramovich, S. Zigerson, I. Mironi-Harpaz, D. Seliktar, and E. Gazit, "Self-assembled Fmoc-peptides as a platform for the formation of nanostructures and hydrogels," *Biomacromolecules*, vol. 10, no. 9, pp. 2646–2651, 2009.

[183] T. Liebmann, S. Rydholm, V. Akpe, and H. Brismar, "Self-assembling Fmoc dipeptide hydrogel for in situ 3D cell culturing," *BMC Biotechnol.*, vol. 7, no. 1, p. 88, 2007.

[184] S. Sutton, N. L. Campbell, A. I. Cooper, M. Kirkland, W. J. Frith, and D. J. Adams, "Controlled Release from Modified Amino Acid Hydrogels Governed by Molecular Size or Network Dynamics," *Langmuir*, vol. 25, no. 17, pp. 10285–10291, Sep. 2009.

[185] A. L. Rodriguez, T. Y. Wang, K. F. Bruggeman, C. C. Horgan, R. Li, R. J. Williams, C. L. Parish, and D. R. Nisbet, "In vivo assessment of grafted cortical neural progenitor cells and host response to functionalized self-assembling peptide hydrogels and the implications for tissue repair," *J. Mater. Chem. B*, vol. 2, no. 44, pp. 7771–7778, 2014.

[186] V. N. Modepalli, A. L. Rodriguez, R. Li, S. Pavuluri, K. R. Nicholas, C. J. Barrow, D. R. Nisbet, and R. J. Williams, "In vitro response to functionalized self-assembled peptide scaffolds for three-dimensional cell culture," *Biopolymers*, vol. 102, no. 2, pp. 197–205, Mar. 2014.

[187] A. L. Rodriguez, C. L. Parish, D. R. Nisbet, and R. J. Williams, "Tuning the amino acid sequence of minimalist peptides to present biological signals via charge neutralised self assembly," *Soft Matter*, vol. 9, no. 15, p. 3915, 2013.

[188] F. A. Somaa, T.-Y. Wang, J. C. Niclis, K. F. Bruggeman, J. A. Kauhausen, H. Guo, S. McDougall, R. J. Williams, D. R. Nisbet, L. H. Thompson, and C. L. Parish, "Peptide-Based Scaffolds Support Human Cortical Progenitor Graft Integration to Reduce Atrophy and Promote Functional Repair in a Model of Stroke," *Cell Rep.*, vol. 20, no. 8, pp. 1964–1977, Aug. 2017.

[189] M. Hughes, P. W. J. M. Frederix, J. Raeburn, L. S. Birchall, J. Sadownik, F. C. Coomer, I.-H. Lin, E. J. Cussen, N. T. Hunt, T. Tuttle, S. J. Webb, D. J. Adams, and R. V. Ulijn, "Sequence/structure relationships in aromatic dipeptide hydrogels formed under thermodynamic control by enzyme-assisted self-assembly," *Soft Matter*, vol. 8, no. 20, p. 5595, 2012.

[190] D. Zanuy, J. Poater, M. Solà, I. Hamley, and C. Aleman, "Fmoc-RGDS based fibrils: Atomistic details of their hierarchical assembly," *Phys. Chem. Chem. Phys.*, pp. 1265–1278, 2015.

[191] Z. Yang, H. Gu, D. Fu, P. Gao, J. K. Lam, and B. Xu, "Enzymatic Formation of Supramolecular Hydrogels," *Adv. Mater.*, vol. 16, no. 16, pp. 1440–1444, Aug. 2004.

[192] M. Hughes, S. Debnath, C. W. Knapp, and R. V. Ulijn, "Antimicrobial properties of enzymatically triggered self-assembling aromatic peptide amphiphiles," *Biomater. Sci.*, vol. 1, no. 11, p. 1138, 2013.

[193] W. Wang, Z. Yang, S. Patanavanich, B. Xu, and Y. Chau, "Controlling self-assembly within nanospace for peptide nanoparticle fabrication," *Soft Matter*, vol. 4, no. 8, p. 1617, 2008.

[194] D. J. Adams, M. F. Butler, W. J. Frith, M. Kirkland, L. Mullen, and P. Sanderson, "A new method for maintaining homogeneity during liquid–hydrogel transitions using low molecular weight hydrogelators," *Soft Matter*, vol. 5, no. 9, p. 1856, 2009.

[195] A. Z. Cardoso, A. E. Alvarez Alvarez, B. N. Cattoz, P. C. Griffiths, S. M. King, W. J. Frith, D. J. Adams, D. J. Adams, S. M. King, A. Paul, S. Furzeland, D. Atkins, and D. J. Adams, "The influence of the kinetics of self-assembly on the properties of dipeptide hydrogels," *Faraday Discuss.*, vol. 166, no. 0, p. 101, 2013.

[196] R. Li, C. C. Horgan, B. Long, A. L. Rodriguez, L. Mather, C. J. Barrow, D. R. Nisbet, and R. J. Williams, "Tuning the mechanical and morphological properties of self-assembled peptide hydrogels via control over the gelation mechanism through regulation of ionic strength and the rate of pH change," *RSC Adv.*, vol. 5, no. 1, pp. 301–307, 2015.

[197] H.-G. Braun and A. Z. Cardoso, "Self-assembly of Fmoc-diphenylalanine inside liquid marbles," *Colloids Surfaces B Biointerfaces*, vol. 97, pp. 43–50, 2012.

[198] S. Debnath, A. Shome, D. Das, and P. K. Das, "Hydrogelation through self-assembly of fmoc-peptide functionalized cationic amphiphiles: Potent antibacterial agent," *J. Phys. Chem. B*, vol. 114, no. 13, pp. 4407–4415, 2010.

[199] G. M. Kavanagh and S. B. Ross-Murphy, "Rheological characterisation of polymer gels," *Prog. Polym. Sci.*, vol. 23, no. 3, pp. 533–562, Jan. 1998.

[200] J. M. Zuidema, C. J. Rivet, R. J. Gilbert, and F. A. Morrison, "A protocol for rheological characterization of hydrogels for tissue engineering strategies," *J. Biomed. Mater. Res. - Part B Appl. Biomater.*, vol. 102, no. 5, pp. 1063–1073, 2014.

[201] S. Sathaye, A. Mbi, C. Sonmez, Y. Chen, D. L. Blair, J. P. Schneider, and D. J. Pochan, "Rheology of peptide- and protein-based physical hydrogels: Are everyday measurements just scratching the surface?," *Wiley Interdiscip. Rev. Nanomedicine Nanobiotechnology*, vol. 7, no. 1, pp. 34–68, 2015.

[202] E. Beniash, J. D. Hartgerink, H. Storrie, J. C. Stendahl, and S. I. Stupp, "Self-assembling peptide amphiphile nanofiber matrices for cell entrapment," *Acta Biomater.*, vol. 1, no. 4, pp. 387–397, 2005.

[203] A. M. Smith, R. J. Williams, C. Tang, P. Coppo, R. F. Collins, M. L. Turner, A.

Saiani, and R. V. Ulijn, "Fmoc-Diphenylalanine Self Assembles to a Hydrogel via a Novel Architecture Based on π–π Interlocked β-Sheets," *Adv. Mater.*, vol. 20, no. 1, pp. 37–41, Jan. 2008.

[204] R. Li, S. Pavuluri, K. Bruggeman, B. M. Long, A. J. Parnell, A. Martel, S. R. Parnell, F. M. Pfeffer, A. J. C. Dennison, K. R. Nicholas, C. J. Barrow, D. R. Nisbet, and R. J. Williams, "Coassembled nanostructured bioscaffold reduces the expression of proinflammatory cytokines to induce apoptosis in epithelial cancer cells," *Nanomedicine Nanotechnology, Biol. Med.*, vol. 12, no. 5, pp. 1397–1407, Jul. 2016.

[205] K. Tao, A. Levin, L. Adler-Abramovich, E. Gazit, J. K. Lam, B. Xu, D. S. Waugh, Z. Y. Zhang, T. R. Burke, C. Ko, M. R. Ghadiri, A. L. Rogach, P. Zhang, S. Link, P. Král, and N. A. Kotov, "Fmoc-modified amino acids and short peptides: simple bio-inspired building blocks for the fabrication of functional materials," *Chem. Soc. Rev.*, vol. 45, no. 14, pp. 3935–3953, 2016.

[206] S. Fleming, P. W. J. M. Frederix, I. Ramos Sasselli, N. T. Hunt, R. V. Ulijn, T. Tuttle, R. Sasselli, N. T. Hunt, and R. V. Ulijn, "Assessing the Utility of Infrared Spectroscopy as a Structural Diagnostic Tool for β-Sheets in Self-Assembling Aromatic Peptide Amphiphiles," *Langmuir*, vol. 29, no. 30, pp. 9510–9515, Jul. 2013.

[207] G. Cheng, V. Castelletto, R. R. Jones, C. J. Connon, and I. W. Hamley, "Hydrogelation of self-assembling RGD-based peptides," *Soft Matter*, vol. 7, no. 4, pp. 1326–1333, 2011.

[208] C. Tang, A. M. Smith, R. F. Collins, R. V Ulijn, and A. Saiani, "Fmoc-Diphenylalanine Self-Assembly Mechanism Induces Apparent p K a Shifts," vol. 25, no. 21, pp. 9447–9453, 2009.

[209] P. W. J. M. Frederix, R. Kania, J. A. Wright, D. A. Lamprou, R. V. Ulijn, C. J. Pickett, and N. T. Hunt, "Encapsulating [FeFe]-hydrogenase model compounds in peptide hydrogels dramatically modifies stability and photochemistry," *Dalt. Trans.*, vol. 41, no. 42, p. 13112, 2012.

[210] Z. Yang and B. Xu, "A simple visual assay based on small molecule hydrogels for detecting inhibitors of enzymes," *Chem. Commun.*, no. 21, p. 2424, 2004.

[211] M. Ma, Y. Kuang, Y. Gao, Y. Zhang, P. Gao, and B. Xu, "Aromatic−Aromatic Interactions Induce the Self-Assembly of Pentapeptidic Derivatives in Water To Form Nanofibers and Supramolecular Hydrogels," *J. Am. Chem. Soc.*, vol. 132, no. 8, pp. 2719–2728, Mar. 2010.

[212] Z. Yang, G. Liang, L. Wang, and B. Xu, "Using a Kinase/Phosphatase Switch to Regulate a Supramolecular Hydrogel and Forming the Supramolecular Hydrogel in Vivo," *J. Am. Chem. Soc.*, vol. 128, no. 10, pp. 3038–3043, Mar. 2006.

[213] V. Castelletto, G. Cheng, B. W. Greenland, I. W. Hamley, and P. J. F. Harris, "Tuning the Self-Assembly of the Bioactive Dipeptide L-Carnosine by Incorporation of a Bulky Aromatic Substituent," *Langmuir*, vol. 27, no. 6, pp. 2980–2988, Mar. 2011.

[214] D. M. Ryan, S. B. Anderson, and B. L. Nilsson, "The influence of side-chain halogenation on the self-assembly and hydrogelation of Fmoc-phenylalanine derivatives," *Soft Matter*, vol. 6, no. 14, p. 3220, 2010.

[215] D. M. Ryan, T. M. Doran, and B. L. Nilsson, "Complementary π–π Interactions Induce Multicomponent Coassembly into Functional Fibrils," *Langmuir*, vol. 27, no. 17, pp. 11145–11156, Sep. 2011.

[216] D. M. Ryan, T. M. Doran, and B. L. Nilsson, "Stabilizing self-assembled Fmoc–F 5 –Phe hydrogels by co-assembly with PEG-functionalized monomers," *Chem. Commun.*, vol. 47, no. 1, pp. 475–477, 2011.

[217] X. Du, J. Zhou, J. Shi, and B. Xu, "Supramolecular Hydrogelators and Hydrogels: From Soft Matter to Molecular Biomaterials," *Chem. Rev.*, vol. 115, no. 24, pp. 13165–13307, Dec. 2015.

[218] R. Orbach, I. Mironi-harpaz, L. Adler-abramovich, E. Mossou, E. P. Mitchell, V. T. Forsyth, E. Gazit, and D. Seliktar, "The Rheological and Structural Properties of Fmoc-Peptide-Based Hydrogels: The Effect of Aromatic Molecular

Architecture on Self- Assembly and Physical Characteristics," 2015.

[219] S. Zhang, T. Holmes, C. Lockshin, and a Rich, "Spontaneous assembly of a self-complementary oligopeptide to form a stable macroscopic membrane.," *Proc. Natl. Acad. Sci. U. S. A.*, vol. 90, no. 8, pp. 3334–3338, 1993.

[220] A. M. McGrath, L. N. Novikova, L. N. Novikov, and M. Wiberg, "BD™ PuraMatrix™ peptide hydrogel seeded with Schwann cells for peripheral nerve regeneration," *Brain Res. Bull.*, vol. 83, no. 5, pp. 207–213, Oct. 2010.

[221] A. Kaneko and Y. Sankai, "Long-term culture of rat hippocampal neurons at low density in serum-free medium: Combination of the sandwich culture technique with the three-dimensional nanofibrous hydrogel PuraMatrix," *PLoS One*, vol. 9, no. 7, 2014.

[222] E. Genové, C. Shen, S. Zhang, and C. E. Semino, "The effect of functionalized self-assembling peptide scaffolds on human aortic endothelial cell function," *Biomaterials*, vol. 26, no. 16, pp. 3341–3351, 2005.

[223] Y. Kumada and S. Zhang, "Significant Type I and Type III Collagen Production from Human Periodontal Ligament Fibroblasts in 3D Peptide Scaffolds without Extra Growth Factors," *PLoS One*, vol. 5, no. 4, p. e10305, Apr. 2010.

[224] S. Koutsopoulos and S. Zhang, "Long-term three-dimensional neural tissue cultures in functionalized self-Assembling peptide hydrogels, Matrigel and Collagen i," *Acta Biomater.*, vol. 9, no. 2, pp. 5162–5169, 2013.

[225] J. H. Collier and P. B. Messersmith, "Enzymatic modification of self-assembled peptide structures with tissue transglutaminase," *Bioconjug. Chem.*, vol. 14, no. 4, pp. 748–755, 2003.

[226] J. P. Jung, A. K. Nagaraj, E. K. Fox, J. S. Rudra, J. M. Devgun, and J. H. Collier, "Co-assembling peptides as defined matrices for endothelial cells," *Biomaterials*, vol. 30, no. 12, pp. 2400–2410, 2009.

[227] S. Boothroyd, A. Saiani, and A. F. Miller, "Controlling network topology and mechanical properties of co-assembling peptide hydrogels," *Biopolymers*, vol.

101, no. 6, pp. 669–680, 2014.

[228] S. Boothroyd, A. Saiani, and A. F. Miller, "Formation of mixed ionic complementary peptide fibrils," *Macromol. Symp.*, vol. 273, no. 1, pp. 139–145, 2008.

[229] F. Stoica, C. Alexander, N. Tirelli, A. F. Miller, and A. Saiani, "Selective synthesis of double temperature-sensitive polymer–peptide conjugatesw," 2008.

[230] Z. Luo, X. Zhao, and S. Zhang, "Self-Organization of a Chiral D-EAK16 Designer Peptide into a 3D Nanofiber Scaffold," *Macromol. Biosci.*, vol. 8, no. 8, pp. 785–791, Aug. 2008.

[231] S. Marchesan, L. Waddington, C. D. Easton, D. a. Winkler, L. Goodall, J. Forsythe, and P. G. Hartley, "Unzipping the role of chirality in nanoscale self-assembly of tripeptide hydrogels," *Nanoscale*, vol. 4, no. 21, p. 6752, 2012.

[232] S. Marchesan, C. D. Easton, F. Kushkaki, L. Waddington, and P. G. Hartley, "Tripeptide self-assembled hydrogels: unexpected twists of chirality," *Chem. Commun.*, vol. 48, no. 16, p. 2195, 2012.

[233] S. Marchesan, L. Waddington, C. D. Easton, F. Kushkaki, K. M. McLean, J. S. Forsythe, and P. G. Hartley, "Tripeptide Self-Assembled Hydrogels: Soft Nanomaterials for Biological Applications," *Bionanoscience*, vol. 3, no. 1, pp. 21–29, 2013.

[234] Z. Luo, X. Zhao, and S. Zhang, "Structural dynamic of a self-assembling peptide d-EAK16 made of only D-amino acids," *PLoS One*, vol. 3, no. 5, 2008.

[235] Z. Luo, S. Wang, and S. Zhang, "Fabrication of self-assembling d-form peptide nanofiber scaffold d-EAK16 for rapid hemostasis," *Biomaterials*, vol. 32, no. 8, pp. 2013–2020, Mar. 2011.

Chapter 2 Materials and Methods

2.1 Methods

2.1.1 Solid phase peptide synthesis

All peptides were synthesized using standard Fmoc solid phase peptide synthesis with HBTU (2-(1H-Benzotriazole-1-yl)-1,1,3,3-tetramethyluronium hexafluorophosphate) activation using chlorotrityl 2-chloride resin for carboxylic acid terminated peptides and rink-amide resin for amidated peptides. Briefly, Fmoc-amino acid deprotection was performed in a sintered funnel, using 20% piperidine in N,N-dimethyl formamide (DMF). Resins were washed three times, for five minutes each. Amino acid activation was performed with 2 equivalents of Fmoc-amino acid, 2 equivalents of HBTU, 2 equivalents of (Hydroxybenzotriazole) HOBt and 4 equivalents N,N-Diisopropylethylamine (DIPEA). Reagents were dissolved in 4ml DMF per gram of resin. Coupling was performed at room temperature for 20 minutes in a sintered funnel with constant mixing via nitrogen bubbling. Final cleavage was carried out using a mixture of trifluroacetic acid (TFA), Triisopropylsilane (TIPS), and water (95:2.5:2.5 ratio). Crude peptides were precipitated from solution using cold ether, then the liquid phase removed, the remaining solid was redissolved acetonitrile/ether and freeze dried overnight. Crude Fmoc-LLY peptides were too hydrophobic to be precipitated in cold ether, thus the majority of TFA was evaporated under nitrogen flow, and the remaining oil was redissolved in a mixture of acetonitrile/water, and then freeze-dried overnight. The freeze-dried product was then purified by reverse-phase high pressure liquid chromatography(HPLC) (Agilent Technologies).

2.1.1 High pressure liquid chromatography

The HPLC was equipped with a preparative gradient pump (1100/1200), preparative C-18 column (Luna, 10 microns, 100 Å, 150 x 21.20 mm, Phenomenex), auto-sampler (G2260), Diode Array detector (G1365D). The gradient used consisted of acetonitrile (AcN) / water with 0.1% TFA. Analytical gradients were performed from 5-95% acetonitrile over 20 minutes.

2.1.2 Fmoc gel preparation using hydrochloric acid

To prepare 1ml of hydrogel, 400uL pH7.4 0.1M phosphate buffer (Sigma) was added to the peptides, followed by 100uL 1M NaOH (Sigma). These are then vortexed until clear. A further 400uL phosphate buffer is added while vortexing. Hydrogels were formed by adding 100uL 1M HCl (Sigma) dropwise while vortexing to achieve a homogeneous hydrogel.

2.1.3 Fmoc gel preparation using carbon dioxide

To prepare 1ml of hydrogel, 450uL pH 7.4 0.1M phosphate buffer (Sigma) was added to the peptide, followed by 100uL 1M NaOH (Sigma). This was vortexed until clear, then a further 450uL PBS was added, and mixed until homogenous. The solution was then pipetted into whatever tube or culture plate it was being used in. This was then placed into a box with a tap connected. A balloon was filled with CO_2 and connected to the tap. The tap was opened and left for 10 min. The high CO_2 content of the air caused formation of carbonic acid in the peptide solution, gradually the pH of the solution decreases, until self-supporting hydrogels have formed.

To ensure physiological pH before seeding, all gels were rinsed with PBS or DMEM before cell experiments are started.

2.1.4 Self-complementary peptide hydrogel preparation

Peptides were dissolved to the desired concentration in PBS (Life Technologies). To homogenise the gels, solutions were heated to 60°C until clear, which redissolved the hydrogel (approximately 5 minutes). Hydrogels form homogenously upon cooling.

2.1.5 Rheology

Rheology was conducted on an Anton Paar Physica MCR 501 rheometer, with the plates heated to 37°C. Gels were prepared as previously described. 150 μL of gel was pipetted onto the bottom plate of the rheometer, using at 25 mm top plate (Chapter 3) or a 15mm plate (Chapter 4 and 5) and a 0.3 mm gap size. Paraffin oil was pipetted carefully around the plate to prevent evaporation of water from the gel. The gelation time and final modulus were measured at a 1 Hz and 0.3% amplitude.

2.1.6 CryoTEM

Gels were prepared as described previously. 4-6 μL was transferred onto copper grids covered in carbon lace (Lacey carbon: ProSci-Tech, Qld, Australia), which had been plasma charged using an Edwards Auto 306 Thermal Evaporator, and sandwiched between filter paper (Whatman 401) for 3-6 seconds. It was then plunged into liquid ethane, and then quickly transferred to liquid nitrogen. Samples were imaged using a Gatan 626 cryoholder (Gatan, Pleasanton, CA, USA) and Tecnai 12 Transmission Electron Microscope (FEI, Eindhoven, The Netherlands) at 120kV with a spot size of 2 in "Low Dose" mode.

2.1.7 Negative staining

Gels were diluted 10-100x in the same buffer used for original preparation of the hydrogel, and pipetted onto a plasma charged copper grid with flat carbon film. Phosphotungstic acid was pipetted onto the grid, wicked away with filter paper (Whatman 401) and reapplied, then wicked and left to dry. The sample was then imaged using a Tecnai 12 Transmission Electron Microscope (FEI, Eindhoven, The Netherlands) at 120kV with a spot size of 2, with a Megaview III CCD camera and AnalySIS camera control software (Olympus).

2.1.8 Tissue culture protocols for L929

L929 fibroblasts were cultured in a 37 °C incubator with 5% CO_2. Culture media was composed of Dulbecco's modified eagle medium(DMEM) with 10% foetal calf serum(FCS), and 1% Penicillin and Streptomycin (Gibco). Media was changed every 2-3 days as needed.

2.1.9 Tissue culture protocols for SN4741

SN4741 cells were maintained at 33°C in a humidity controlled incubator at 5% CO_2. Growth medium consisted of DMEM supplemented with 10% FCS, 1% Glutamax (Gibco) and 1% Penicillin and Streptomycin (Gibco). Media wash changed every 2-3 days as needed, and plates were subcultured at 1:10 to 1:40 depending on requirements.

2.1.10 Tissue culture protocols for SH-SY5Y cells

SH-SY5Y cells were grown in high glucose DMEM containing 10% FCS, 1% Glutamax and 2% Pen/Strep, in a humidity controlled incubator at 37 °C with 5% CO_2. Media was changed every 2-3 days as required. When confluent, cells were subcultured at 1:4-1:10.

2.1.11 Tissue culture protocols for NIH-3T3 cells transfected with TrkB

Cells were maintained at 37°C in a humidity controlled incubator at 5% CO_2. Growth medium consisted of DMEM supplemented with 10% Newborn Calf Serum, 1% Glutamax (Gibco), 1% Penicillin and Streptomycin (Gibco) and 100ug/mL G418 (Gibco) to maintain transgene expression. Media wash changed every 2-3 days as needed, and plates were subcultured at 1:20 each week.

2.1.12 Primary cell culture

Mixed cortical and hippocampal neurons were isolated from embryonic day 14-16 embryos as previously described (Taylor et al., 2005). Breifly … Cultures were treated at 7 days *in vitro* with the Trk inhibitor 120nM GNF5837 for 30 min. This was followed by either fresh media with or without 20ng/mL BDNF, or a thin layer of pre-conditioned hydrogels. Hydrogels were pre-conditioned with growth media.

2.1.13 Preparation of substrates for cell experiments

After forming hydrogels as previously described, they were left between 1 and 24 hours until stable, depending upon gel concentration. Then rinsed twice culture medium to ensure they are at an appropriate pH for cell experiments.

2.1.14 Live/dead cell stain

Media was removed from wells. 100 µl of the staining solution was added to each well, containing 4µM each of Calcein AM and ethidium homodimer-1 (Life Technologies). The plate was then incubated for 20 min at 37 °C and images collected on a Nikon Eclipse Ti-S fluorescent microscope within 1 hour of stain being added. Wells were not rinsed between removal of media and addition of stain to avoid removal of cells.

2.1.15 MTS assay

Cells were grown in 96 well culture plates. Media was aspirated, and wells rinsed once with PBS. 3-(4,5-dimethylthiazol-2-yl)-5-(3-carboxymethoxyphenyl)-2-(4-sulfophenyl)-2H-tetrazolium(MTS) reagent was mixed with serum free DMEM at a 1:5 ratio. PBS was aspirated, and 120uL of the prepared MTS and DMEM was added to each well. The plates were left to incubate at 37°C for at least 2 hours, until the MTS reagent had developed sufficient colour. 100uL of reagent was collected from each well, and transferred to a new plate. Absorbance was measured at 490 nm.

2.1.16 Conditioned media experiments

6 wells in a 96 well plate of hydrogel for each condition were prepared. After stabilising the hydrogel, and rinsing as described previously, 100µl complete culture media was added to all wells, and left overnight in an incubator. At this point, NIH 3T3 cells were seeded into a 96 well plate, at a 6000cells per well. The media on the hydrogels was removed and collected. Serial dilutions of this media were performed, media on the cells was removed and replaced with this conditioned media. After 24 hours, and MTS assay was conducted on all wells.

2.1.17 Mixed cortical and hippocampal neuron isolation

Primary neurons were isolated as previously described[1]. Cells were prepared from C57Bl/6 J embryos (day 14–16) and initially cultured in Neurobasal Media (Gibco-BRL Life Technologies, Ont., Canada) [containing 10% fetal bovine serum] in poly-L-lysine-coated plates and allowed to adhere for 4 h before their media was changed (serum-free media). Half the media was subsequently replaced every 2 days. After 3 days, cultures were treated with 2 µM aArabinoside-C (Ara-C) for 24 h to remove contaminating glial and other proliferative cells.

2.1.18 Primary cell culture treatment and lysis

Cultures were treated at 7 days in vitro with 120 nM GNF5837 for 30 min, followed by either fresh media with or without 20ng/mL BDNF, or a thin layer of the hydrogels, which had been pre-conditioned in growth media. Hydrogels were pre-formed by the relevant method, and equilibrated overnight in PBS, to ensure an appropriate pH for the cells. The gels were then warmed to 37°C. Media was

removed from the cells, and gel transferred on top using a 1mL micropipette. After 30 min, media/hydrogel was removed and wells rinsed with ice cold PBS. Cells were lysed in radioimmunoprecipitation assay (RIPA) buffer, containing phosphatase and protease inhibitors. 100uL of cold buffer was added to each well in a 6 well plate, then samples were scraped and collected into 1.7ml centrifuge tubes. After a total of 15 min exposure to the buffer with everything on ice, tubes were sonicated in a bath for 10 seconds at a time, then returned to ice for 5 minutes a total of 3 times to assist with homogenising the samples. Samples were then stored at -20 degrees until further analysis.

2.1.19 Bradford assay

Cell lysates were thawed on ice. The Bradford protein reagent was diluted 1:5 in MilliQ water, and filtered. Lysates were diluted to 1:50 and 1:100 in MilliQ. Serial dilutions of bovine serum albumin (BSA) were prepared as a standard curve, from 1mg/mL to 0.031mg/mL. 10 µL of each sample or BSA standard was added to a 96 well plate, all in triplicate. 200 µL of the Bradford reagent was added to each well, and left for 5 minutes at room temperature. Using a plate reader, absorbance at 595nm was measured. Triplicate readings were averaged, and a standard curve drawn from the BSA results. Using this, the protein concentration in the lysate samples was calculated.

2.1.20 Western blot

Referring to the Bradford assay results, the amount of protein to be loaded was calculated. Lysates were diluted 1:1 with loading buffer, to a maximum 30µL per well. Lysates were vortex mixed and centrifuged in a benchtop centrifuge, then incubated at 99°C for 5 min. The gel was loaded into the tank, and filled with running buffer. Wells were cleared by aspirating running buffer into them repeatedly. Samples and protein marker (Bio-Rad Precision Plus Protein WesternC Blotting Standard) were carefully pipetted into the wells in the gel. Samples were run at 80V until the dye front was well into the gel, then voltage was increased to 120V, until the dye front reached the end of the gel.

The gel was removed from the slide, loaded into a Bio-Rad Trans-Blot Turbo Transfer System. Transfer was conducted using the 'Turbo' protocol for mini gels. After transfer, the membrane was removed, and blocked with TBS-T (tris buffered saline with tween-20) containing 4% skim milk for 30 min. Primary antibodies (TrkB, pTrkB, β-actin) were prepared in 1% skim milk, and applied overnight at 4°C. The following day, membranes were washed 3 times in TBS-T before secondary antibodies (goat anti-rabbit HRP [horseradish peroxidase]) in 1% skim milk were applied at room temperature for one hour. Membranes were washed 3 times in TBS-T, followed by incubation for 5 min in the ECL reagents (GE Life Sciences). Images were collected on a Bio-Rad ChemiDock blot imaging system.

If re-probing a membrane, rinse 3 times in TBS-T, and apply the relevant primary antibody, and follow instructions as before.

2.1.21 Gel preparation for in vivo injections

All hydrogels were synthesised and prepared according to the CO_2 diffusion method, as described previously. The hydrogels were then loaded into the barrel of a 23G needle, which was sealed with parafilm until use.

2.1.22 Hydrogel implantation into the mouse brain

All animal experiments were approved by the Howard Florey Institute Ethics committee and were in accordance with the National Health and Medical Research Council guidelines. The animals were housed two Mice per cage, given free access to food and water and kept on a 12/12 h light/dark cycle. NesCreER2-Rosa26eYFP Mice were administered an intramuscular injection of a predrug mix consisting of 0.1 ml atropine and 0.2 ml xylazine diluted in 0.7 ml saline. Anesthesia was induced with 3% isofluorane in oxygen at a constant flow rate of 1.0 lmin^{-1}. When anaesthetised, the mice were placed into a stereotaxic frame, and the skull was fixed in place. Bilateral craniotomies were performed at the following coordinates: anteroposterior +0.5mm AP and lateral +1.5mm ML (medial–lateral) from the bregma. A 32mm 23 G needle preloaded with the hydrogel was loaded onto the stereotactic frame, and the hydrogel was implanted into the brain to a depth of 4.0mm dorsal–ventral. Phosphate buffer (20mM) was implanted as a control. For

each mouse (n=4), the same material was implanted into both the left and right hemispheres, to increase the chance of finding the injection site, and to compensate for possible failed injections. The experiments were set for two time points, 7 and 14 days. After surgery, an antiseptic ointment was applied to the edges of the sutured wound. The mice were allowed to fully recover in warm cages prior to being returned to their home cages.

2.1.23 Immunohistochemistry

Mice were killed by cardiac perfusion under terminal anaesthesia with 0.1 ml Lethabarb and ice-cold saline, followed by 4%paraformaldehyde solution. After removing the brain, it was equilibrated with 30%sucrose, and 30 μm transverse sections were obtained on a cryostat. The sections were then permeabilized with 0.5% Triton X-100, blocked with 10% normal goat serum+1% bovine serum albumin+0.2% Tween 20 and incubated with rabbit monoclonal primary antibodies against glial fibrillary acidic protein (GFAP; 1:1000; DAKO, Sydney, NSW, Australia) and IBA1 (1:250; Wako Pure Chemical Industries, Osaka, Japan). Goat anti-rabbit HRP secondary antibodies were used, followed by incubation in avidin peroxidase. Colour was developed using DAB (3,3'-diaminobenzidine tetrahydrochloride) substrate. Slides were then counterstained with Neutral Red. Images were obtained on a Leica DM2500 optical microscope equipped with a 20x dry lens 0.5 NA.

2.2 References

[1]   J. M. Taylor, U. Ali, R. C. Iannello, P. Hertzog, and P. J. Crack, "Diminished Akt phosphorylation in neurons lacking glutathione peroxidase-1 (Gpx1) leads to increased susceptibility to oxidative stress-induced cell death," *J. Neurochem.*, vol. 92, no. 2, pp. 283–293, 2005.

Chapter 3 Fmoc-LLY hydrogels for the delivery of neurotrophic signals to the brain

3.1 Abstract

Self-assembling peptide hydrogels, composed of the peptide Fmoc-LLY have been investigated as a drug delivery vehicle, for small molecule BDNF mimetics. A BDNF derived self-assembling peptide was also developed, and co-gelled with Fmoc-LLY. The hydrogels were characterised using a combination of rheology and TEM. The preparation of Fmoc based peptide hydrogels using CO_2 to trigger gelation is also described in this chapter.

3.2 Introduction

Self-assembled 3D scaffolds, which mimic the structures of the extracellular matrix, are of interest for their potential in supporting cell growth *in vitro* and *in vivo*[1]–[3]. A variety of structures have been reported, ranging from peptide amphiphiles[4], to self-complementary peptides such as RADA16[5]–[7]. Additionally, there is a family of smaller peptides, based on aromatic peptide derivatives, which self-assemble through π-β interactions[2], [8]–[10]. The smaller size of these peptides offers several advantages over other reported systems. They are easier to synthesise, and the scaffolds they form are scalable. Fmoc self-assembling peptides have been widely investigated with regards to their structure and the effect this has on the sequence's ability to form a hydrogel[2], [11], [12].

The peptide Fmoc-LLY had been previously developed by CSIRO, with preliminary mechanical testing and cytotoxicity analysis conducted with L929 fibroblasts (Unpublished work).

This chapter outlines the development of a novel method for preparing Fmoc hydrogels, inspired by the work by Braun et al. in which they created a nanofibrous capsule on the surface of liquid marbles. In their protocol, *Lycopodium clavatum* spores were used to encapsulate a solution containing 10 mmol L^{-1} Fmoc-FF, these were then placed in a nested petri dishes. The outer dish contained dry ice, which

increased CO_2 gas concentration within the dishes. A network of Fmoc-FF fibres formed at the gas/liquid interface on the liquid marbles, creating a capsule. The thickness of the fibrous layer formed was 50-500 nm.[13].

Peptide hydrogels are a promising material for the development of a treatment for neurodegenerative diseases, such as Parkinson's disease. Current therapies for Parkinson's disease are only able to at best manage the symptoms[14], [15], with no options available that actually treat the cause, or even slow the progression of the disease[15]–[17]. Neurotrophic therapies are a promising approach, as they harness the brain's ability to repair itself. Studies have shown that neurotrophins improve dopaminergic cell survival in vitro[18], and *in vivo* studies have shown BDNF treatment is beneficial in a Parkinsonian mouse model[19], [20]. Neurotrophins alone however are unlikely to be a complete solution to the problem, as they have poor *in vivo* half-life, and blood brain barrier penetration mean some combination of invasive surgeries and/or repeated injections for prolonged periods would be required for effective treatment. The use of a hydrogel as a combined cell scaffold and drug delivery reservoir may help overcome some of these issues – allowing prolonged delivery of the neurotrophic compound to the required region of the brain for as long as is required, while also providing the physical support necessary for cells to grow and develop new connections.

Brain derived neurotrophic factor activates the receptor TrkB with high specificity, the function of BDNF in neural cell populations is to promote the survival, differentiation and synaptic function[21]–[24]. BDNF was first identified in 1982[25] and exists in the adult brain in 2 forms, a pro-BDNF state, and the mature BDNF. After secretion of pro-BDNF from cells, the pro-domain of the protein is cleaved by plasmin or metalloproteases yielding the mature BDNF protein[26]. Mature BDNF is the predominant form of BDNF found in the adult human central nervous system[27] and has significant and potent effects on several cell populations.

A limitation of BDNF as a therapeutic is its very poor pharmacokinetic properties. The half-life *in vivo* is only a matter of minutes and it has very poor blood brain barrier penetration. The development of TrkB agonists, which achieve a

neuroprotective effect with superior pharmacokinetic properties, is currently an area of active research. Synthetic and naturally derived small molecule BDNF mimetics have been reported[28], [29]. For integration into a self-assembling peptide (SAP) system, the use of a short peptide as the functional molecule has numerous advantages. The short peptides, Ac-Ser-Lys-Lys-Arg-NH_2 and Ac-Ile-Lys-Arg-Gly-NH_2 were identified as partial TrkB agonists[30]. Introducing functional peptide sequences into Fmoc gels has so far focused on the incorporation of short binding sequences, such as RGD[31] from fibronectin and IKVAV or YIGSR[32] from laminin. These peptides have all been reported in various materials for improving cell adhesion and spreading on substrates[33]. In order to achieve a stable gel at physiological pH, additional residues need to be added to the functional motif, to either adjust the pK_a[9] or add aromatic and hydrophobic[34] components to the system.

Herein we present the peptide Fmoc-FDIKRG-OH the first Fmoc self-assembling peptide to contain a neurotrophic signal. The action and regulation of neurotrophins in the brain is highly concentration dependent. While an increase in BDNF signalling is advantageous in many psychological disorders[35] the benefits may be outweighed if there is an inadvertent increase in BDNF stimulation in areas of the brain that are functioning normally, or the level of signalling is too high within the targeted area. This could lead to an increase in tumour cell survival and neuronal excitotoxicity[36]. As demonstrated by the functional Fmoc peptides containing the functional sequences RGD[8], [37] and IKVAV[38], bioactive motifs conjugated to these systems are bioavailable. Our hypothesis is that the sequence will be available to cells in direct contact with the hydrogel. If correct, this will induce phosphorylation of TrkB, and subsequent activation of the pro survival pathways[39], [40]. The spatial effect of this material would be well constrained, as the neurotrophic signal is an integral part of the hydrogel. In order to control the level of BDNF signal presented and to stabilise the hydrogel, it was blended with Fmoc-LLY.

3.3 Results and discussion

3.3.1 Physical characterisation

Fmoc-LLY self-assembles into a self-supporting hydrogel at neutral pH following a pH switch from high pH to pH 7.4. Thorough mixing is required to achieve a homogeneous, transparent hydrogel. The mechanical properties of the resulting hydrogel can be controlled through concentration of the peptide used.

Rheological analysis of the properties of the formed hydrogel are shown in Figure 3.1. At 37°C, the storage modulus begins to plateau after approximately 30 minutes for all concentrations. This value was therefore used for subsequent experiments as a minimum time for curing. The average peak modulus is controlled here by the concentration of peptide used, with an upper limit of 10mg/mL. Above this concentration, complete dissolution of the peptide is extremely difficult, using NaOH in PBS. Self-supporting hydrogels – as shown by the inversion test are possible bellow 1mg/mL, but it was extremely fragile. Even gently knocking the vial containing the gel was enough to make the gel collapse and begin flowing. Gels were prepared from 1mg/ml up to 10mg/ml. The storage modulus ranged from 180 to 1250 Pa over this concentration range. The ability to control the mechanical properties of the hydrogels through this range is beneficial, as the modulus of brain tissue ranges from 0.5-1kPa[1].
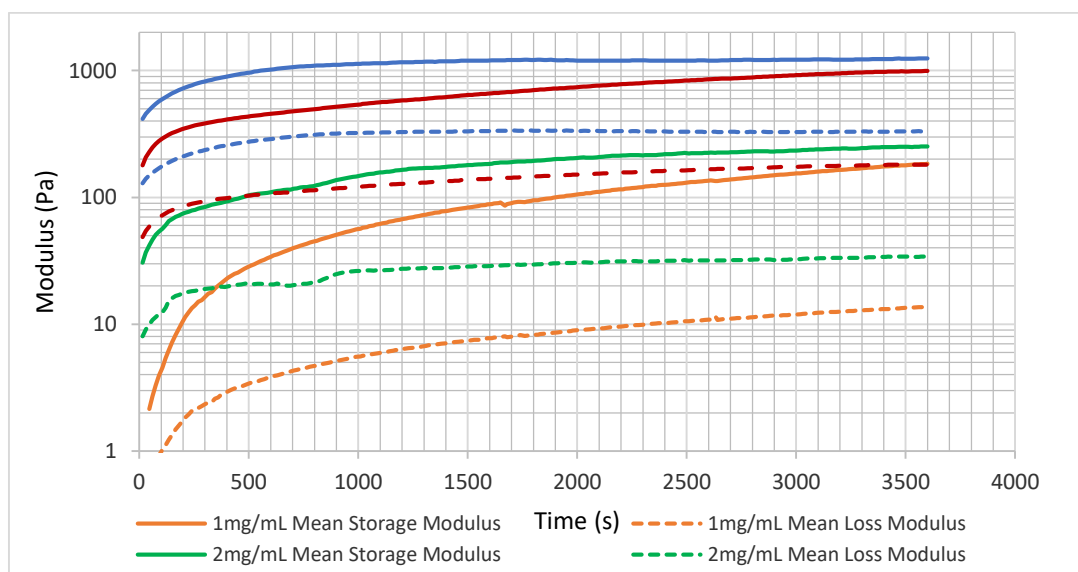
Figure 3.1: Parallel plate rheology of Fmoc-LLY hydrogels

3.3.2 Release of small molecule BDNF mimetic from Fmoc-LLY hydrogel

The small molecule BDNF mimetic LM22A-4 (Figure 3.2) has been widely published, and shown to be effective at phosphorylating the TrkB receptor *in vivo*[41]. In order to impart a neurotrophic function into the Fmoc-LLY hydrogels, LM22A-4 was added to the dissolved peptide solution before forming the hydrogel.
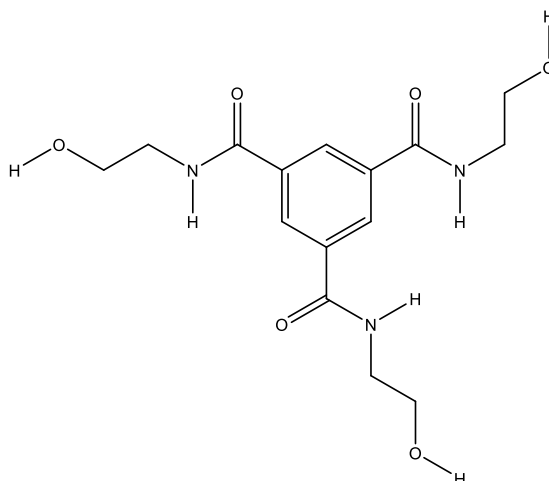

Figure 3.2: Chemical structure of the small molecule BDNF mimetic LM22A-4.

After allowing the hydrogels to stabilise overnight, PBS was pipetted on top of the formed hydrogels. PBS was collected, and replaced at regular intervals. The collected PBS was analysed using HPLC. The release profile is shown in Figure 3.3. The diffusion of LM22A-4 out of this hydrogel exhibits burst release characteristics, reaching 80% total release in only 6 hours.
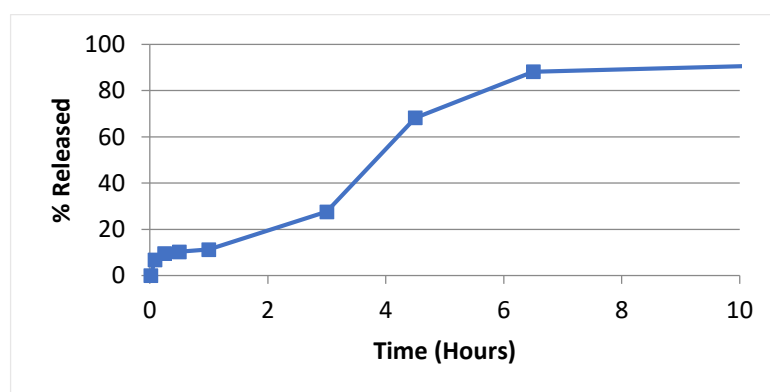
Figure 3.3: Release of LM22A-4 from Fmoc-LLY hydrogel as characterised by HPLC

Systems which successfully used an Fmoc self-assembling hydrogel to deliver a drug in a controlled manner have use whole proteins[42] or reasonably hydrophobic, with planar aromatic regions[43]. As seen in Figure 3.2, LM22A-4 does contain a central

aromatic ring, but was too hydrophilic to interact well with the peptide hydrogel. Burst release drug delivery will not provide the control required for effective treatment of Parkinson's disease. Following this, alternative options were investigated.

3.3.3 Synthesis of a new peptide hydrogel

After identifying the IKRG and SKKR peptide sequences from the full BDNF protein[30], these were investigated to see if it was possible to incorporate one of these into an Fmoc hydrogel system. The IKRG sequence was selected, as it contained less hydrophobic residues and would therefore be easier to incorporate into a hydrophobic self-assembling hydrogel. Initially, several new peptides were synthesised. The first peptide synthesised was Fmoc-IKRG-OH, to see if the Fmoc group alone was sufficient to form a hydrogel containing this functional sequence. This sequence was very hydrophilic, and simply dissolved in neutral solutions tested (PBS, DMEM and water) with no evidence of self-assembly.

Co-assembly with Fmoc-LLY was tested, in which Fmoc-IKRG-OH was dissolved alongside Fmoc-LLY when forming a hydrogel. The gel formed as normal, for Fmoc-LLY, with release of Fmoc-IKRG-OH characterised by HPLC, shown in Figure 3.4. A rapid burst release profile resulted, indicating that the Fmoc modification alone was not sufficient to achieve hydrogel formation, or co-assembly with Fmoc-LLY.
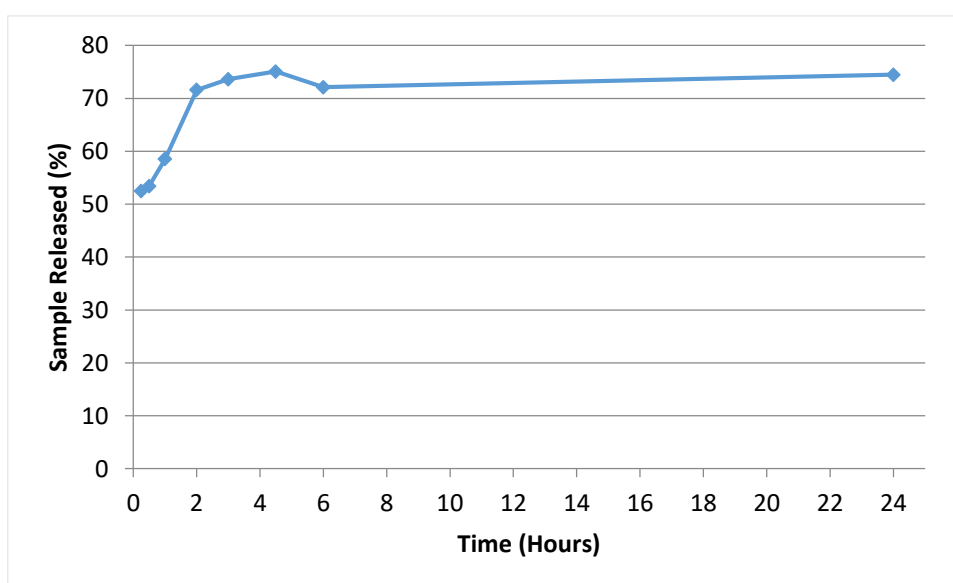
Figure 3.4: Release of Fmoc-IKRG from Fmoc-LLY hydrogels, as characterised by HPLC.

It was hypothesised that the IKRG containing peptide needed to be made more hydrophobic for self-assembly to occur. Given the role of aromatics in the self-assembly of these systems, Phenylalanine was added to subsequently synthesised peptides. The peptides synthesised were Fmoc-FIKRG-OH, Fmoc-FFIKRG-OH and Fmoc-FFFIKRG-OH. Of these, Fmoc-FFIKRG-OH and Fmoc-FFFIKRG-OH were too hydrophobic, with little, if any of the peptide dissolving even at very high pH values. Fmoc-FIKRG-OH was soluble at very low pH, and formed a weak hydrogel at approximately pH 3. If the pH was raised any higher than this, the peptide would precipitate, and destabilise the hydrogel.

Work by Wiliams et al. demonstrated that addition of Aspartic acid residues to a peptide can shift the pH required for self-assembly[9], so 2 more peptides were prepared, Fmoc-FDIKRG-OH and Fmoc-FDDIKRG-OH. Of these, Fmoc-FDDIKRG-OH was too hydrophilic, and did not form a hydrogel. However, Fmoc-FDIKRG-OH could form a self-supporting hydrogel, following a pH switch from a basic solution to approximately 7.4. This gel however was not perfect, and over hours to days would begin to grow cloudy, and eventually precipitate.

3.3.4 Co-gelling Fmoc peptides

As Fmoc-LLY is a very robust gel-forming sequence, able to form a hydrogel at very low concentrations, it was thought that it may be able to stabilise the Fmoc-FDIKRG-OH peptide hydrogels, making a temporally stable biofunctional peptide hydrogel. Since both peptides are soluble at high pH, both were dissolved in phosphate buffer with NaOH added until clear. Various ratios of the dissolved peptides mixed together. These were then neutralised dropwise using HCl, and diluted to 10mg/mL, and left overnight to see which were stable, and which were not. Figure 3.5 shows the vials of hydrogel inverted after 1 hour. This preparation of Fmoc-LLY was quite cloudy from the start, but formed a very stable, and rigid hydrogel. Fmoc-FDIKRG is still partially gelled, but has started to collapse, with visible aggregates visible after 24 hours. B was marginally better, but at 24 hours still had small visible aggregates. The gels C-E were still clear and stable. Therefore, a minimum 20% Fmoc-LLY was required for a stable gel to form. The optimum ratio of these materials needs to be

temporally stabilised, and therefore requires at least 20% Fmoc-LLY, as well as containing an acceptable amount of Fmoc-FDIKRG to stimulate the TrkB receptor. It is important to be able to balance the material properties and biological response, so having a large window if freedom is beneficial.
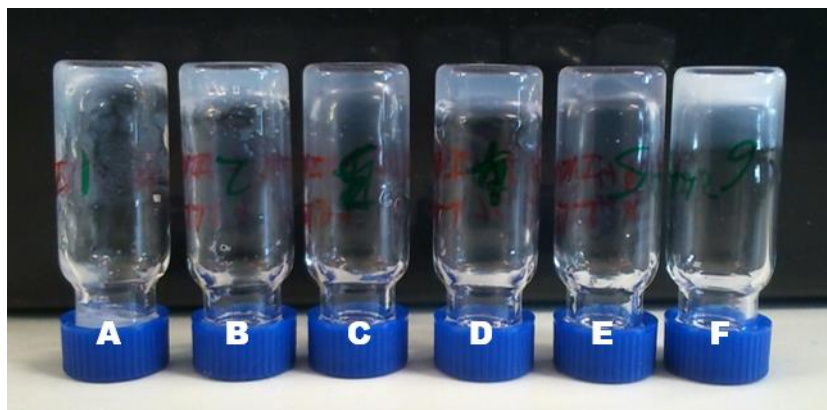

Figure 3.5: Fmoc-LLY and Fmoc-FDIKRG peptide hydrogel blends after 1 hour. A: Fmoc-FDIKRG, B: 90% Fmoc-FDIKRG, C: 80% Fmoc-FDIKRG, D: 70% Fmoc-FDIKRG,E: 60% Fmoc-FDIKRG, F: Fmoc-LLY

3.3.5 TEM Characterisation of hydrogels

In order to compare and differences in the structure of the hydrogel blends, TEM microscopy was used. Two complementary methods were implemented. Negative stain, and CryoTEM. This is done, as each method shows different information. Negative staining a sample enables fast sample preparation, and shows in high contrast many of the features present in the sample. However, since preparation of the sample requires dilution and dehydration onto a grid, the arrangement and interactions of the fibres may have altered. CryoTEM is the method best able to preserve the native hydrated state of the hydrogel, and observe the arrangement, packing and morphology of the hydrogel as they exist in the native state. CryoTEM however suffers from poor contrast, and a low signal to noise ratio, since the sample is imbedded in a film of vitreous ice, and there are no heavy elements in the sample to provide significant contrast.

Fmoc-FDIKRG alone was only able to form a hydrogel for short periods, before beginning to precipitate. TEM samples were prepared while the hydrogel was still optically clear. The morphology of Fmoc-FDIKRG is shown in Figure 3.6. This hydrogel is composed of a mixture of twisted ribbon-like fibres, and a larger helical fibre structure. In Figure 3.6b, a collapsed helix can be seen. A hydrated helix is

shown in Figure 3.6c. It is likely growth of these large fibres that eventually leads to cloudiness of the hydrogel, followed by precipitation, and collapse of the system.
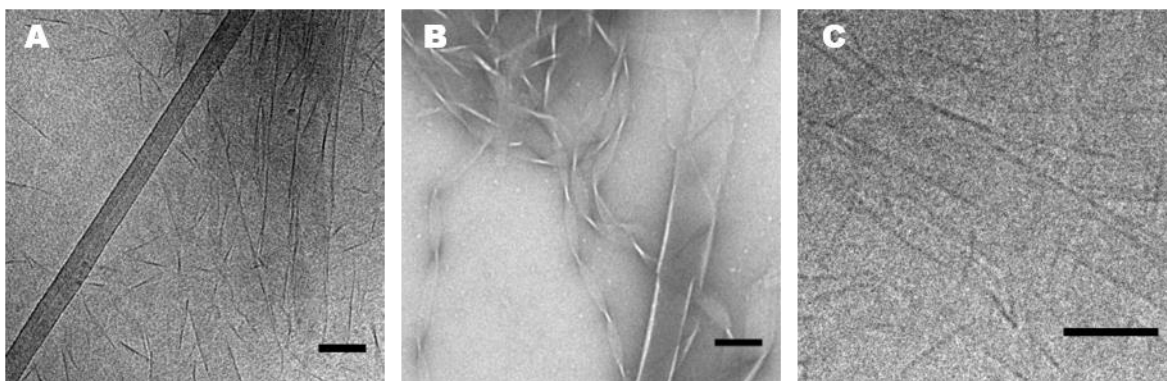

Figure 3.6: Macromolecular structure of Fmoc FDIKRG by A: CryoTEM and B: Negative Stain. C: CryoTEM image showing a clearer helical fibre. Scale bars: 100nm

Blends of the peptides Fmoc-LLY and Fmoc-FDIKRG were able to form self-supporting hydrogels, which were temporally stable. These blends were all examined by CryoTEM and negative stain. Interestingly, blends of the hydrogels show a morphology entirely like that seen for Fmoc-LLY alone. The consistent morphology in the gel-forming blends shows that Fmoc-LLY, as a robust gelator is able to stabilise other peptides. This is supported by previous work, which showed that a robust gel-forming Fmoc peptide, when blended with a non-gel forming peptide led to co-assembly[44].
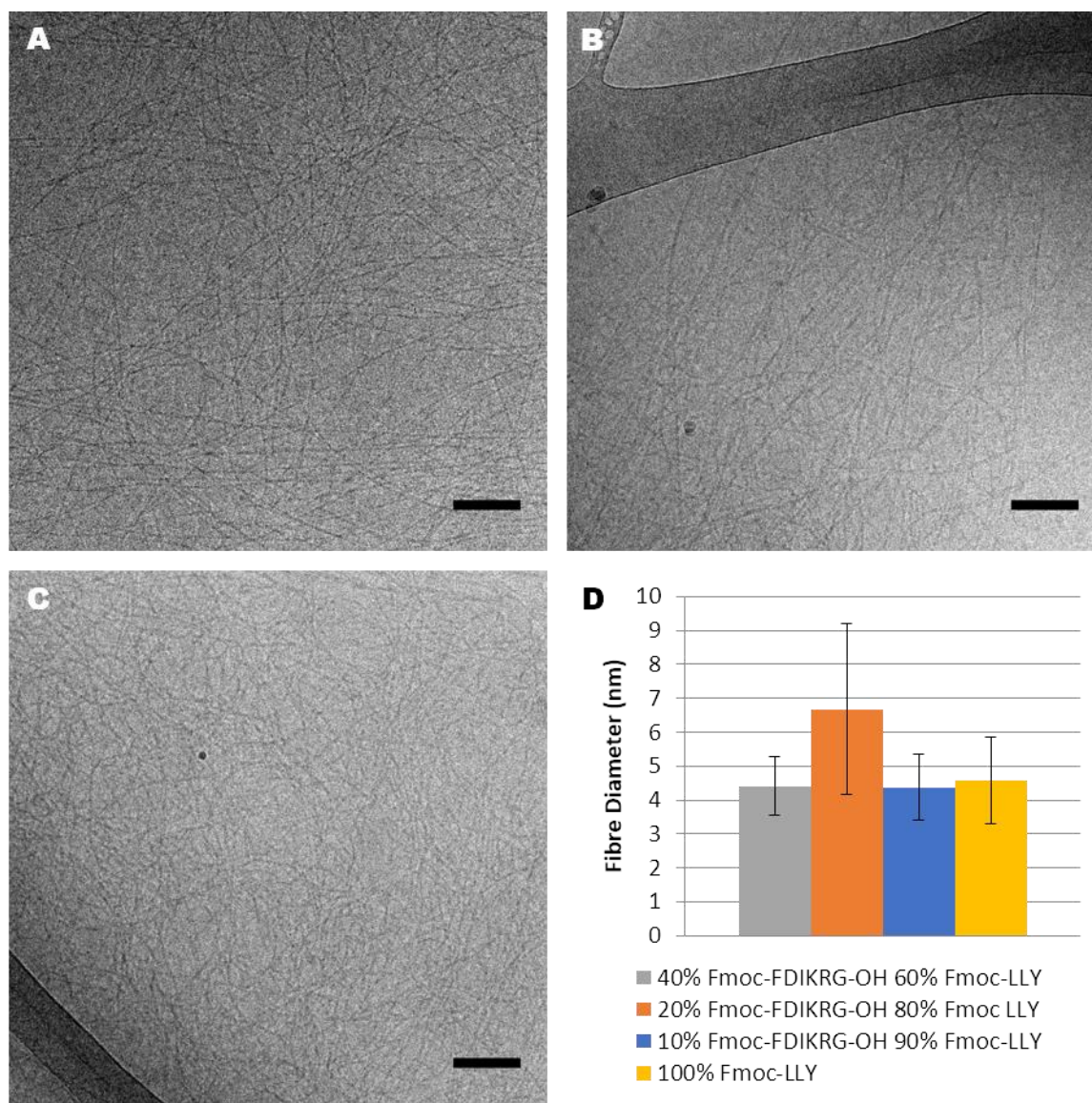
Figure 3.7: CryoTEM micrographs of Fmoc-LLY and Fmoc-FDIKRG hydrogel blends. A: 10%, B: 20% and C: 40%. Scale bars: 100nm D: Fibre diameter of Fmoc hydrogel blends, as measured by CryoTEM.

Comparing these 2 methods of characterisation. The measurements obtained for fibre diameter were consistently smaller than those obtained via negative stain. The differences were not consistent, as would be expected if this were caused simply by the relaxation/spreading of the fibres as they were dried onto the grid for negative staining. Therefore, for the most accurate measure of fibre size, CryoTEM is the preferred method.
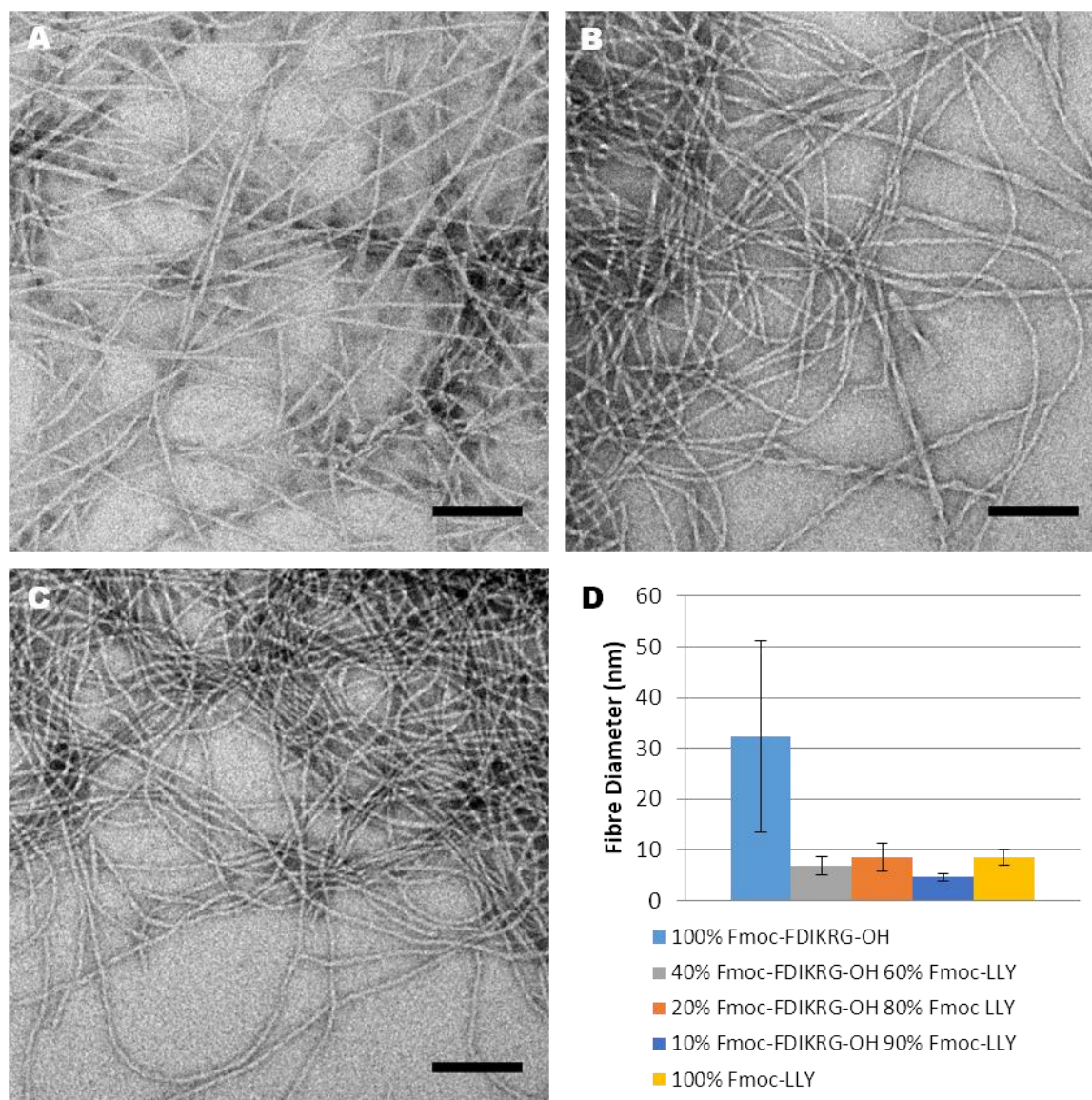
Figure 3.8: Fmoc-LLY and Fmoc-FDIKRG peptide blends imaged by negative stain. A: 10%, B: 20% and C: 40%. Scale bars: 100nm D: Fibre diameter of Fmoc hydrogel blends, as measured by negative stain.

However, in the case of Fmoc-FDIKRG, the fibres are very large, and the relative contrast in cryoTEM quite poor, so it was not possible to measure the width of enough fibres. Negative stain TEM is still a valuable tool in the characterisation of these materials, especially when the low contrast of Cryo imaging leads to an ambiguous interpretation of the macromolecular structure. The difference between a twisted ribbon structure, and 2 intertwined fibres for example, being very difficult to differentiate in cryoTEM, but is easy to resolve in a negatively stained sample.

3.3.6 A novel approach to the preparation of bulk Fmoc hydrogels

Formation of a hydrogel from peptide Fmoc-LLY requires it to first be dissolved at high pH, with gelation triggered by subsequently lowering the pH back down to pH

7.4. It has been reported that forming Fmoc hydrogels using the pH switching method can lead to inhomogeneity and inconsistency[45]. By using the slow hydrolysis of glucono-δ-lactone (GDL) to reduce the pH of the peptide solution, a stronger and more homogeneous hydrogel resulted[45]. This method has now been used by several groups working with these peptide systems [34], [46]–[48]. These works demonstrated the benefits of homogenous gradual pH changes upon the properties of the hydrogels formed. Based on the work in which a high concentration of gaseous CO_2 was used to form nanofibers on the surface of liquid marbles containing solubilised Fmoc peptides[13]. Therefore, a new approach to bulk hydrogel preparation was proposed. Peptides are dissolved in PBS or DMEM and 1M NaOH. They are then pipetted into the required vessel for the work (culture dish or plate, rheometer plate, Eppendorf tube etc) which is then placed into a box, with a tap connected to a side. A balloon filled with CO_2 is connected to the tap, and allowed to fill the box (the container is not airtight). When using DMEM, containing phenol red, the pH change is easy to see, due to the colour change as pH decreases. After 30 minutes, for thin layers (less than 2 mm) the colour change has penetrated the gel, and upon inversion, the hydrogels are fully self-supporting. For thicker layers (5mm or greater) a colour gradient can be seen. Leaving these thicker layers for longer times results in homogeneous colour, and stable hydrogels. Precise control of the pH is difficult by this method, so samples are always rinsed multiple times in PBS or DMEM before any cell work is conducted, to ensure a physiologically relevant environment.

The use of CO_2 gas for making hydrogels from Fmoc-LLY, compared with the dropwise HCl method has led to much more homogeneous gels by appearance, and greater consistency in mechanical properties, when compared to the HCl method.
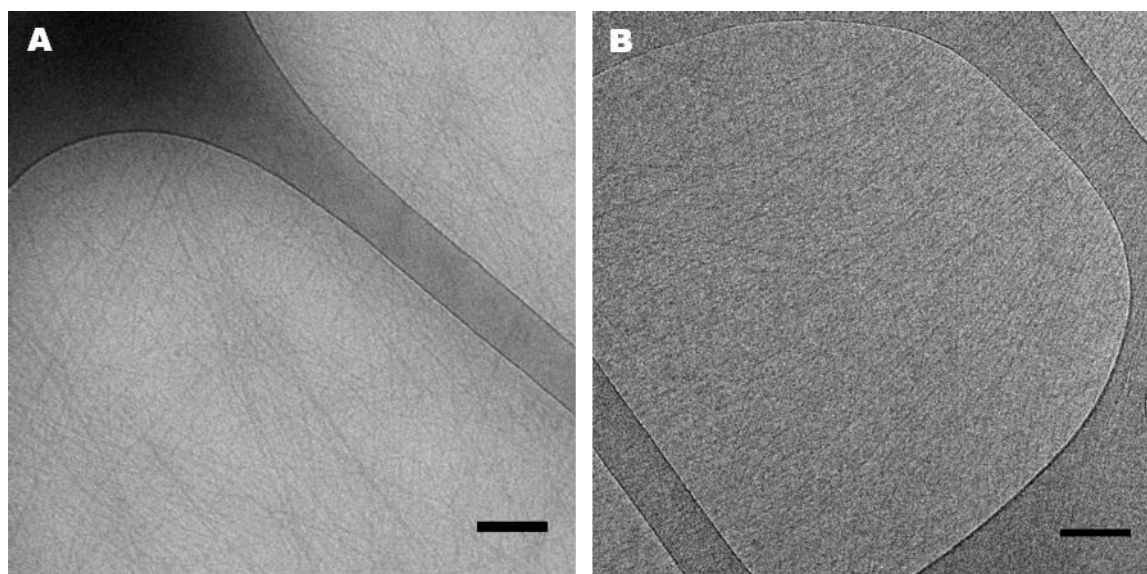
Figure 3.9: CryoTEM micrographs of Fmoc-LLY hydrogels prepared both by A: dropwise addition of HCl, and by B: CO_2 diffusion. Scale bars:100nm

The structure of Fmoc-LLY as prepared by each method was investigated using the TEM methods implemented previously. The cryoTEM micrographs can be seen in Figure 3.9. The fibre diameters as characterised by negative stain and cryoTEM are in Table 3.1. By both methods the fibre diameters were found to be significantly different (P<0.005). While both methods resulted in the formation of a transparent hydrogel, the nanostructure has changed. This difference is possibly caused by the rate of gel formation, as noted when preparing Fmoc hydrogels with GDL[34].

Table 3.1: Fibre diameter of Fmoc LLY hydrogels prepared by HCl addition and CO_2 diffusion methods, as characterised by both CryoTEM and Negative stain.

	HCl	CO2
Negative Stain	8.56±1.54 nm	5.24±1.28 nm
CryoTEM	4.61±1.28 nm	4.04±0.93 nm

3.3.7 Biocompatibility of Hydrogels

Cell culture was conducted on these gels. Initial results using L929 fibroblasts, involved using a live/dead fluorescent stain, 24 hours after seeding cells onto Fmoc-LLY. Fmoc-LLY hydrogels at 10mg/mL were prepared, in a 96 well plate. After leaving the gels to stabilise for at least an hour, they were rinsed with PBS twice, to ensure pH was neutral, and any residual TFA from synthesis was removed. Cells were seeded on top of the hydrogels, and images collected using a fluorescent microscope. These results are shown in Figure 3.10. The ratio of live to dead cells

observed was very favourable, although very few total cells were observed. This was thought to be caused by low cells adhesion to the hydrogels. There is some auto fluorescence of these hydrogels in the red channel, but dead cells are brighter, and therefore still observable. After the initial L929 live-dead results were obtained, cell work was performed using a neural cell type for further analysis, as this provided a better model of the intended application.
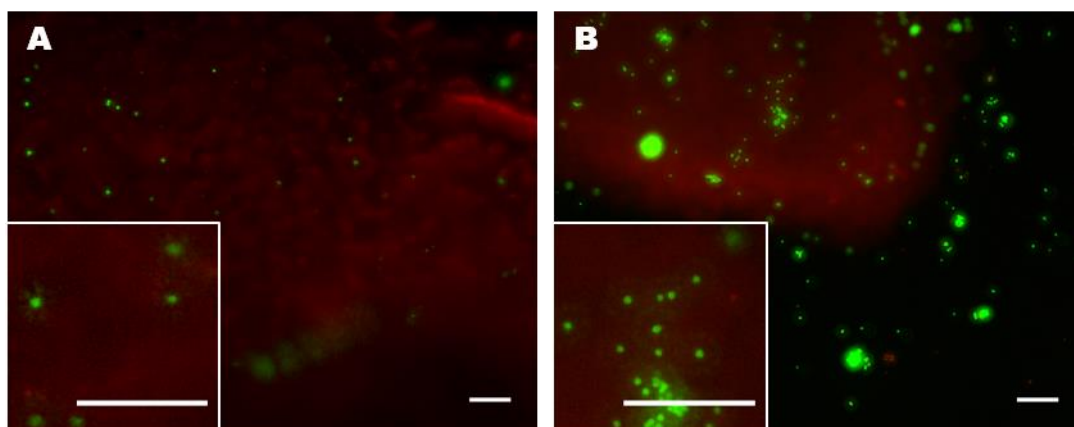

Figure 3.10: L929 fibroblast cells grown on Fmoc-LLY and a 5% Fmoc-FDIKRG blended hydrogel for 24 hours. Live cells are stained with Calcein AM (Green) and dead cells are stained using ethidium homodimer (red) – Due to the different focal planes in image B, 2 exposures have been combined here to give a better representation of the live/dead staining. Scale for main images: 100µm. Scale bar for insets: 250 µm.

SN4741 is a mouse cell line derived from the Substantia Nigra and is an appropriate model for dopaminergic neurons in vtro. Given our intended target for this project is Parkinson's disease, this was an ideal cell type for our next series of cell experiments. Using the SN4741 cell line, live/dead assays were conducted. Figure 3.11 shows cells grown on the surface of Fmoc-LLY, Fmoc-FDIKRG, and a 1:1 blend of these two hydrogels after 1 day in vitro. The cells grown on Fmoc-LLY are almost entirely dead, as are those grown on the 1:1 blend hydrogel. Fmoc-FDIKRG was not stable enough, and after 24 hours, most of the hydrogel has degraded, meaning the cells imaged here were growing on the culture plate. While not an ideal case, it does indicate however that the degradation products of Fmoc-FDIKRG are biocompatible, and unlikely to cause cell death.
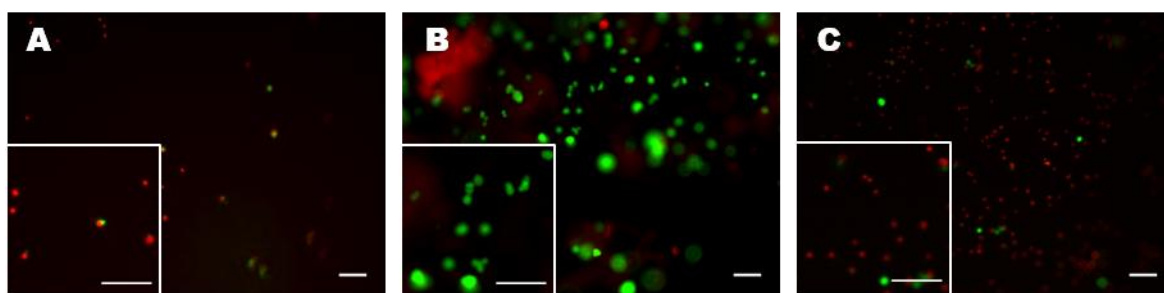
Figure 3.11: Live (green) / Dead (red) staining of SN4741 cells grown on A: Fmoc-LLY, B: Fmoc-FDIKRG and C: a 1:1 blend of these peptides. After 24 hours, there was very little hydrogel remaining in the Fmoc-FDIKRG wells, so the cells seen are those grown on the culture plate Scale bars: 100µm.

Following this initial experiment, a hydrogel with better stability than Fmoc-FDIKRG alone, but also better biocompatibility was required. Blends of Fmoc-LLY and Fmoc-FDIKRG were prepared as described in Table 3.2. All thee gel blends were more stable than Fmoc-FDIKRG alone, and showed a favourable ratio of live to dead cells at 24 hours (Figure 3.12).

Table 3.2: Peptide hydrogel blends for Live/Dead testing

	Fmoc-FDIKRG	Fmoc-LLY
Gel 1	100%	0%
Gel 2	82%	18%
Gel 3	62%	38%
Gel 4	58%	62%
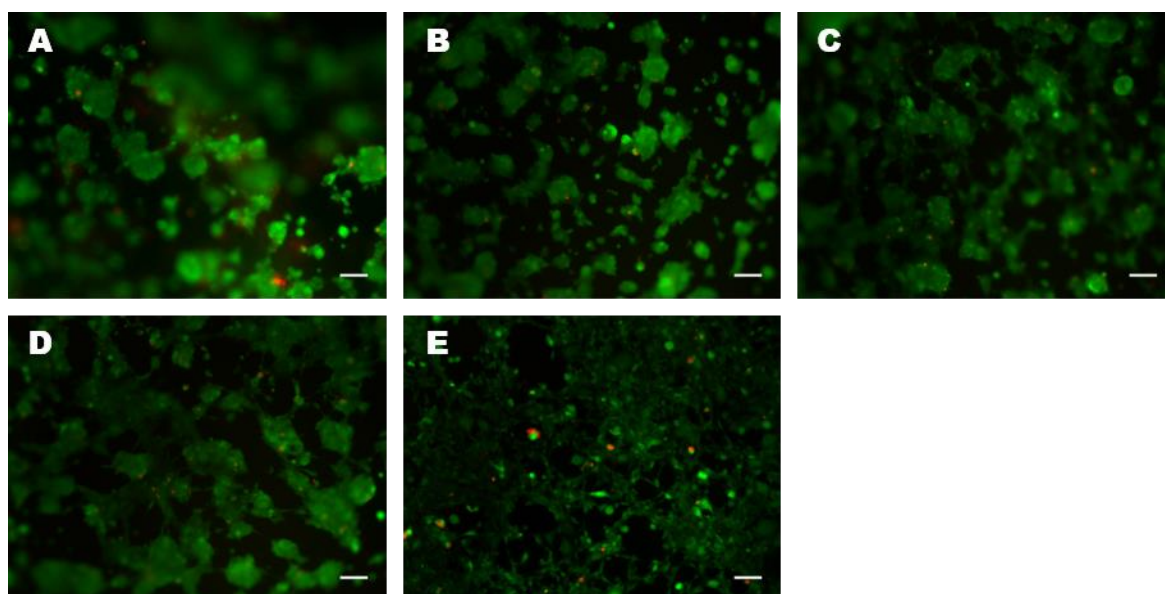
Figure 3.12: Follow-up experiment using lower concentrations of Fmoc-LLY in blended gels to reduce potential toxicity. A: Gel 1, B: Gel 2, C: Gel 3, D: Gel 4 and E: a TCPS (Untreated culture plate) control. Scale bar: 100 µm.

During the process of optimising these experiments, continued attempts at Live/Dead assays to longer time points had been made. Results were inconsistent, with some assays showing entirely dead cells after 24 hours, while others still had live cells after longer time points.

3.3.8 Conditioned media experiment

A cell toxicity assay was conducted using NIH-3T3 cells, a robust fibroblast cell line. Gels were prepared as normal, and had complete culture media placed on top overnight. This media was then collected, and serial dilutions made. Cells were cultured for 24 hours, then their media was exchanged for the pre-conditioned media. After 24 hours, an MTS assay was conducted, the results are shown in Figure 3.13. This clearly shows that a component of the hydrogels is diffusing into the culture media, and causing cell death. It has been shown that components of Fmoc hydrogels leeching out is sufficient to cause necrosis once concentration gets high enough[49]. In that study, it took 72 hours for Fmoc-FF to trigger this response, however the Fmoc-LLY peptide may have a lower critical concentration for this effect, or leech out of the hydrogel faster.
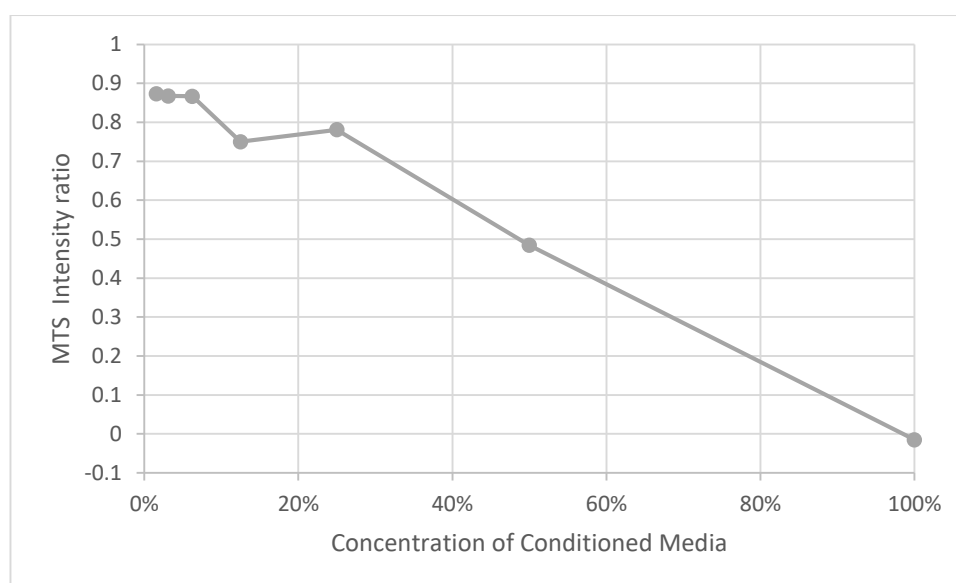

Figure 3.13: MTS Assay using conditioned media to grow NIH-3T3 cells in media conditioned with Fmoc-LLY.

After several months of inconsistent results using the Fmoc-LLY hydrogel system, these combined results convinced us that it was no longer worth pursuing. It may be

possible to adapt the Fmoc-LLY hydrogel to another application in future, but for neural cell types at least, it appears to be cytocoxic.

3.4 Conclusion

While the Fmoc-LLY hydrogel appears to be compatible with robust cell types, and therefore is promising as a biomaterial for some applications. It is not biocompatible with neural cells which are the focus of this project. The mechanical properties are reproducible, easily modified within a wide range, and make it an easy material to work with. The CO_2 diffusion method of hydrogel preparation developed in this chapter has been carried over into subsequent work, as it enables far easier preparation of reproducible hydrogels than the HCl method. The novel peptide Fmoc-FDIKRG is further developed upon in chapters 4 and 6.

3.5 References

[1]   J. T. S. Pettikiriarachchi, C. L. Parish, M. S. Shoichet, J. S. Forsythe, and D. R. Nisbet, "Biomaterials for Brain Tissue Engineering," *Aust. J. Chem.*, vol. 63, no. 8, p. 1143, 2010.

[2]   S. Fleming and R. V Ulijn, "Design of nanostructures based on aromatic peptide amphiphiles.," *Chem Soc Rev*, vol. 8150, no. 43, pp. 8150–8177, 2014.

[3]   J. B. Matson, R. H. Zha, and S. I. Stupp, "Peptide self-assembly for crafting functional biological materials," *Curr. Opin. Solid State Mater. Sci.*, vol. 15, no. 6, pp. 225–235, 2011.

[4]   E. Beniash, J. D. Hartgerink, H. Storrie, J. C. Stendahl, and S. I. Stupp, "Self-assembling peptide amphiphile nanofiber matrices for cell entrapment," *Acta Biomater.*, vol. 1, no. 4, pp. 387–397, 2005.

[5]   E. Genové, C. Shen, S. Zhang, and C. E. Semino, "The effect of functionalized self-assembling peptide scaffolds on human aortic endothelial cell function," *Biomaterials*, vol. 26, no. 16, pp. 3341–3351, 2005.

[6]   N. Ni, Y. Hu, H. Ren, C. Luo, P. Li, J. B. Wan, and H. Su, "Self-assembling peptide nanofiber scaffolds enhance dopaminergic differentiation of mouse pluripotent stem cells in 3-dimensional culture," *PLoS One*, vol. 8, no. 12, pp. 1–11, 2013.

[7]   Y. Chau, Y. Luo, A. C. Y. Cheung, Y. Nagai, S. Zhang, J. B. Kobler, S. M. Zeitels, and R. Langer, "Incorporation of a matrix metalloproteinase-sensitive substrate into self-assembling peptides - A model for biofunctional scaffolds," *Biomaterials*, 2008.

[8]   V. N. Modepalli, A. L. Rodriguez, R. Li, S. Pavuluri, K. R. Nicholas, C. J. Barrow, D. R. Nisbet, and R. J. Williams, "In vitro response to functionalized self-assembled peptide scaffolds for three-dimensional cell culture," *Biopolymers*, vol. 102, no. 2, pp. 197–205, Mar. 2014.

[9]   A. L. Rodriguez, C. L. Parish, D. R. Nisbet, and R. J. Williams, "Tuning the amino acid sequence of minimalist peptides to present biological signals via charge neutralised self assembly," *Soft Matter*, vol. 9, no. 15, p. 3915, 2013.

[10]   T. Liebmann, S. Rydholm, V. Akpe, and H. Brismar, "Self-assembling Fmoc dipeptide hydrogel for in situ 3D cell culturing," *BMC Biotechnol.*, vol. 7, no. 1, p. 88, 2007.

[11]   V. Jayawarna, M. Ali, T. a. Jowitt, A. F. Miller, A. Saiani, J. E. Gough, and R. V. Ulijn, "Nanostructured hydrogels for three-dimensional cell culture through self-assembly of fluorenylmethoxycarbonyl-dipeptides," *Adv. Mater.*, vol. 18, no. 5, pp. 611–614, Mar. 2006.

[12]   S. Fleming, S. Debnath, P. W. J. M. Frederix, T. Tuttle, and R. V Ulijn, "Aromatic peptide amphiphiles: significance of the Fmoc moiety.," *Chem. Commun. {(Camb.)}*, vol. 49, no. 90, pp. 10587–10589, 2013.

[13]   H.-G. Braun and A. Z. Cardoso, "Self-assembly of Fmoc-diphenylalanine inside liquid marbles," *Colloids Surfaces B Biointerfaces*, vol. 97, pp. 43–50, 2012.

[14]   W. Dauer and S. Przedborski, "Parkinson's Disease," *Neuron*, vol. 39, no. 6, pp. 889–909, 2003.

[15]   S. Fahn, D. Oakes, I. Shoulson, K. Kieburtz, A. Rudolph, A. Lang, C. W. Olanow, C. Tanner, K. Marek, and Parkinson Study Group, "Levodopa and the Progression of Parkinson's Disease," *N. Engl. J. Med.*, vol. 351, no. 24, pp. 2498–2508, 2004.

[16]   P. Hickey, "Available and emerging treatments for Parkinson ' s disease : a review," pp. 241–254, 2011.

[17]   C. L. Tomlinson, R. Stowe, S. Patel, C. Rick, R. Gray, and C. E. Clarke, "Systematic Review of Levodopa Dose Equivalency Reporting in Parkinson ' s Disease," vol. 25, no. 15, pp. 2649–2685, 2010.

[18]   J. H. Son, H. S. Chun, T. H. Joh, S. Cho, B. Conti, and J. W. Lee, "Neuroprotection and neuronal differentiation studies using substantia nigra

dopaminergic cells derived from transgenic mouse embryos.," *J. Neurosci.*, vol. 19, no. 1, pp. 10–20, Jan. 1999.

[19]   T. F. Oo, D. M. Marchionini, O. Yarygina, P. D. O'Leary, R. A. Hughes, N. Kholodilov, and R. E. Burke, "Brain-derived neurotrophic factor regulates early postnatal developmental cell death of dopamine neurons of the substantia nigra in vivo," *Mol. Cell. Neurosci.*, vol. 41, no. 4, pp. 440–447, Jul. 2009.

[20]   T. Tsukahara, M. Takeda, S. Shimohama, O. Ohara, and N. Hashimoto, "Effects of brain-derived neurotrophic factor on 1-methyl-4-phenyl-1,2,3,6-tetrahydropyridine-induced parkinsonism in monkeys.," *Neurosurgery*, vol. 37, no. 4, pp. 733-9; discussion 739-41, Oct. 1995.

[21]   A. H. Nagahara and M. H. Tuszynski, "Potential therapeutic uses of BDNF in neurological and psychiatric disorders," *Nat. Rev. Drug Discov.*, vol. 10, no. 3, pp. 209–219, Mar. 2011.

[22]   L. N. Gillespie, G. M. Clark, P. F. Bartlett, and P. L. Marzella, "BDNF-induced survival of auditory neurons in vivo: Cessation of treatment leads to accelerated loss of survival effects," *J. Neurosci. Res.*, vol. 71, no. 6, pp. 785–790, Mar. 2003.

[23]   D. Rejali, V. A. Lee, K. A. Abrashkin, N. Humayun, D. L. Swiderski, and Y. Raphael, "Cochlear implants and ex vivo BDNF gene therapy protect spiral ganglion neurons.," *Hear. Res.*, vol. 228, no. 1–2, pp. 180–7, Jun. 2007.

[24]   H. Staecker, R. Kopke, B. Malgrange, P. Lefebvre, and T. R. Van De Water, "NT-3 and/or BDNF therapy prevents loss of auditory neurons following loss of hair cells," *Neuroreport*, vol. 7, no. 4, pp. 889–894, Mar. 1996.

[25]   Y. A. Barde, D. Edgar, and H. Thoenen, "Purification of a new neurotrophic factor from mammalian brain.," *EMBO J.*, vol. 1, no. 5, pp. 549–553, 1982.

[26]   V. Nikoletopoulou, H. Lickert, J. M. Frade, C. Rencurel, P. Giallonardo, L. Zhang, M. Bibel, and Y.-A. Barde, "Neurotrophin receptors TrkA and TrkC cause neuronal death whereas TrkB does not," *Nature*, vol. 467, no. 7311, pp. 59–63, Sep. 2010.

[27]   S. Rauskolb, M. Zagrebelsky, A. Dreznjak, R. Deogracias, T. Matsumoto, S. Wiese, B. Erne, M. Sendtner, N. Schaeren-Wiemers, M. Korte, and Y.-A. Barde, "Global deprivation of brain-derived neurotrophic factor in the CNS reveals an area-specific requirement for dendritic growth.," *J. Neurosci.*, vol. 30, no. 5, pp. 1739–1749, 2010.

[28]   J. Xu, M. H. Lacoske, and E. a. Theodorakis, "Neurotrophic Natural Products: Chemistry and Biology," *Angew. Chemie - Int. Ed.*, vol. 53, no. 4, pp. 956–987, 2014.

[29]   F. M. Longo, S. M. Massa, and S. Gupta, "Non-peptide bdnf neurotrophin mimetics," *US Pat. App. 13/117*, 2011.

[30]   M. D. C. Cardenas-Aguayo, S. F. Kazim, I. Grundke-Iqbal, and K. Iqbal, "Neurogenic and Neurotrophic Effects of BDNF Peptides in Mouse Hippocampal Primary Neuronal Cell Cultures," *PLoS One*, vol. 8, no. 1, p. e53596, 2013.

[31]   G. Cheng, V. Castelletto, R. R. Jones, C. J. Connon, and I. W. Hamley, "Hydrogelation of self-assembling RGD-based peptides," *Soft Matter*, vol. 7, no. 4, pp. 1326–1333, 2011.

[32]   A. L. Rodriguez, T. Y. Wang, K. F. Bruggeman, C. C. Horgan, R. Li, R. J. Williams, C. L. Parish, and D. R. Nisbet, "In vivo assessment of grafted cortical neural progenitor cells and host response to functionalized self-assembling peptide hydrogels and the implications for tissue repair," *J. Mater. Chem. B*, vol. 2, no. 44, pp. 7771–7778, 2014.

[33]   G. Orive, E. Anitua, J. L. Pedraz, and D. F. Emerich, "Biomaterials for promoting brain protection, repair and regeneration.," *Nat. Rev. Neurosci.*, vol. 10, no. 9, pp. 682–692, 2009.

[34]   R. Li, C. C. Horgan, B. Long, A. L. Rodriguez, L. Mather, C. J. Barrow, D. R. Nisbet, and R. J. Williams, "Tuning the mechanical and morphological properties of self-assembled peptide hydrogels via control over the gelation mechanism through regulation of ionic strength and the rate of pH change," *RSC Adv.*, vol. 5, no. 1, pp. 301–307, 2015.

[35]   A. E. Autry and L. M. Monteggia, "Brain-Derived Neurotrophic Factor and Neuropsychiatric Disorders," *Pharmacol. Rev.*, vol. 64, no. 2, pp. 238–258, Apr. 2012.

[36]   R. D. Price, S. a. Milne, J. Sharkey, and N. Matsuoka, "Advances in small molecules promoting neurotrophic function," *Pharmacol. Ther.*, vol. 115, no. 2, pp. 292–306, 2007.

[37]   V. Castelletto, C. M. Moulton, G. Cheng, I. W. Hamley, M. R. Hicks, A. Rodger, D. E. López-Pérez, G. Revilla-López, and C. Alemán, "Self-assembly of Fmoc-tetrapeptides based on the RGDS cell adhesion motif," *Soft Matter*, vol. 7, no. 24, p. 11405, 2011.

[38]   F. L. Maclean, Y. Wang, R. Walker, M. K. Horne, R. J. Williams, and D. R. Nisbet, "Reducing Astrocytic Scarring after Traumatic Brain Injury with a Multifaceted Anti-Inflammatory Hydrogel System," *ACS Biomater. Sci. Eng.*, vol. 3, no. 10, pp. 2542–2549, Oct. 2017.

[39]   G. Tejeda and M. Díaz-Guerra, "Integral Characterization of Defective BDNF/TrkB Signalling in Neurological and Psychiatric Disorders Leads the Way to New Therapies," *Int. J. Mol. Sci.*, vol. 18, no. 12, p. 268, Jan. 2017.

[40]   K. Obata and K. Noguchi, "BDNF in sensory neurons and chronic pain," *Neurosci. Res.*, vol. 55, no. 1, pp. 1–10, May 2006.

[41]   S. M. Massa, T. Yang, Y. Xie, J. Shi, M. Bilgen, J. N. Joyce, D. Nehama, J. Rajadas, and F. M. Longo, "Small molecule BDNF mimetics activate TrkB signaling and prevent neuronal degeneration in rodents," *J. Clin. Invest.*, vol. 120, no. 5, pp. 1774–1785, May 2010.

[42]   K. F. Bruggeman, A. L. Rodriguez, C. L. Parish, R. J. Williams, and D. R. Nisbet, "Temporally controlled release of multiple growth factors from a self-assembling peptide hydrogel," *Nanotechnology*, vol. 27, no. 38, p. 385102, Sep. 2016.

[43]   X.-D. Xu, L. Liang, C.-S. Chen, B. Lu, N. Wang, F.-G. Jiang, X.-Z. Zhang, and R.-X. Zhuo, "Peptide Hydrogel as an Intraocular Drug Delivery System for Inhibition

of Postoperative Scarring Formation," *ACS Appl. Mater. Interfaces*, vol. 2, no. 9, pp. 2663–2671, Sep. 2010.

[44]   R. Orbach, I. Mironi-harpaz, L. Adler-abramovich, E. Mossou, E. P. Mitchell, V. T. Forsyth, E. Gazit, and D. Seliktar, "The Rheological and Structural Properties of Fmoc-Peptide-Based Hydrogels: The Effect of Aromatic Molecular Architecture on Self- Assembly and Physical Characteristics," 2015.

[45]   D. J. Adams, M. F. Butler, W. J. Frith, M. Kirkland, L. Mullen, and P. Sanderson, "A new method for maintaining homogeneity during liquid–hydrogel transitions using low molecular weight hydrogelators," *Soft Matter*, vol. 5, no. 9, p. 1856, 2009.

[46]   D. J. Adams, L. M. Mullen, M. Berta, L. Chen, and W. J. Frith, "Relationship between molecular structure, gelation behaviour and gel properties of Fmoc-dipeptides," *Soft Matter*, vol. 6, no. 9, p. 1971, 2010.

[47]   X. Mu, K. M. Eckes, M. M. Nguyen, L. J. Suggs, and P. Ren, "Experimental and Computational Studies Reveal An Alternative Supramolecular Structure for Fmocdipeptide Self-assembly."

[48]   B. Adhikari, J. Nanda, and A. Banerjee, "Multicomponent hydrogels from enantiomeric amino acid derivatives: helical nanofibers, handedness and self-sorting," *Soft Matter*, vol. 7, no. 19, p. 8913, 2011.

[49]   W. T. Truong, Y. Su, D. Gloria, F. Braet, and P. Thordarson, "Dissolution and degradation of Fmoc-diphenylalanine self-assembled gels results in necrosis at high concentrations in vitro," *Biomater. Sci.*, vol. 3, no. 2, pp. 298–307, 2015.

Chapter 4 Bi-Functional Fmoc Peptide Hydrogels

4.1 Abstract

In the previous chapter, the peptide Fmoc-FDIKRG was developed, and blended with Fmoc-LLY to form hydrogels. Fmoc-LLY was incompatible with neural cells, so alternative peptides were investigated for blending with Fmoc-FDIKRG, in order to improve compatibility of the hydrogels with neural cell types. Several Fmoc peptide hydrogels from the literature were identified as potential candidates, three were selected because of proven biocompatibility in the literature and the presence of integrin binding motifs. Of these, Fmoc-FRGDF was able to co-assemble with Fmoc-FDIKRG most effectively, so these materials were investigated further. Hydrogels formed from blends of these two peptides were characterised by TEM methods and rheology. Following physical characterisation, the hydrogels formed were tested for biocompatibility and for their ability to activate the TrkB receptor.

4.2 Introduction

In order to produce a bi-functional hydrogel, containing integrin binding peptides in addition to the BDNF derived IKRG motif, a literature search was conducted, and Fmoc hydrogels containing functional motifs investigated. Three published Fmoc hydrogels, Fmoc-FRGDF[1]–[6], Fmoc-DIKVAV[6], [7] and Fmoc-DYIGSRF[6] were identified as potential candidates for co-gelation with the Fmoc-FDIKRG peptide. It has been shown that the Fmoc-FRGDF and Fmoc-DIKVAV peptides can co-assemble[3]. Depending of the method of co-assembly, the properties, and macromolecular structure could be controlled. If the peptides were gelled separately, and then mixed, the gels consisted of 2 distinct populations of fibres, intertwined, where if both peptides were dissolved and gelled as one, they co-assembled into the same fibres. These peptides have been shown to be non-cytotoxic *in vivo*[6]. The Fmoc-FRGDF material tested *in vivo* in the brain induced an inflammatory response[6], with heightened astrocyte and microglia density surrounding the injection site. It was hypothesised that this was due to the absence of fibronectin in the brain ECM. Many studies have been published, finding that the density of RGD present on a surface has a significant effect on the response of cells or tissue to that

substrate[8], [9], with evidence that too high an RGD concentration is sub-optimal for neurite outgrowth[10]. Therefore, in the case of Fmoc-FRGDF, where the entire material is presenting the RGD motif, the density of signalling may be too high for successful culture of neural cells. By blending Fmoc-FRGDF with other self-assembling peptides, it may be possible to sufficiently reduce the RGD motif density, and improve the response of cells to the material.

Of the three peptides investigated for blending with Fmoc-FDIKRG, only Fmoc-FRGDF was able to co-assemble under the conditions tested into a stable hydrogel, with the others precipitating within 24 hours, therefore work with the Fmoc-FRGDF peptide was continued.

By blending these peptides into a single material, we can harness the proven biocompatibility and integrin binding of the Fmoc-FRGDF hydrogel, and provide additional neurotrophic function through the Fmoc-FDIKRG peptide. The intention here being to enable the formation of a bi-functional hydrogel, which can physically support neural cells in an ECM-like environment, while stimulating growth and proliferation through the TrkB receptor.

These hydrogels were prepared using the CO_2 diffusion method developed in Chapter 3. The gels were physically characterised by rheology and TEM methods, as described previously. Biological testing involved live/dead staining and MTS assays, to determine the biocompatibility of the hydrogels. Further testing of the hydrogels involved treating primary cells with the hydrogels, and using western blots to determine the ability of these peptide hydrogels to activate the TrkB receptor *in vitro*.

4.3 Results and Discussion

4.3.1 New blended peptides

One of the reasons for developing an Fmoc based peptide with the IKRG moiety was the number of other peptides that have been developed using this assembly system. This gives the option of blending these together to achieve a combination of integrin binding and BDNF activating sequences in a single hydrogel. Fmoc-FRGDF[2], Fmoc-DIKVAV and Fmoc-DYIGSRF[6] were all synthesised, and blends of the peptides prepared. Stable hydrogels only formed from the combination of Fmoc-FRGDF and Fmoc-FDIKRG, so this system was explored further. Table 4.1 shows the ratios of Fmoc-FDIKRG and Fmoc-FRGDF which are able to form a stable self-supporting hydrogel.

Table 4.1: Fmoc peptide ratios investigated

Fmoc-FDIKRG	Fmoc-FRGDF	Clear Self Supporting Gel?
100%	0%	No
75%	25%	No
50%	50%	Yes
25%	75%	Yes
10%	90%	Yes
5%	95%	Yes

4.3.2 Mechanical testing

Mechanical characterisation of the hydrogels at 10mg/mL was conducted in a parallel plate rheometer. Due to the rapid rate of gelation in these materials, the tests were invariably started once the gel had already formed, then vortexed to allow them to flow, and transferred to the rheometer. All gels showed an initial rapid increase in storage modulus. The storage modulus continues to gradually climb up to 2 hours, where the rate of change was marginal. As seen in Figure 4.1, Fmoc-FRGDF has the highest storage modulus, and this decreased with greater Fmoc-FDIKRG content in the hydrogels. All gels had an order of magnitude difference between their storage and loss modulus, indicating that these are all elastic and solid-like

hydrogels[11]. This gelation behaviour informed subsequent experiments, and all gels were left for a minimum of two hours to stabilise before use.
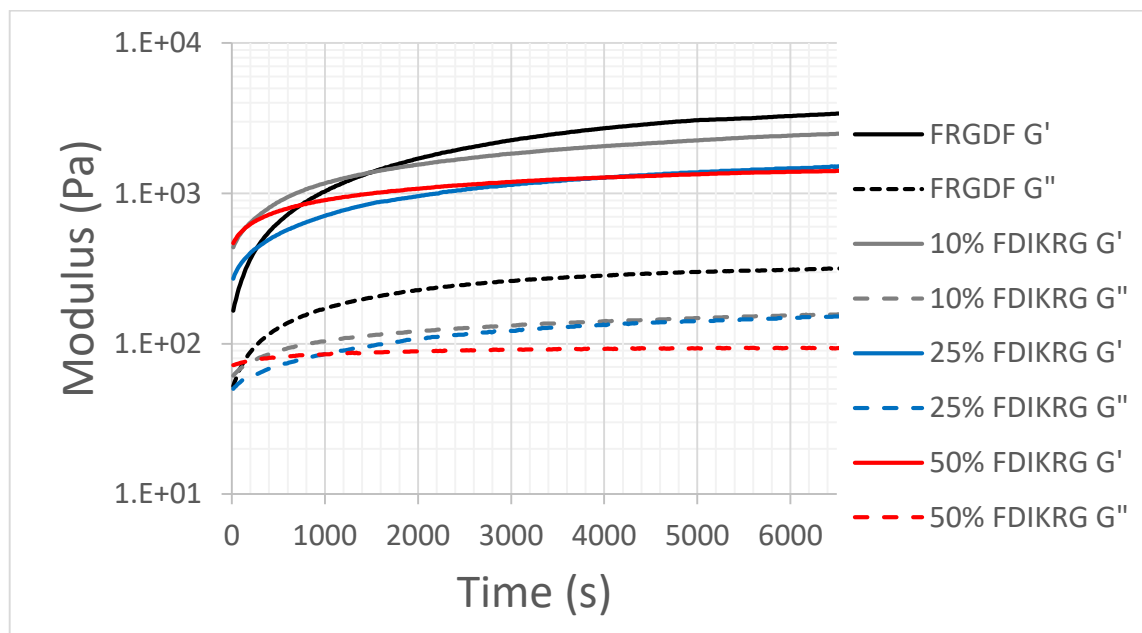

Figure 4.1: Storage and loss modulus of 10mg/ml Fmoc hydrogel blends, as measured with a parallel plate rheometer at 37 degrees.

4.3.3 TEM Characterisation of hydrogels

As in Chapter 3, the hydrogels were analysed using a combination of cryoTEM, for the most accurate representation of the hydrogels in their hydrated state, and negative stain, which is used to reveal features that may not be apparent in cryoTEM. Representative micrographs of the structures visible in each hydrogel formed are shown in Figure 4.2.

Analysis of the structure of the hydrogels reveals a nanofibrous network for Fmoc-FRGDF, agreeing with the literature[4]. Fibre diameter are shown in Figure 4.2F. The diameter and structure of the fibres present in 100% Fmoc-FRGDF gels are straight narrow fibres, averaging 10±3.4 nm in diameter, which is similar to reported atomic force microscopy measurements for this peptide[1]. Fmoc-FDIKRG, as discussed in chapter 3, had a very distinct structure, consisting of significantly larger fibres and sheets. A structure similar to Fmoc-FRGDF is observed for all blended hydrogels. As seen in the Fmoc-LLY blends in Chapter 3, the stable blends have fibre sizes much closer to those found in the more robust gel-forming peptide system, with the

relatively small standard deviation in these systems indicating a homogeneous fibre population.
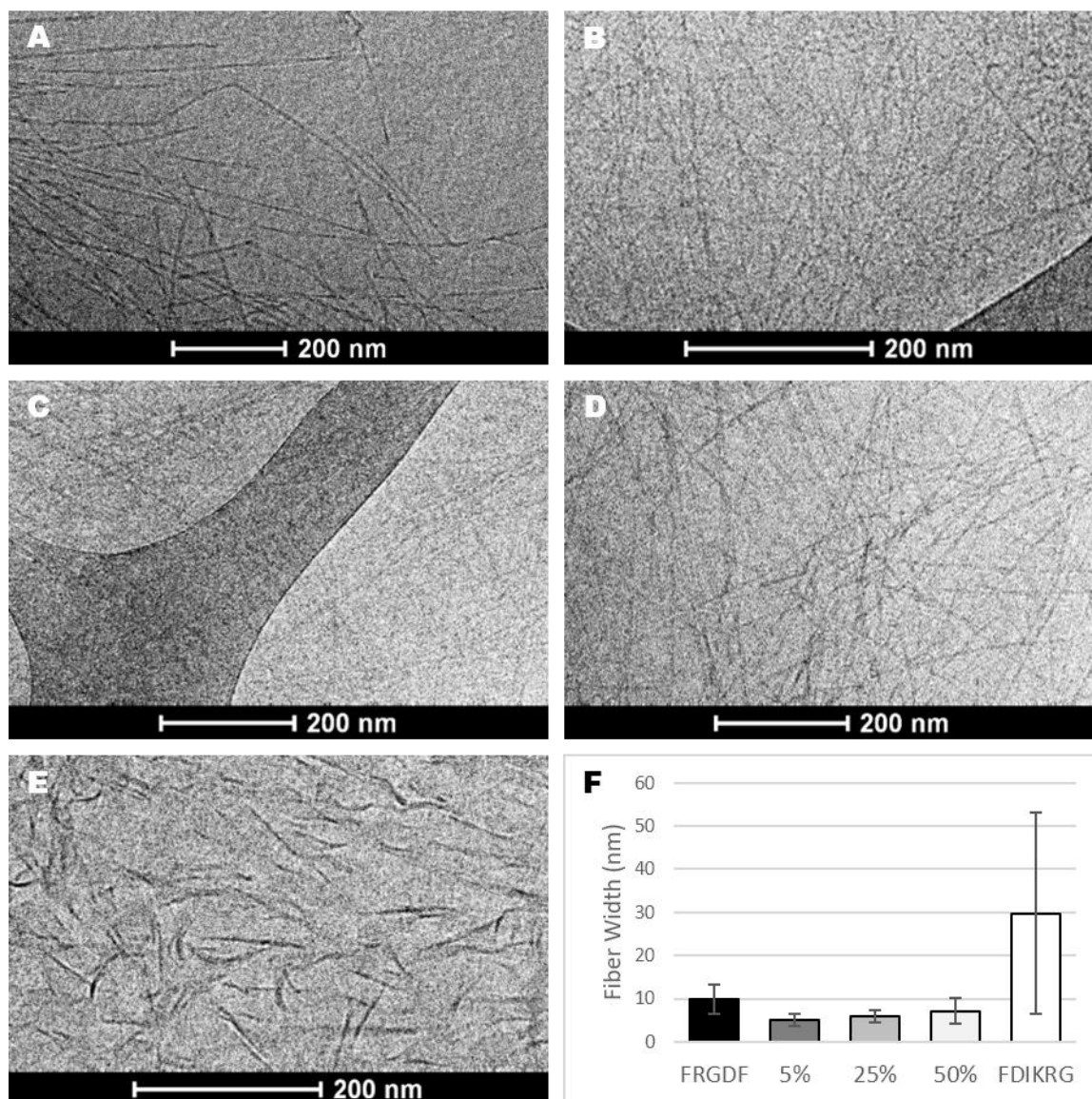

Figure 4.2: CryoTEM micrographs of A: Fmoc-FRGDF, B: 95% Fmoc-FRGDF with 5% Fmoc-FDIKRG C: 75% Fmoc-FRGDF with 25% Fmoc-FDIKRG D: 50% Fmoc-FRGDF with 50% Fmoc-FDIKRG E: Fmoc-FDIKRG F: Average fibre diameter, measured from cryoTEM micrographs in imageJ.

In the blended hydrogels, there are two predicted mechanism of co-assembly. The first is that each peptide would self-assemble with itself, resulting in observed structures that are combination of the large fibres seen in Fmoc-FDIKRG, and the smaller fibres seen in Fmoc-FRGDF. The other mechanism being the peptides co-assembling into the same fibres, showing a single type of fibre. Since there are none of the large fibres observed in Fmoc-FDIKRG in any of the blended hydrogels, the peptides are clearly interacting, resulting in smaller nanofibers, much closer in

morphology to Fmoc-FRGDF, which is a more stable hydrogel. This is supported by work in which Fmoc-FRGDF and Fmoc-DIKVAV were co-assembled by two mechanisms, in the first, both peptides were solubilised together, the gels formed by this method were found to be composed of homogenous nanofibers containing both peptides, while the gels formed by preparing each peptide separately, then mixing them together resulted in more heterogeneous fibres[3]. The absence of the larger fibres seen in Fmoc-FDIKRG alone also means that the blended hydrogels are optically transparent, as the smaller nanofibers do not cause significant light scattering.
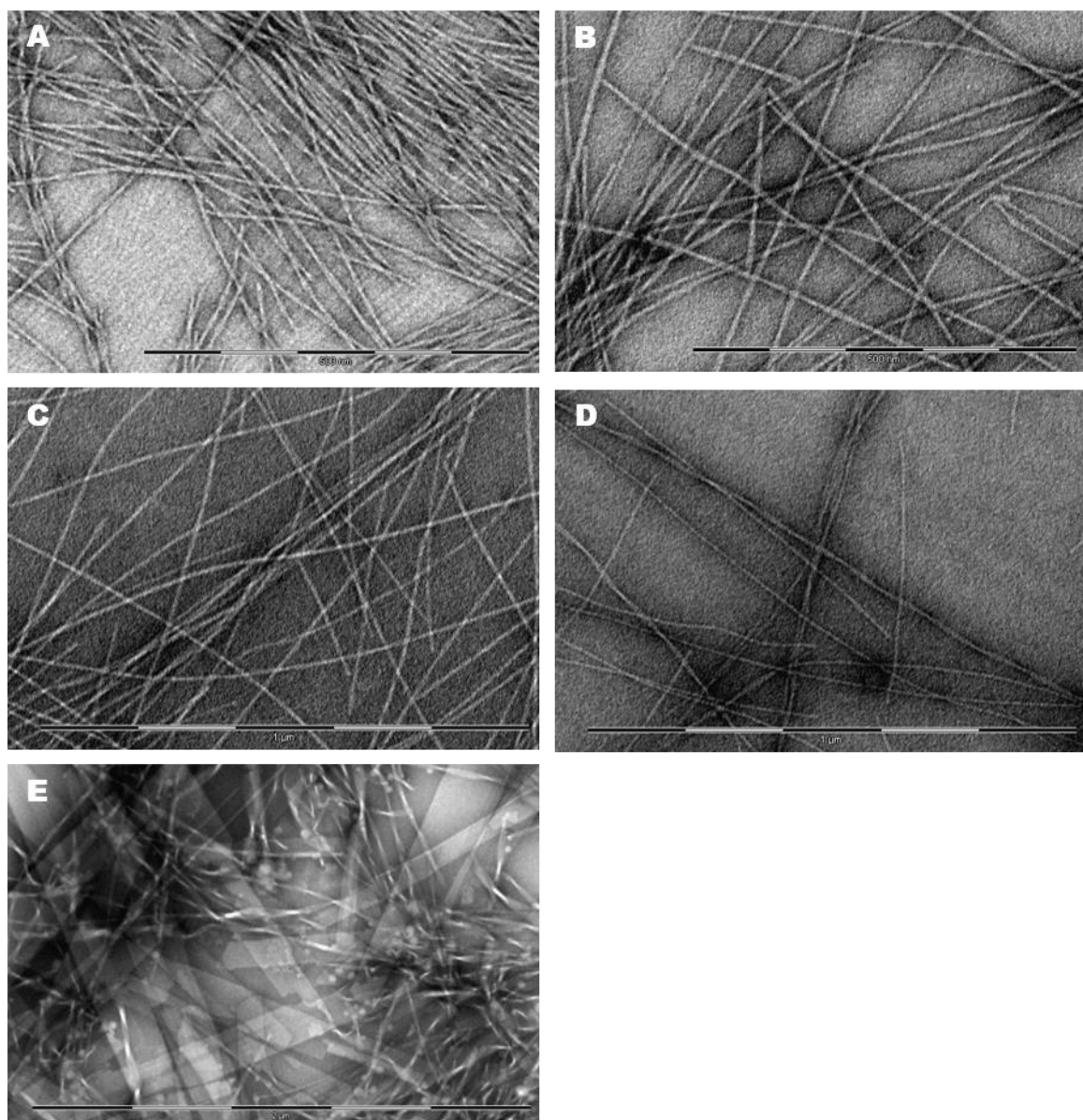
Figure 4.3: Negatively stained TEM imaged of A: Fmoc-FRGDF, B: 95% Fmoc-FRGDF with 5% Fmoc-FDIKRG C: 75% Fmoc-FRGDF with 25% Fmoc-FDIKRG D: 50% Fmoc-FRGDF with 50% Fmoc-FDIKRG E: Fmoc-FDIKRG.

Negative stained TEM micrographs are shown in Figure 4.3. The structures shown in this set of images are much clearer, with the greater contrast making it simpler to distinguish individual fibres. The hydrogels can be seen to consist of a composition-dependent mixture of straight or twisted fibres. In the Fmoc-FRGDF containing hydrogels, some twisted fibres are visible, some of these are more apparent than others. In the Fmoc-FDIKRG sample, we see a combination of ribbon like fibres, the twisted region, and large sheet like fibres. Many of these structures are suggested by the cryoTEM images of the same compositions. By combining these complementary methods, we can confidently interpret the morphology of these hydrogels.

The negative stain reveals an interesting feature, as seen in Figure 4.3D. At least some of the highly twisted fibres 50% Fmoc-FDIKRG are actually 2 smaller fibres twisting around each other. Possibly explaining the larger fibre diameter and standard deviation measured in this sample compared to the other blended hydrogels.

Fibre diameters were not measured from the negatively stained micrographs, as it was possible to determine the diameter of the fibres from the CryoTEM micrographs, giving the most accurate measure of fibre size.

4.3.4 Biocompatibility of Fmoc hydrogel blends

SH-SY5Y cells are a human derived cell line, which is frequently used as an *in vitro* model for neuronal function and differentiation. These cells were used to assess the biocompatibility of these materials. MTS assays and fluorescent Live/Dead stain were used in combination, as this gives a good indication of not only the survival of cells, but also the proliferation of cells over time on these materials.

Table 4.2: Hydrogel compositions used in biocompatibility assays.

		Composition	
		Fmoc-FRGDF-OH	Fmoc-FDIKRG-OH
Gel	1	100%	0%
	2	90%	10%
	3	75%	25%
	4	50%	50%

Hydrogels were prepared at 10 mg/mL. Compositions used are outlined in Table 4.2. They were prepared in a 96 well culture dish, using the CO_2 diffusion method. They were then equilibrated to physiological pH by rinsing twice with 200 µl PBS. Complete culture media was then left on the hydrogels overnight. Cells were seeded at 10^5 cells per well. Live/Dead assays and MTS assays were conducted on cells grown on the hydrogels at 24 hours after seeding.

After 1 day *in vitro*, the only hydrogel of this series which showed significant cell survival was the 50% Fmoc-FDIKRG condition, as seen in Figure 4.4. All other hydrogels showed poor survival. Unfortunately, due to the clustering of the cells on this material, it is difficult to quantify the live-dead ratio.
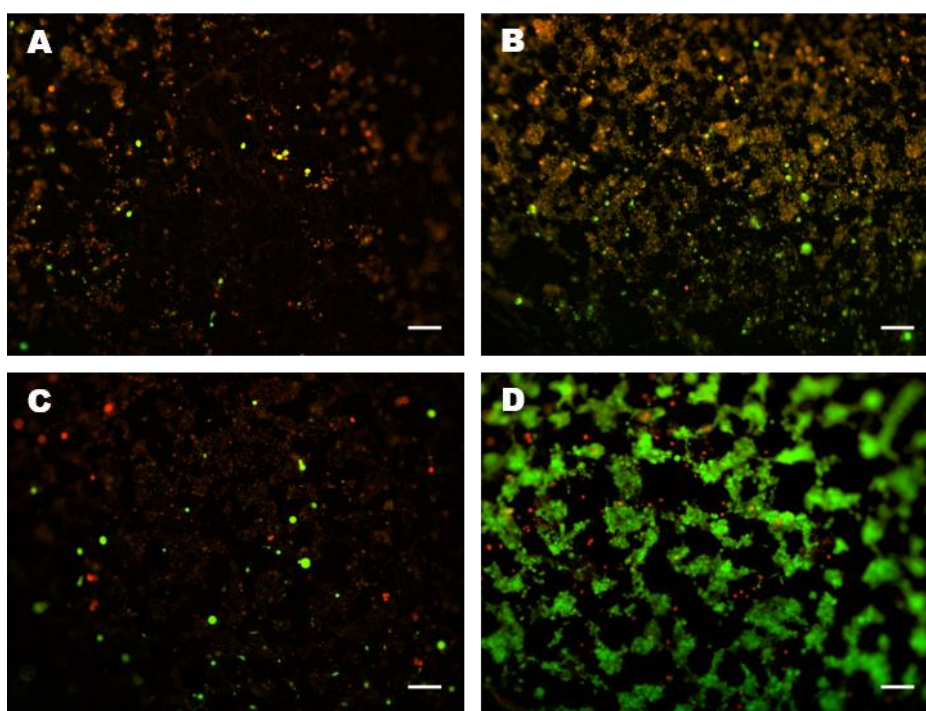
Figure 4.4: Micrographs of cells cultured for 24 hours, and stained using a Live/Dead assay. A: Gel 1 B: Gel 2 C: Gel 3 D: Gel 4. Scale Bar 250 micron.

An MTS assay was conducted in parallel with the live/dead assay (Figure 4.5). After subtracting the background, and normalising the readings to the highest absorbance, the 50% FDIKRG showed 10 times the metabolic activity of any other tested hydrogel, which supports the live/dead data.
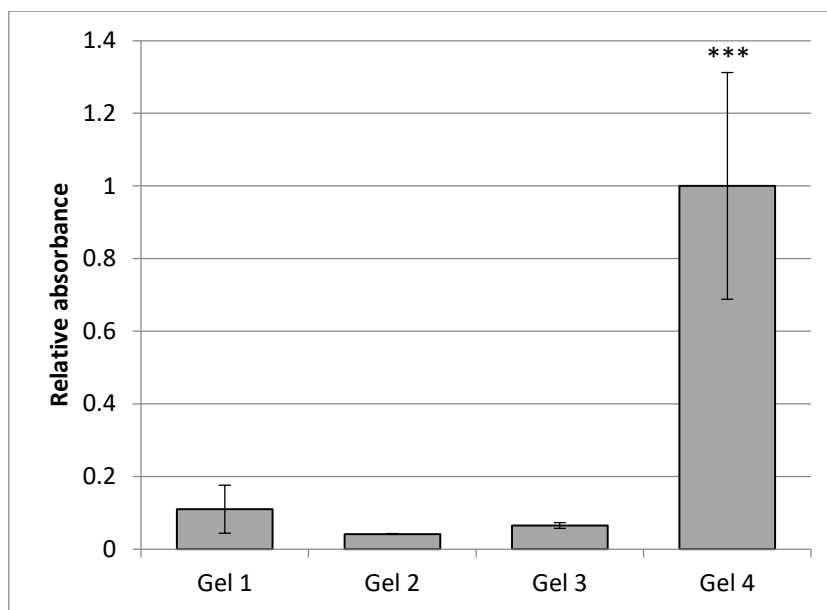
Figure 4.5: Relative MTS absorbance from cells grown on different hydrogels. Gel 4 is significantly greater than all other conditions (P<0.001)

To determine the cause of the cell death observed in Gel 1, 2 and 3, a conditioned media experiment was conducted. The aim was to determine if a component of the hydrogels was leeching out and causing the toxicity observed. It has been shown that at high concentrations, degradation products of Fmoc hydrogels (specifically Fmoc-FF) cause cell necrosis in a variety of cell lines in vitro[12]. Gels were prepared as previously described. Then, complete culture media was left on top of the gels overnight. This modified media was then collected, and serial dilutions were made. Cells cultured on TCPS were incubated in this media overnight. An MTS assay was conducted on these cells and MTS readings were normalised to a TCPS control after subtracting background absorbance. Results are shown in Figure 4.6. All conditions at 100% concentration of the conditioned media led to reduced MTS reading, but the conditioned media from Gel 4 was significantly better than the other compositions tested, with cells grown on this gel exhibiting 50% the metabolic activity of untreated cells, compared to <20% for all other hydrogels. The 50% FDIKRG conditioned media continues to be the least detrimental over several serial dilutions of the media.
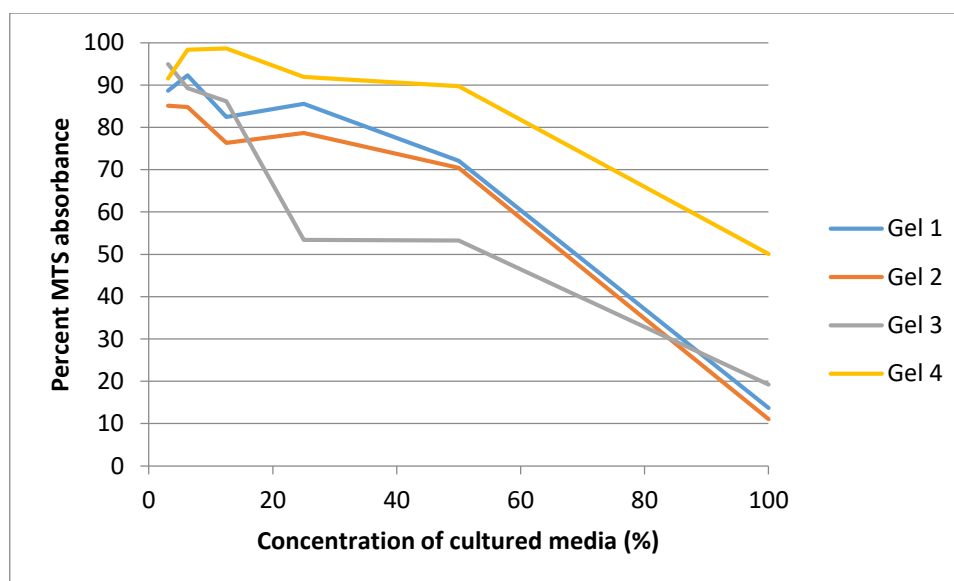
Figure 4.6: Relative absorbance from an MTS assay conducted with conditioned media from different hydrogels.

This indicates that a compound present in the Fmoc-FRGDF hydrogel and the blended hydrogels containing a majority of Fmoc-FRGDF is leeching out of the gels, and causing the cell death. This trend in unexpected, as the gel modulus increases with higher Fmoc-FRGDF content as seen in Figure 4.1. These high modulus gels would be expected to release fewer peptide fragments than the softer Fmoc-FDIKRG rich gels. All gels were prepared identically, with multiple rinses of PBS before preparing the conditioned media, so TFA residue is unlikely to be the cause[13]. Published studies suggested that the Fmoc-FRGDF hydrogel would be biocompatible with neural cell lines.

Self-assembled Fmoc hydrogels are typically prepared using HCl[14], [15] or GDL[16], [17] to obtain the appropriate pH and trigger gelation. The gels in this chapter are prepared using CO_2 diffusion. Therefore, it was deemed necessary to compare cell growth on CO_2 gels to growth on the same composition created *via* a more conventional method. In the literature, Fmoc-FRGDF is usually prepared by the HCl method[1], [5], so this was used for the comparison. This would determine whether the cause of cell death was associated with the pH trigger used in preparation of the hydrogels. SN4741 neural cells were seeded at 1000 cells per well on 100% Fmoc-FRGDF gels prepared using CO_2 or HCl, alongside untreated cells in a culture dish as a positive control, or cells plus DMSO as a negative control. MTS assays were conducted after 24 hours. As seen in Figure 4.7, cell metabolism was

very low on both Fmoc-FRGDF gels regardless of preparation method. These results suggest that the method of hydrogel preparation is not the cause of the observed cell death.
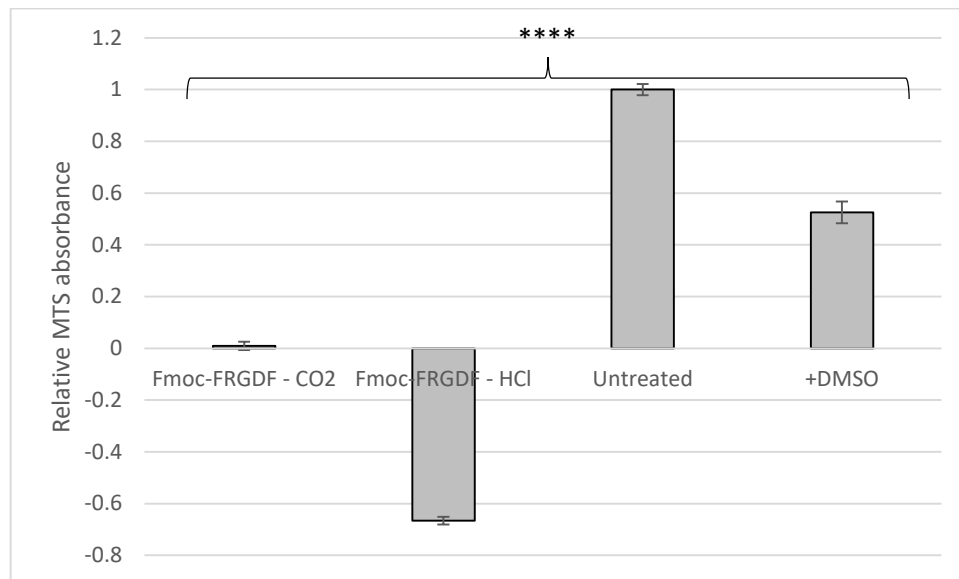

Figure 4.7: MTS assay of SN4741 cells grown on Fmoc-FRGDF prepared using either CO_2 diffusion or HCl addition, with untreated cells, and cells +DMSO as controls. All values are significantly different (P<0.0001)

One possible cause for the improved cell survival observed in cultures of SH-SY5Y and SN4741 cells is that both of these cell lines express the TrkB receptor, and that at high enough concentrations, Fmoc-FDIKRG is able to activate TrkB, and improve cell survival. Alternatively, as Fmoc-FRGDF appears to be cytotoxic to these cells, simply reducing the concentration of this component may be sufficient to explain the cause of improved cell survival.

4.3.5 Measuring the biological activity of Fmoc-FDIKRG

It was hypothesised in chapter 3 that the Fmoc-FDIKRG peptide gel is able to activate the TrkB receptor in a similar fashion to free BDNF. This was initially assessed using the SHSY5Y and SN4741 cell lines. Cells were treated with 20ng/mL BDNF, as was used in the paper which originally described the IKRG peptide[18]. GNF5837, a selective pan-Trk inhibitor[19] was used to block the TrkB receptor, and therefore the activity of BDNF or the peptides. Controls for these tests were untreated cells on TCPS, as a baseline. Activation of TrkB was examined via Western Blot. Initial experiments were unsuccessful in detecting pTrkB, even after multiple repeats. It was unclear if this result was due to the cells or antibodies, so further testing was

conducted with NIH 3T3 cells, which were transfected to express TrkB (Kindly donated by David Kaplan). However, after finally optimising the western blot and staining protocol, and using a whole brain lysate as a positive control, no pTrkB was detectable (Figure 4.8). This was despite culturing the cells with G418 to maintain transgene expression.
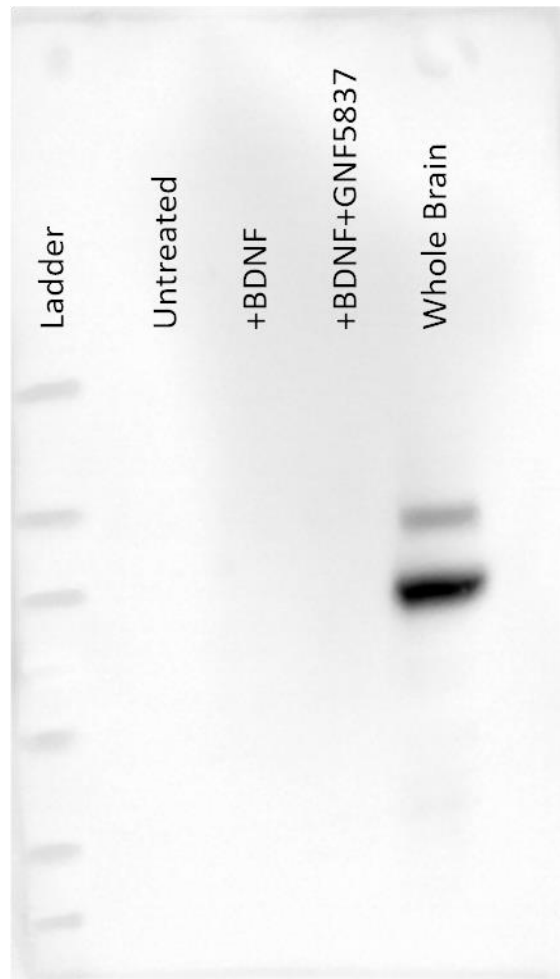

Figure 4.8: Negative result for TrkB receptor in NIH 3T3 cells transfected with TrkB

In order to determine whether the Fmoc-FDIKRG peptide is able to activate the TrkB receptor as hypothesised, western blots were repeated using primary mixed hippocampal/cortical neuron cultures. Primary cells remove the uncertainty of protein expression, and therefore give the greatest chance of observing the desired result, as well as being a more accurate model than cell lines.
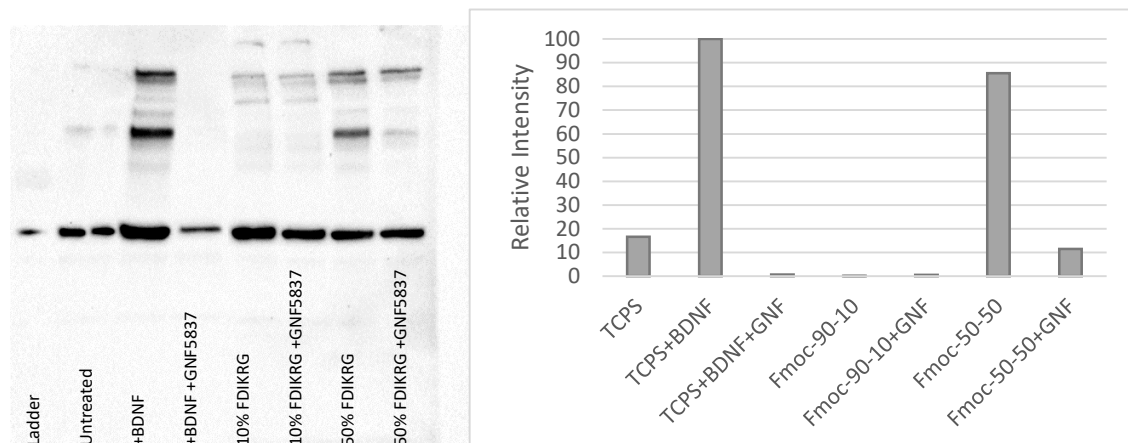
Figure 4.9: TrkB and β-tubulin stained western blot, Intensity of pTrkB band normalised first to β-tubulin, then to the highest signal, +BDNF.

Controls used were, untreated cells, cells treated with 20ng/mL soluble BDNF protein, and cells pre-treated with GNF5837, then treated with soluble BDNF. The hydrogels tested in this experiment were blended Fmoc-FRGDF and Fmoc-FDIKRG hydrogels, containing 10% and 50% Fmoc-FDIKRG respectively, each with an inhibited condition. The first series of experiments is shown in Figure 4.9, in which the function of soluble BDNF and the inhibitor perform as expected, with BDNF potently activating TrkB, and GNF5837 inhibiting this. The 10% Fmoc-FDIKRG hydrogel was unable to phosphorylate TrkB in the primary cells. The 50% Fmoc-FDIKRG hydrogel produced 85% of the activity of soluble BDNF, indicating that the IKRG motif is bioavailable, and highly functional in this state. In the paper which first described the IKRG peptide, treatment with 20 ng/mL soluble BDNF resulted in six times more pTrkB than the control condition, and 1 μM IKRG peptide resulted in approximately 1.8 times the activation of the control[18], indicating that the gel 4 is more effective than 1 μM of soluble IKRG peptide at activating TrkB.
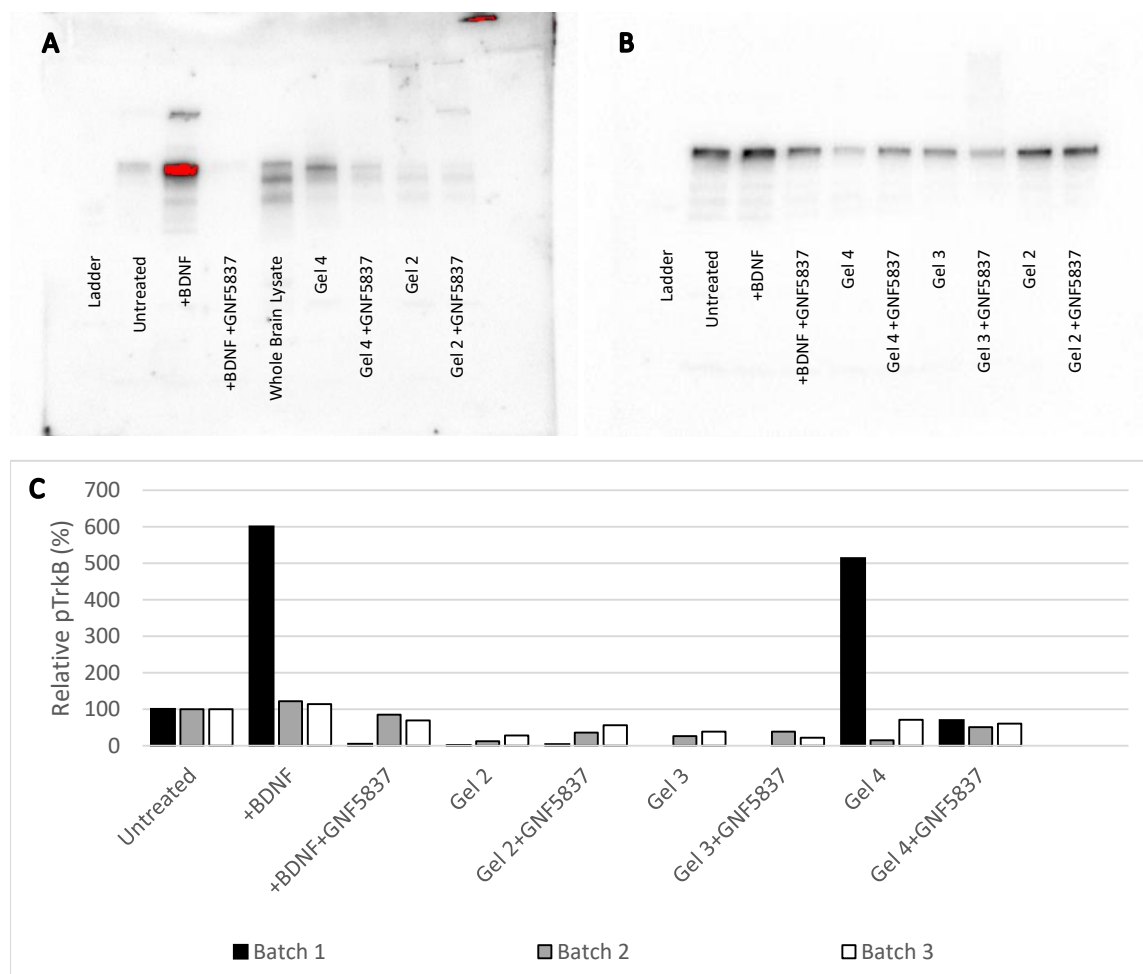
Figure 4.10: Western blots of the A: first and B: second set of lysates. C: Graphed pTrkB intensity for 3 sets of western blots. No results are statistically significant.

This experiment was repeated with a 25% FDIKRG condition added, to determine whether there was a dose response effect for the IKRG containing peptide gels. The results of all repeats of this experiment are shown in Figure 4.10C. The three control conditions used were the same, but showed considerably less difference than in the first experiment. This indicated that both the BDNF and GNF5837 had potentially deteriorated between experiments. None of the hydrogels from the repeated experiment had any more pTrkB than any of the three control samples, including 50% Fmoc-FDIKRG. The method and times of incubation did not change between repeats. This inconsistency between experiments, leaves us uncertain as to the biological function of these materials. Unfortunately, due to time constraints, further repeats of this experiment were not possible, so a conclusive result was not achieved.

4.4 Conclusion

The functional small peptide, Fmoc-FDIKRG developed in this chapter has proven to be biocompatible, and capable of co-assembly with the previously published Fmoc-FRGDF peptide. Fmoc-FRGDF was found to be incompatible with the cell lines tested in this work, although this effect was significantly reduced when blended 1:1 with the Fmoc-FDIKRG peptide. Cells treated with the 1:1 peptide blend for 20 minutes showed TrkB phosphorylation equivalent to 85% of 20ng/mL BDNF full protein, which is significantly higher than that reported for IKRG alone [18]. Repeated testing however did not support this early result. Repeated experiments, with fresh reagents would hopefully enable a conclusive result.

4.5 References

[1]   V. N. Modepalli, A. L. Rodriguez, R. Li, S. Pavuluri, K. R. Nicholas, C. J. Barrow, D. R. Nisbet, and R. J. Williams, "In vitro response to functionalized self-assembled peptide scaffolds for three-dimensional cell culture," *Biopolymers*, vol. 102, no. 2, pp. 197–205, Mar. 2014.

[2]   R. Li, C. C. Horgan, B. Long, A. L. Rodriguez, L. Mather, C. J. Barrow, D. R. Nisbet, and R. J. Williams, "Tuning the mechanical and morphological properties of self-assembled peptide hydrogels via control over the gelation mechanism through regulation of ionic strength and the rate of pH change," *RSC Adv.*, vol. 5, no. 1, pp. 301–307, 2015.

[3]   C. C. Horgan, A. L. Rodriguez, R. Li, K. F. Bruggeman, N. Stupka, J. K. Raynes, L. Day, J. W. White, R. J. Williams, and D. R. Nisbet, "Characterisation of minimalist co-assembled fluorenylmethyloxycarbonyl self-assembling peptide systems for presentation of multiple bioactive peptides," *Acta Biomater.*, vol. 38, pp. 11–22, Jul. 2016.

[4]   R. Li, S. Pavuluri, K. Bruggeman, B. M. Long, A. J. Parnell, A. Martel, S. R. Parnell, F. M. Pfeffer, A. J. C. Dennison, K. R. Nicholas, C. J. Barrow, D. R. Nisbet, and R. J. Williams, "Coassembled nanostructured bioscaffold reduces the expression of proinflammatory cytokines to induce apoptosis in epithelial cancer cells," *Nanomedicine Nanotechnology, Biol. Med.*, vol. 12, no. 5, pp. 1397–1407, Jul. 2016.

[5]   R. Li, M. Boyd-Moss, B. Long, A. Martel, A. Parnell, A. J. C. Dennison, C. J. Barrow, D. R. Nisbet, and R. J. Williams, "Facile Control over the Supramolecular Ordering of Self-assembled Peptide Scaffolds by Simultaneous Assembly with a Polysacharride," *Sci. Rep.*, vol. 7, no. 1, p. 4797, Dec. 2017.

[6]   A. L. Rodriguez, T. Y. Wang, K. F. Bruggeman, C. C. Horgan, R. Li, R. J. Williams, C. L. Parish, and D. R. Nisbet, "In vivo assessment of grafted cortical neural progenitor cells and host response to functionalized self-assembling peptide hydrogels and the implications for tissue repair," *J. Mater. Chem. B*, vol. 2, no. 44, pp. 7771–7778, 2014.

[7]   F. L. Maclean, Y. Wang, R. Walker, M. K. Horne, R. J. Williams, and D. R. Nisbet, "Reducing Astrocytic Scarring after Traumatic Brain Injury with a Multifaceted Anti-Inflammatory Hydrogel System," *ACS Biomater. Sci. Eng.*, vol. 3, no. 10, pp. 2542–2549, Oct. 2017.

[8]   X. Du, J. Zhou, J. Shi, and B. Xu, "Supramolecular Hydrogelators and Hydrogels: From Soft Matter to Molecular Biomaterials," *Chem. Rev.*, vol. 115, no. 24, pp. 13165–13307, Dec. 2015.

[9]   J. Z. Gasiorowski and J. H. Collier, "Directed Intermixing in Multicomponent Self-Assembling Biomaterials," *Biomacromolecules*, vol. 12, no. 10, pp. 3549–3558, Oct. 2011.

[10]   J. C. Schense and J. A. Hubbell, "Three-dimensional Migration of Neurites Is Mediated by Adhesion Site Density and Affinity," *J. Biol. Chem.*, vol. 275, no. 10, pp. 6813–6818, Mar. 2000.

[11]   Y. Xie, X. Wang, R. Huang, W. Qi, Y. Wang, R. Su, and Z. He, "Electrostatic and Aromatic Interaction-Directed Supramolecular Self- Assembly of a Designed Fmoc-Tripeptide into Helical Nanoribbons," 2015.

[12]   W. T. Truong, Y. Su, D. Gloria, F. Braet, and P. Thordarson, "Dissolution and degradation of Fmoc-diphenylalanine self-assembled gels results in necrosis at high concentrations in vitro," *Biomater. Sci.*, vol. 3, no. 2, pp. 298–307, 2015.

[13]   S. Motamed, M. P. Del Borgo, K. Kulkarni, N. Habila, K. Zhou, P. Perlmutter, J. S. Forsythe, and M. I. Aguilar, "A self-assembling β-peptide hydrogel for neural tissue engineering," *Soft Matter*, vol. 12, no. 8, pp. 2243–2246, 2016.

[14]   A. M. Smith, R. J. Williams, C. Tang, P. Coppo, R. F. Collins, M. L. Turner, A. Saiani, and R. V. Ulijn, "Fmoc-Diphenylalanine Self Assembles to a Hydrogel via a Novel Architecture Based on π–π Interlocked β-Sheets," *Adv. Mater.*, vol. 20, no. 1, pp. 37–41, Jan. 2008.

[15]   V. Jayawarna, M. Ali, T. A. Jowitt, A. F. Miller, A. Saiani, J. E. Gough, and R. V. Ulijn, "Nanostructured Hydrogels for Three-Dimensional Cell Culture Through

Self-Assembly of Fluorenylmethoxycarbonyl–Dipeptides," *Adv. Mater.*, vol. 18, no. 5, pp. 611–614, Mar. 2006.

[16]   D. J. Adams, "Dipeptide and Tripeptide Conjugates as Low-Molecular-Weight Hydrogelators," *Macromol. Biosci.*, vol. 11, no. 2, pp. 160–173, Feb. 2011.

[17]   D. J. Adams, M. F. Butler, W. J. Frith, M. Kirkland, L. Mullen, and P. Sanderson, "A new method for maintaining homogeneity during liquid–hydrogel transitions using low molecular weight hydrogelators," *Soft Matter*, vol. 5, no. 9, p. 1856, 2009.

[18]   M. D. C. Cardenas-Aguayo, S. F. Kazim, I. Grundke-Iqbal, and K. Iqbal, "Neurogenic and Neurotrophic Effects of BDNF Peptides in Mouse Hippocampal Primary Neuronal Cell Cultures," *PLoS One*, vol. 8, no. 1, p. e53596, 2013.

[19]   P. Albaugh, Y. Fan, Y. Mi, F. Sun, F. Adrian, N. Li, Y. Jia, Y. Sarkisova, A. Kreusch, T. Hood, M. Lu, G. Liu, S. Huang, Z. Liu, J. Loren, T. Tuntland, D. S. Karanewsky, H. M. Seidel, and V. Molteni, "Discovery of GNF-5837, a Selective TRK Inhibitor with Efficacy in Rodent Cancer Tumor Models," *ACS Med. Chem. Lett.*, vol. 3, no. 2, pp. 140–145, Feb. 2012.

Chapter 5 Self-Complementary Peptide Hydrogels

5.1 Abstract

Developed in parallel with the Fmoc peptides discussed in chapters 3 and 4, another family of self-assembling peptide was investigated. It was hypothesised that changing the gel system would result in a different presentation of the IKRG ligand to cells, and thus yield a different cellular response. The system investigated was based around the self-complementary peptide H-FEFQFK-NH$_2$ (MBG-6). A variant of MBG-6 was synthesised, containing the IKRG motif, H-FEFQFKGGIKRG-NH (MBG-B5). This peptide was found to be biocompatible, stable under culture conditions, and was capable of phosphorylating TrkB *in vitro*.

5.2 Introduction

The self-complementary peptide hydrogel H-FEFQFK-NH$_2$ (MBG-6) has been used in the literature for the *in vivo* delivery of drugs[1], [2], and is the smallest self-complementary peptide hydrogel currently in the literature, at only 6 amino acids. Unlike the Fmoc peptide systems, the MBG-6 gel is capable of self-assembling in aqueous solutions without a pH switch, or other external stimulus. This was an attractive option, as it would simplify the potential development of this material as a 3D cell scaffold, as the gel could form around cells at physiological pH. In the Fmoc systems, where a pH or solvent switch is required to form the gel, the pre-gelled environment is unsuitable for cells, and therefore cell encapsulation is more difficult to achieve.

Self-complementary peptide hydrogels have been widely reported for use in biological applications[3]–[5], including some commercially available sequences. One commercially available example is PuraMatrix[6], [7], which is based the RADA family of peptides[8] and is used as a cell culture substrate[9]. Functionalisation of self-complementary peptides is far simpler than in Fmoc based peptide systems, as functional ligands can be conjugated to either the C or N terminal of the peptide and hydrogels still from the resulting peptides[3], [10]–[13]. In some instances, this has minimal effects on the hydrogels properties[13] while sometimes it can have a significant effect[3]. The functionalised version of the peptide can then be used alone,

or blended with the base peptide from which it was derived. Often, one or two glycine residues are used to separate the functional region of the peptide, and the self-assembly region[4], [13], [14]. This is done to improve bioavailability of the functional ligand. Within the self-complementary peptide hydrogel family, the hexa-peptide MBG-6 is the smallest, making it the simplest and cheapest to synthesise, while still possessing robust self-assembly under physiological pH and temperatures.

The MBG-6 self-assembling peptide system is attractive due to the ease of hydrogel formation. Ballet et al. have used it to investigate the *in vivo* delivery of opioids[1] and other biologically relevant small molecules[15]. This chapter focuses on the modification of the peptide MBG-6 with the IKRG functional group, which is of interest due to its ability to stimulate neural growth as previously discussed. Published self-complementary peptides with functional modifications frequently use glycine residues as a means of separating the biofunctional motif from the self-assembling region of the peptide, allowing for greater bioavailability of the functional motif[16]. This work involved the synthesis of a peptide, H-FEFQFKGGIKRG-NH (MBG-B5), which is capable of forming a self-supporting hydrogel in pH 7.4 PBS, at 37 degrees, much like MBG-6. Physical characterisation of the synthesised peptide, was conducted via rheology and TEM methods. Co-assembly of MBG-B5 and MBG-6 was investigated. Hydrogels composed of MBG-B5 were tested for biocompatibility, and the ability of the MBG-B5 peptide hydrogel to activate the TrkB receptor.

5.3 Results and discussion

5.3.1 Physical characterisation

The peptide hydrogel MBG-6 forms a self-supporting hydrogel within the concentration range of 10 to 20 mg/mL[1], [15]. Initially, 10 mg/mL was used to determine whether the modified peptide MBG-B5 was likely to form a hydrogel. After dissolving the peptide in PBS, and heating it to 60 degrees to ensure a homogenous solution, a soft hydrogel formed once the solution had cooled.

Following this, a series of vials were prepared consisting of a mixture of MBG-6 and MBG-B5 all at 10 mg/mL. All formed a self-supporting hydrogel following heating, mixing and cooling.

Figure 5.1: Hydrogels formed from A: MBG-6 and B: MBG-B5.

Rheological testing of MBG-B5 and MBG-6 revealed that MBG-B5 is a softer hydrogel compared to MBG-6. This is to be expected, as the functional section of the peptide, while containing both hydrophilic and hydrophobic residues, does not conform to the pattern used in the base self-assembling sequence. Modification of the widely investigated RADA hydrogels with functional groups has been shown to significantly influence the mechanical properties of the resulting hydrogels[3], which likely explains the significantly lower storage and loss modulus of it versus MBG-6 alone. The storage modulus of MBG-B5 at 10mg/mL is above 10kPa, making it appropriate for use in a range of applications in the body, and within the range of what is found in the central nervous system[17].
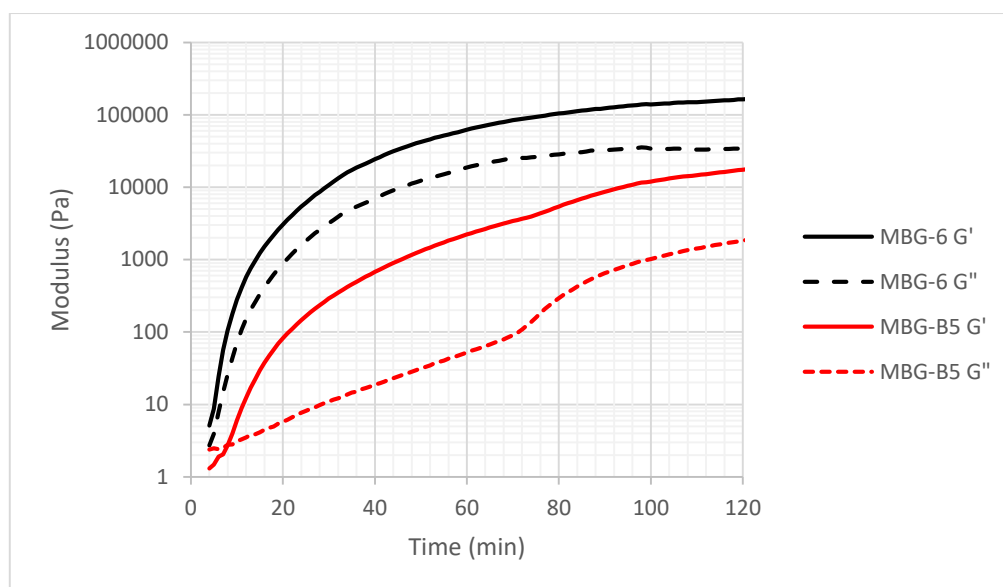
Figure 5.2: Storage and loss modulus of MBG-6 and MBG-B5 at 10mg/mL

As in previous chapters, the hydrogel morphology was investigated using a combination of CryoTEM and Negative stain. CryoTEM micrographs are shown in Figure 5.4. All hydrogels were composed of a dense network of nanofibers, the diameters of which are shown in

Figure 5.3. MBG-6 is composed of the narrowest fibres, at 3.7 nm, with MBG-B5 being 4.8 nm. The blended peptides fall between 5.4 and 4.2 nm diameter. Given the small difference between the fibre diameters in all samples, and similar morphology, it is difficult to say whether the fibres in the blended system are composed of two intertwined populations of fibres, or a single co-assembled type of fibre.

Negatively stained TEM micrographs are shown in Figure 5.5, in these, it is much easier to distinguish individual fibres. The heavy metal stain used, phosphotungstic acid allows for significant improvements in contrast, while still allowing for high resolution imaging. Drying samples onto the grid tends to increase the fibre density. Given the fibres observed in CryoTEM were already very densely packed, the samples were diluted 1:10 with PBS to disperse the fibres, and make imaging easier. If undiluted gels are used, the fibre density is too high, and distinguishing fibres becomes very difficult, and over-crowding of the grid also makes it difficult for the negative stain to settle around fibres.
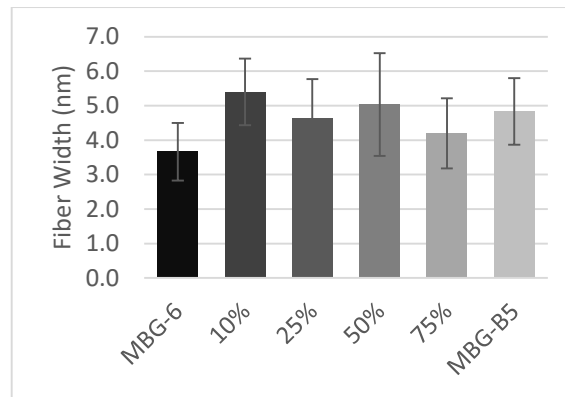
Figure 5.3: Fibre diameters for peptide hydrogels as determined using CryoTEM.

Comparing the two imaging methods, the fibres seen in negative stain appear similar in morphology to those observed by cryoTEM. Negative stain of MBG-B5, Figure 5.5 f) shows a bundling of the fibres not seen in the other samples, but by cryo methods, this is not observed. This bundling is likely an artefact caused either by the dilution process, when the mat of fibres was separated, or by the drying of the hydrogel on the carbon support grid. Other areas of the grid contained single fibres, similar to those seen in the other samples.
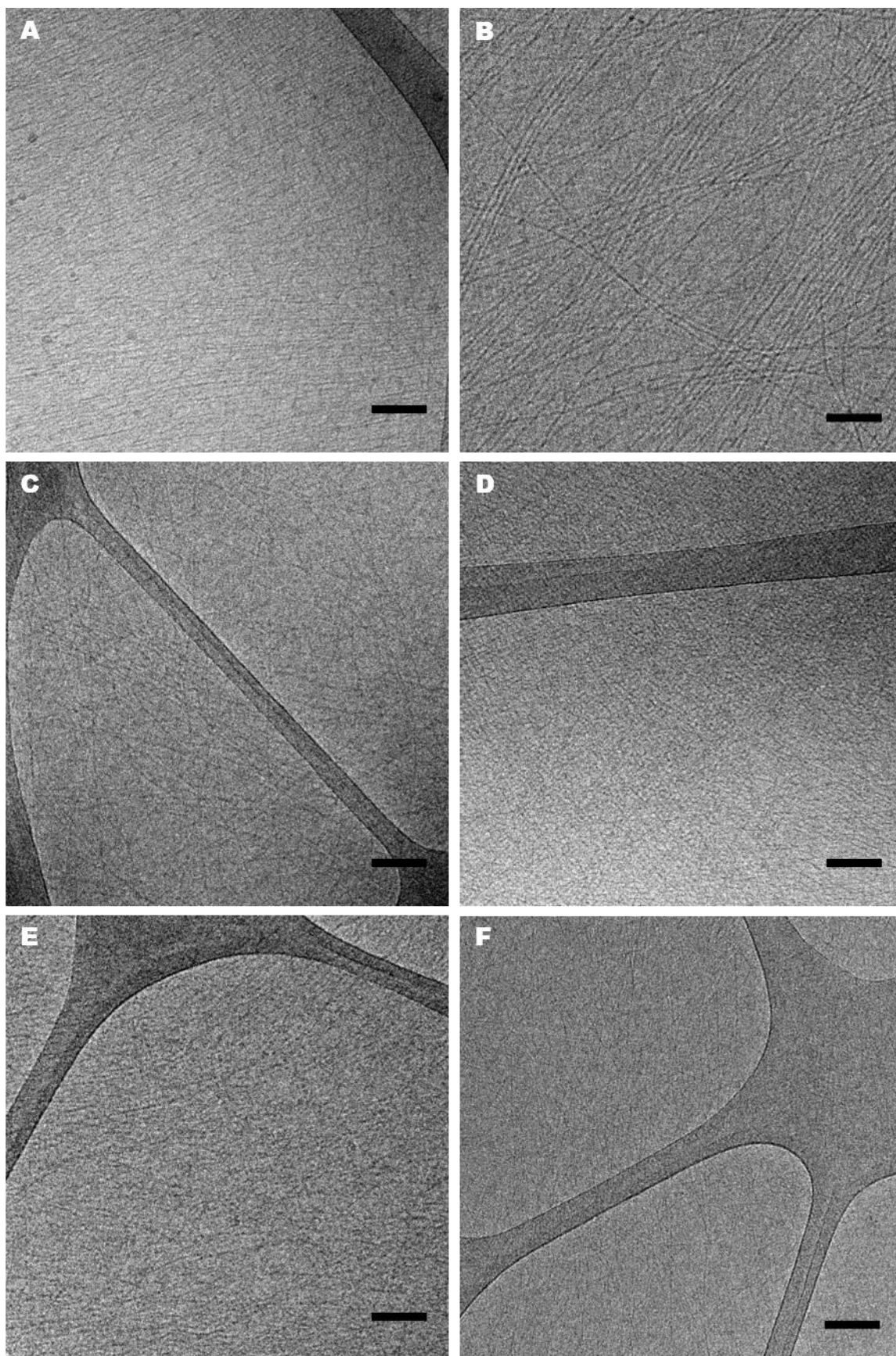
Figure 5.4: CryoTEM micrographs of A: MBG-6, B: 90% MBG-6 with 5% MBG-B5 C: 75% MBG-6 with 25% MBG-B5 D: 50% MBG-6 with 50% MBG-B5 E: 25% MBG-6 with 75% MBG-B5 F: MBG-B5. These images are cropped and brightness/contrast adjust to allow for easier viewing of fibres Scale Bars = 100nm
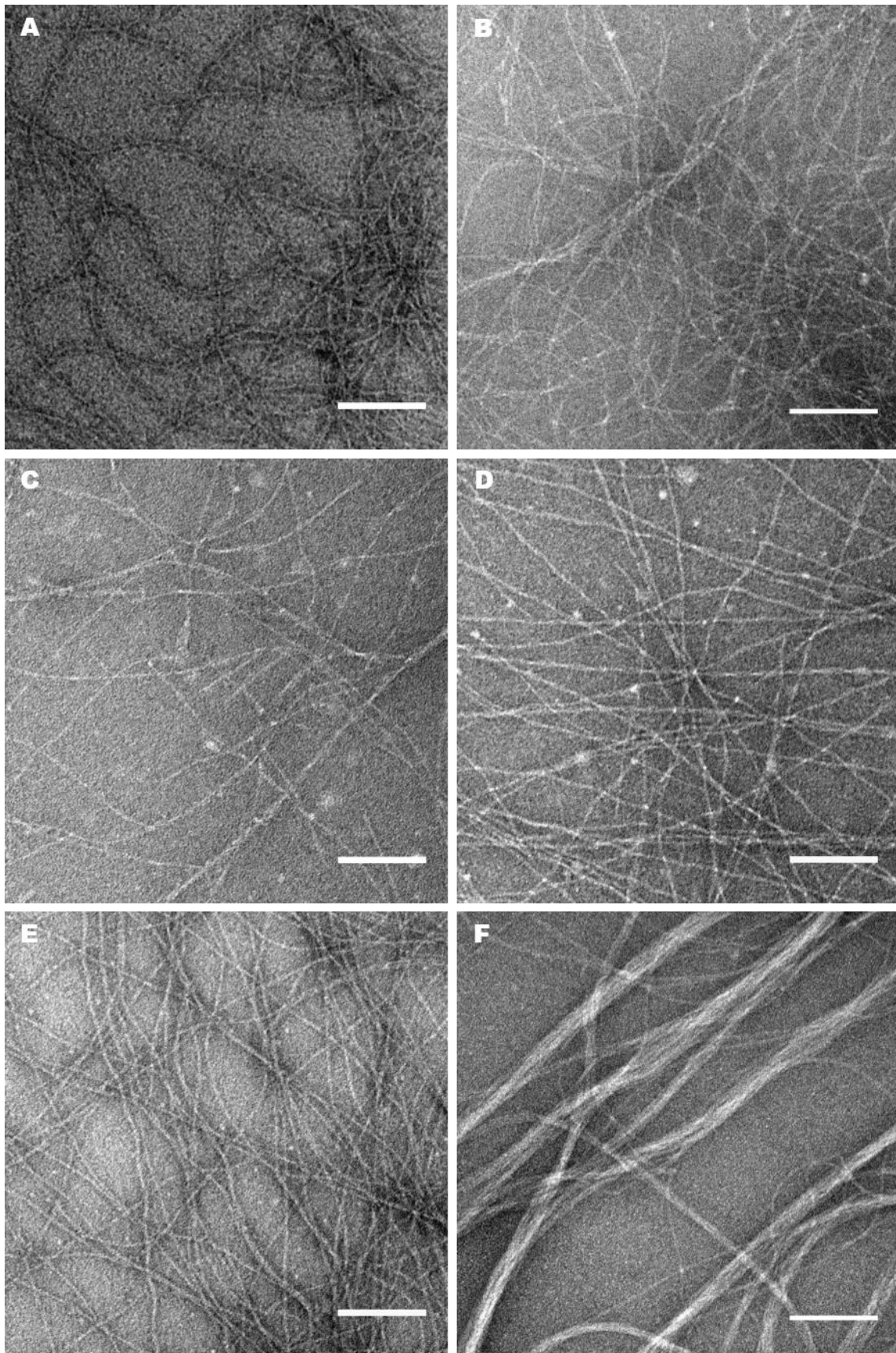
Figure 5.5: Negative Stain micrographs of hydrogels. A: MBG-6, B: 90% MBG-6 with 5% MBG-B5 C: 75% MBG-6 with 25% MBG-B5 D: 50% MBG-6 with 50% MBG-B5 E: 25% MBG-6 with 75% MBG-B5 F: MBG-B5. These images are cropped and brightness/contrast adjust to allow for easier viewing of fibres. Scale bars are 100nm

5.3.2 Biocompatibility

To understand the biocompatibility of these materials, MTS assays were used to investigate the metabolic activity of cells grown on MBG-6 and MBG-B5. NIH-3T3 cells grown on untreated culture plates were used as a positive control for these experiments, and all results were normalised to the TCPS reading.

The first MTS assay showed that at 2 days *in vitro*, MBG-6 and MBG-B5 had 67% and 5% respectively of the metabolic activity of the positive control. These gels were prepared at 20mg/mL. In MBG-6 wells, the gel had almost entirely degraded by the time this reading was made, despite the high peptide concentration. MBG-B5 however, was still present. This results however is questionable, as the MBG-B5 hydrogel was seen to develop a strong colour upon incubation in the MTS reagent. This was insoluble, and did not get transferred into the plate reader.

Following this initial MTS assay, MBG-6 was tested for biocompatibility using a fluorescent live/dead stain. Gels were prepared at 20mg/mL, and left to stabilise overnight before seeding with cells. After 24 hours incubation with cells, the cells were alive as seen in Figure 5.6, but the gels again, had entirely degraded, either by the cells, or the combination of temperature, and a component of the complete culture media. The rapid degradation of MBG-6 is undesirable for our application. Previous studies have shown favourable outcomes with materials that degrade over a period of 2-4 weeks[18], so somewhere in this window would be ideal. Despite this, the cells grown under these conditions have been shown to be alive. Therefore, the gels themselves, and their degradation products are unlikely to cause biocompatibility issues.
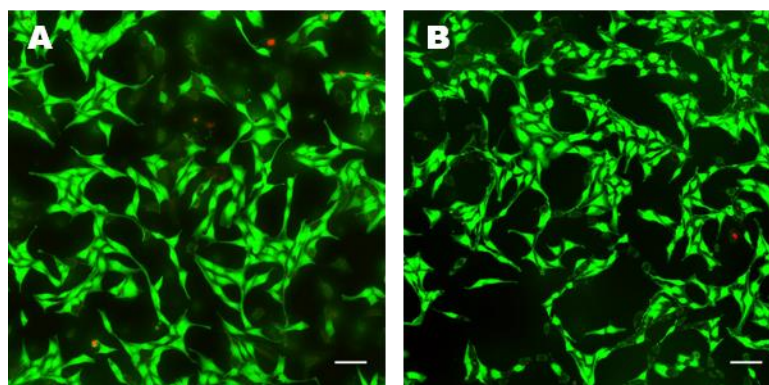
Figure 5.6: Live/Dead staining of cells grown on A: 20mg/ml MBG-6 and B: untreated cells. Scale bars 100 µm.

It has been demonstrated that this hydrogel is stable for greater that 24 hours in PBS[19], and it has been applied *in vivo,* where some degradation was observed within 12 hours of injection, but the hydrogel remained present for several days[15], so the cause of the observed degradation is not clear.

Follow up experiments on MBG-6 at 10mg/mL involved time points at day 2 and day 5, indicated that the cells grown under these conditions had 100% ±8.5% and 92.6% ±0.6% of the metabolic activity of the positive control respectively (Figure 5.7).
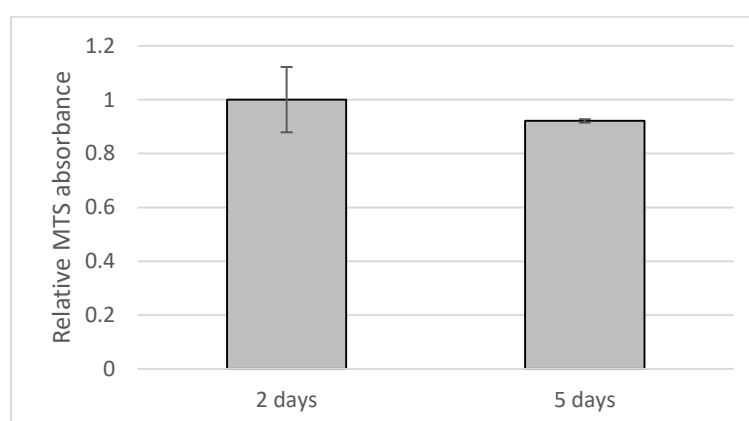

Figure 5.7: MTS results of 2 and 5 days in vitro cultures on MBG-6.

MBG-6 gels were prepared containing 5wt% MBG-B5 and live dead assays were conducted. Micrographs of cells grown on these materials and untreated controls are shown in Figure 5.9. The live to dead cell ratio is very favourable, and, for MBG-6 agrees with the MTS data. By day 2, the hydrogels had completely degraded, and cells were growing on the base of the culture plate. This showed us that at 10mg/mL, MBG-6 is not cytotoxic. Additionally, the inclusion of 5% MBG-B5 into the hydrogel had no significant effect on cell viability.
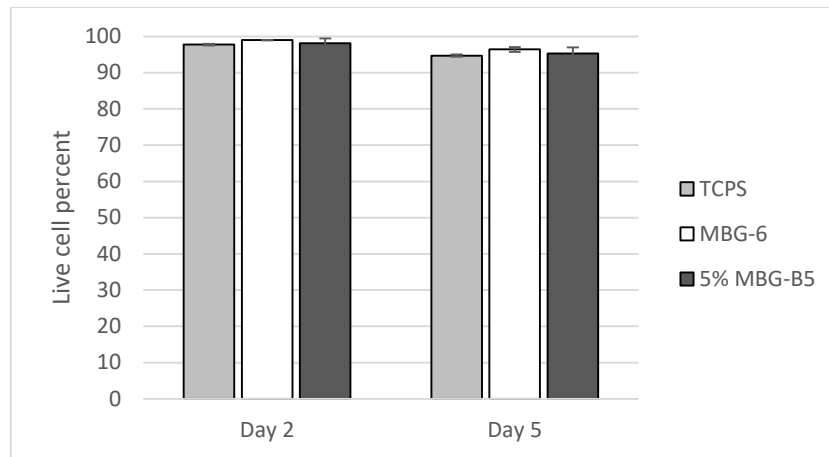
Figure 5.8: Live:Dead cell percent for cells cultures on MBG-6 hydrogels and a control, at 2 and 5 days in vivo.
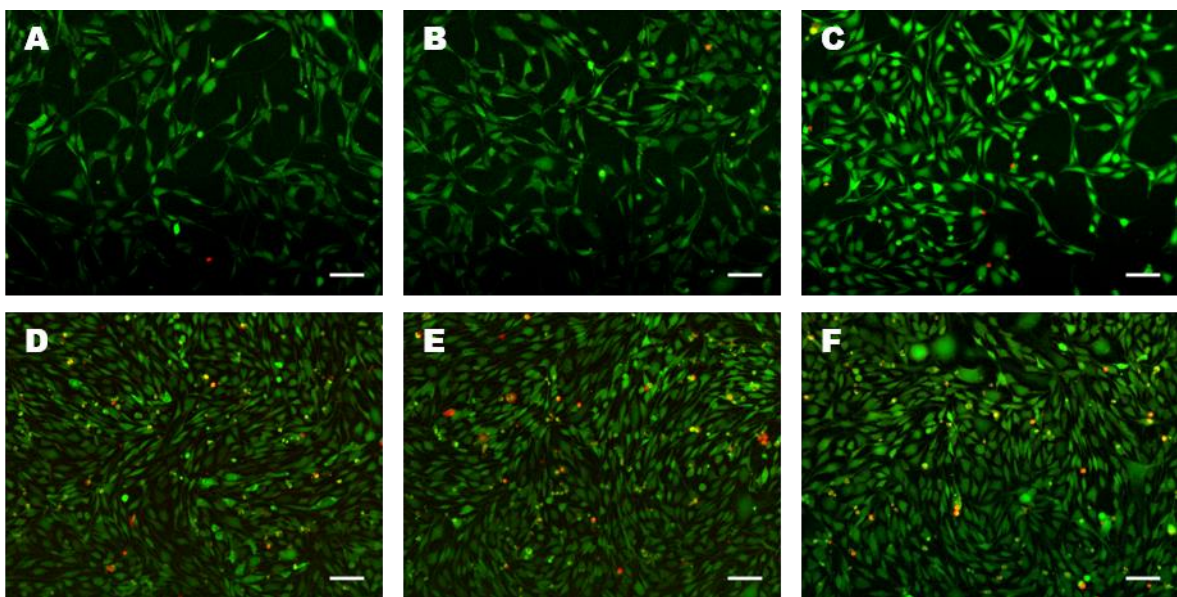

Figure 5.9: NIH-3T3 cells cultured for 2 days. A: MBG-6, B: MBG-6 +5% MBG-B5 and C: Control. And for 5 days. D: MBG-6, E: MBG-6 +5% MBG-B5 and F: Control. Scale bars 100 μm.

A conditioned media experiment was conducted, in which gels were incubated in complete culture media overnight, this was collected, and serial 2x dilutions performed. Cells were plated into untreated wells. After 24 hours their media was exchanged for the conditioned media. After a further 24 hours, the MTS assay was conducted. Figure 5.10 shows that there is a component of the hydrogels which is leeching out, and negatively affecting the growth of these cells, in a concentration dependant manner.
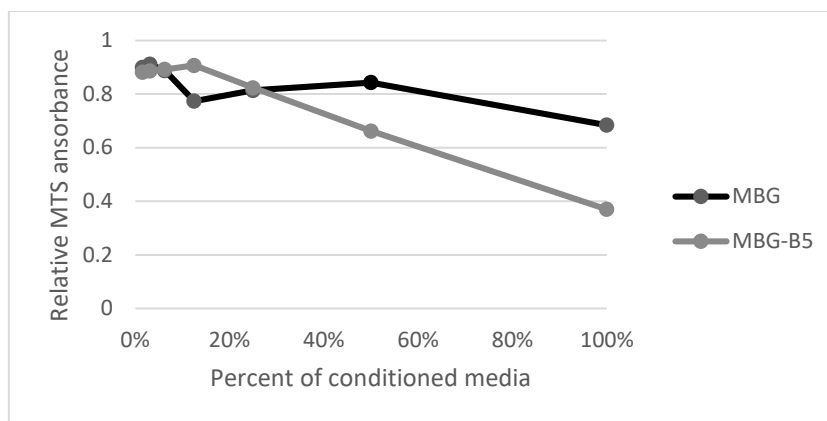
Figure 5.10: MTS results of conditioned media experiment. A component of the MBG hydrogels appears to be leeching out, and affecting cell activity. At a quarter concentration, the effect is considerably reduced.

MTS assays were also repeated with MBG-B5 at 10mg/mL. Since the gel is stable long term under culture conditions, a lower peptide concentration may reduce the leeching effect demonstrated in the conditioned media experiment, and improve cell survival. The MTS assay was conducted at 24 hours *in vitro*. These follow up assays indicated metabolic activity 72% ± 26% compared to untreated cells, a significant improvement over previous results. At 10mg/mL, MBG-B5 hydrogels provide a good environment for cell growth. At a lower peptide concentration, the colour absorbtion of the MTS reagent observed previously was less pronounced.
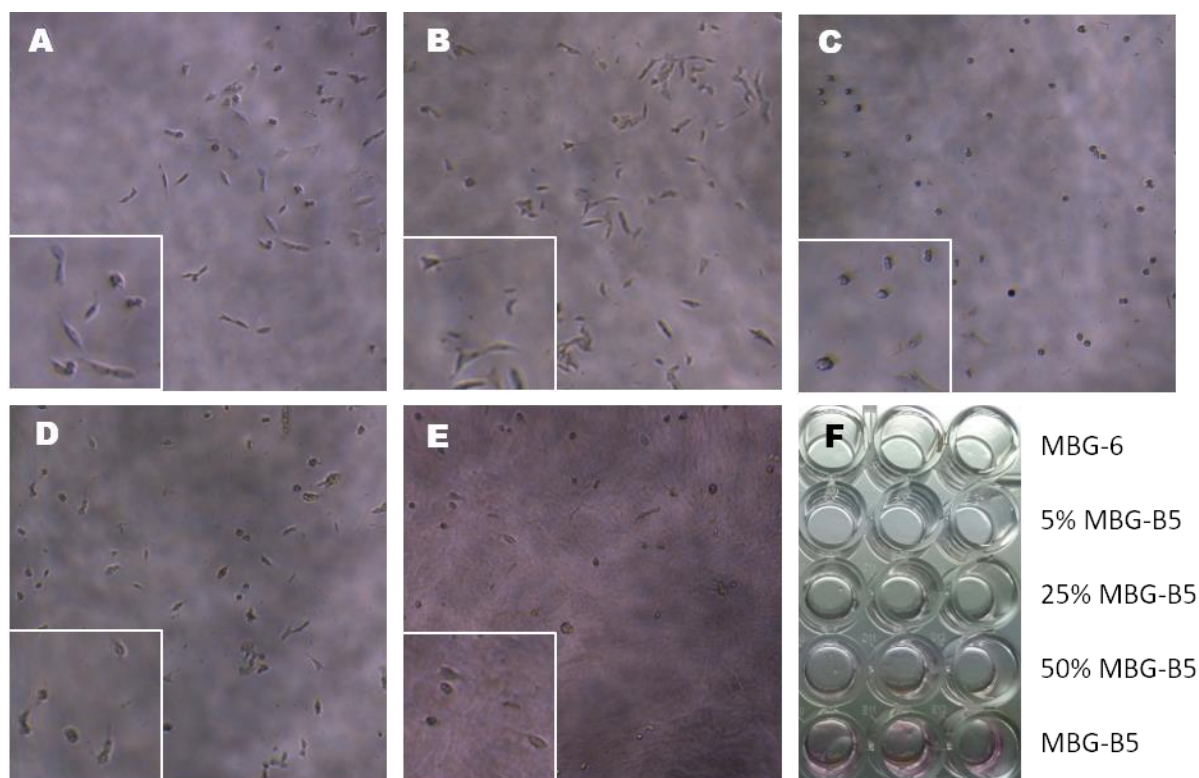
Figure 5.11: Micrographs of hydrogels composed of A: MBG-6, B: 5% MBG-B5, C: 25% MBG-B5, D: 50% MBG-B5 and E MBG-B5 and F: an image of culture plate containing MBG hydrogels after24 hours cell culture.

Figure 5.11F shows the typical state of the hydrogels after 24 hours in culture conditions. MBG-B5 is the only gel still present after this time. Cells were still growing in all wells. Unstained micrographs of each condition are also shown. In Figure 5.11A-C, the cells are all in a single focal plane, and show well developed processes. Figure 5.11F clearly shows that the gel in the 50% MBG-B5 wells has degraded, however these cells do not have elongated processes. Figure 5.11E shows cells growing on MBG-B5. Some processes are visible, but these are less elongated, and not present for every cell, and the cells are in different focal planes.
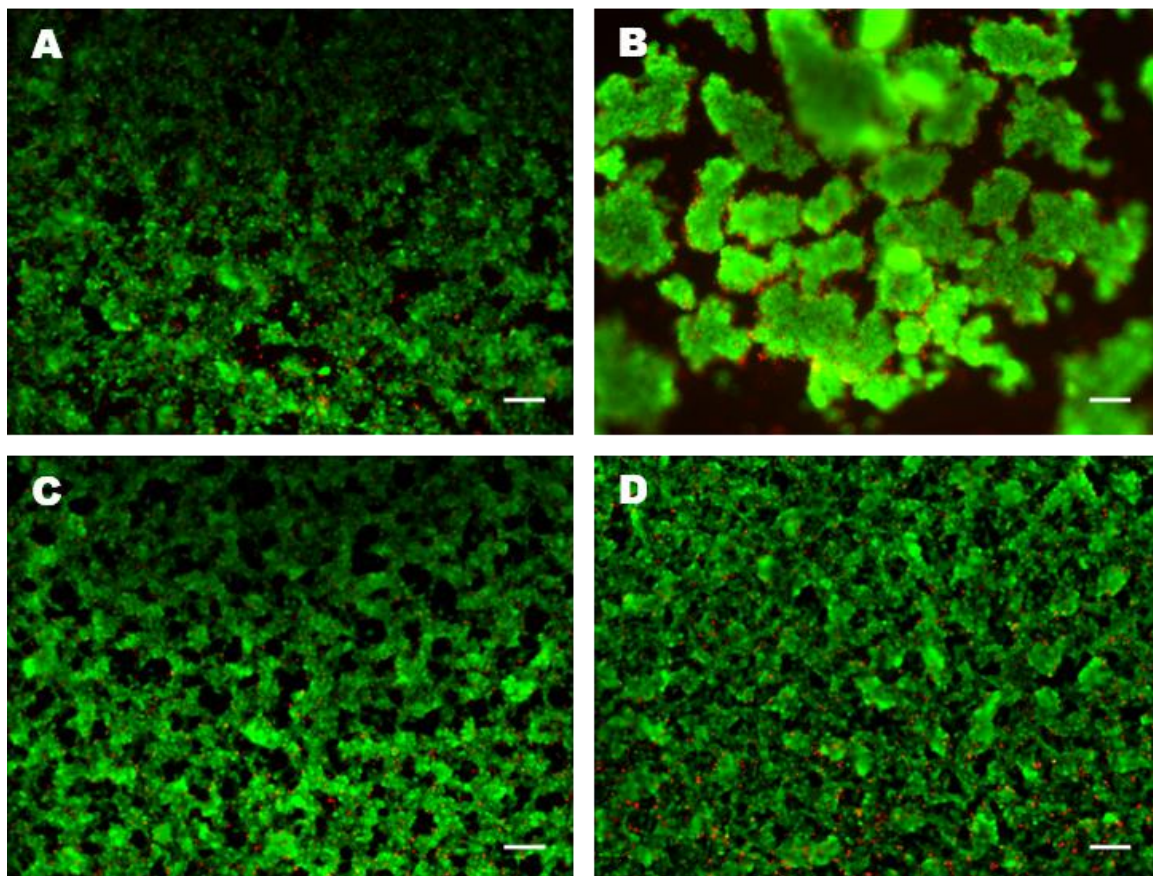

Figure 5.12: SH-SY5Y cells grown on MBG-B5 at A: 1 day and B: 5 days, and untreated cells at C: 1 day and D: 5 days.

Having now demonstrated the ability of MBG-B5 to survive in culture conditions, and that it is able to support the growth of mammalian cells, MBG-B5 hydrogels were tested for biocompatibility with a neural cell line, SH-SY5Y, with a 1 and 5 day time point used for both MTS and live/dead staining. The MTS results showed that cells grown on these gels had only 16% and 24% the metabolic activity of untreated cells at 1 and 5 days respectively. However, the live/dead staining showed a more

favourable live to dead cell ratio at both time points. Unfortunately, it was very difficult to quantify the differences, as the cells tended to cluster on the hydrogel, especially at 5 days. The large number of stained live cells indicated that MBG-B5 is biocompatible with the SH-SY5Y neural cell line. There was noticeable auto-fluorescence of the hydrogel in the red channel, which meant characterisation of a live : dead ratio by thresholding and comparing the relative area of red to green cells was not possible. Percent area coverage of live cells was the best metric available for characterisation of these samples, however, due to the 3D nature of the hydrogels, there are likely some cells out of plane which are not captured in the image, and therefore distort this characterisation.

Repeats of this experiment were undertaken with a lower cell seeding density, 5000 cells per well, in order to simplify characterisation of the biocompatibility of the hydrogel, and reduce overcrowding ass seen in Figure 5.12. Results were also collected at day 1 and 3, to reduce the chances of over-crowding of the hydrogels as cells proliferate. Additionally, serum-free conditions were included, to investigate whether cells are capable of adhering to the hydrogel in the absence of serum proteins.
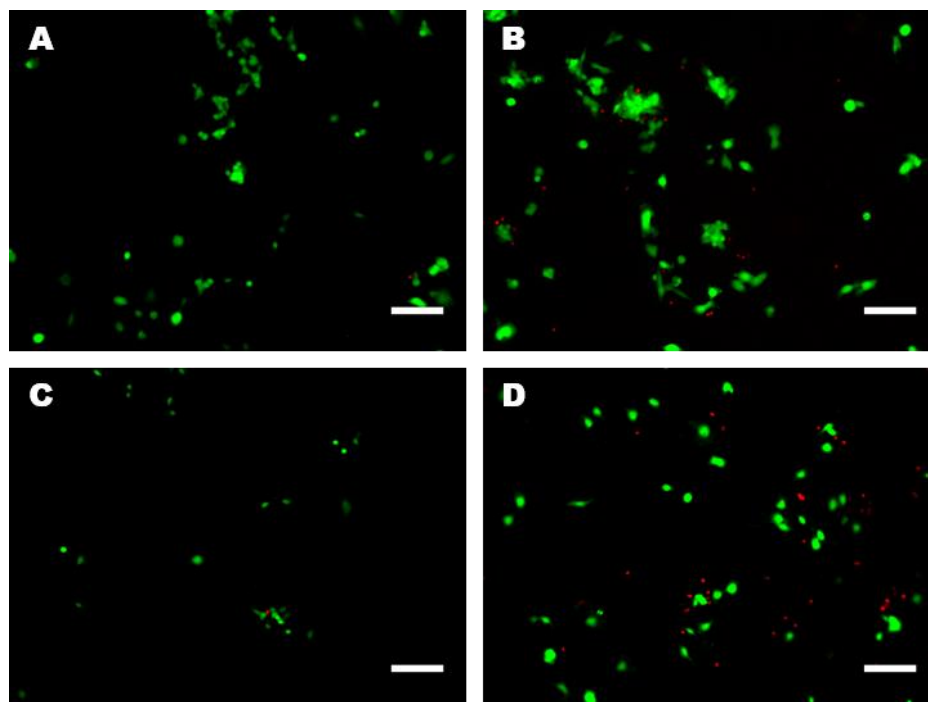

Figure 5.13: SH-SY5Y cells after 1 day culture. A: Control, B: MBG-B5 hydrogel, C: Cells plated and cultured in serum-free media, and D: Cells growing on MBG-B5 hydrogels plated and cultured in serum-free media. Scale bar: 100 µm.

Day 1 images are shown in Figure 5.13. With serum, there is a small difference in live : dead ratio between the control and MBG-B5 hydrogel, as shown in Figure 5.14A, with evidence of cells spreading in both conditions. In the serum-free wells, the cells grown in an untreated well have a favourable live : dead ratio. This ratio however is likely caused due to most of the dead cells detatching during a wash, and therefore not being present to count. The low number of live cells in the image indicates this is likely. Cells grown on MBG-B5 in serum free conditions show some spreading, more than observed on the untreated serum-free plate, indicating the cells are able to adhere to some extent to the hydrogel, the live : dead ratio however is much lower than all other conditions at 50±3%.

There are more dead cells present in the hydrogel wells than in the controls, particularly in the serum free condition. However, these cells are likely embedded in the hydrogel, and therefore were not washed off when exchanging media for the live : dead staining solution, as would have happened in the control plates. If you compare the live cell count, which is graphed in Figure 5.14B, in the presence of serum proteins MBG-B5 is comparable to the control, indicating a biocompatible environment for these cells. In serum-free conditions, MBG-B5 has more cells adhered than the control, 46±12 versus 32±28 respectively. This suggests that in serum free growth conditions, MBG-B5 offer a better environment for cell growth than the culture plate.
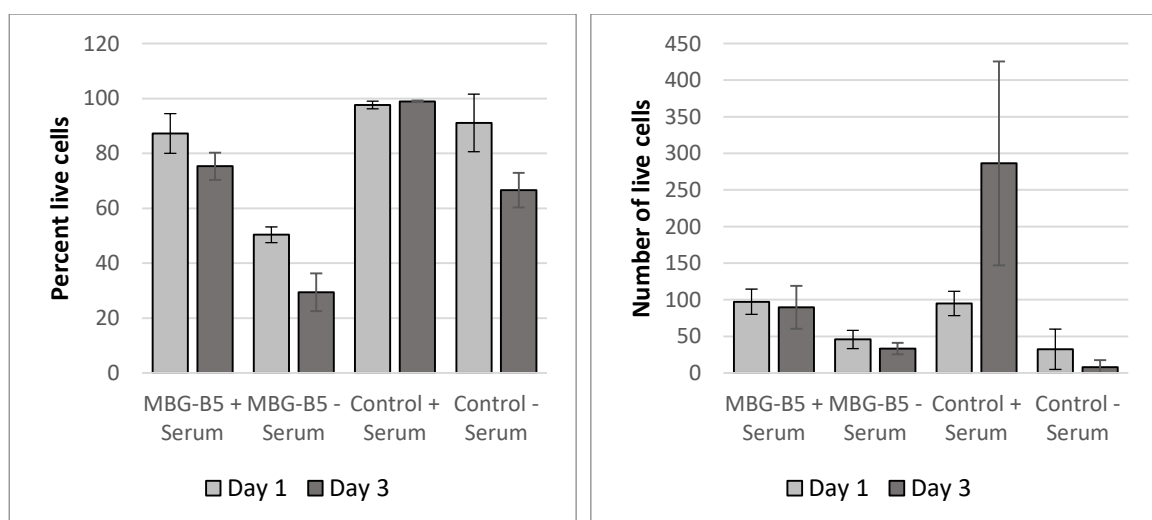

Figure 5.14: A: percent Live : Dead cell ratio for SH-SY5Y cells cultured for 1 and 3 days, and B: Number of live cells observed per condition.

SH-SY5Y cells cultured for three days are shown in Figure 5.15. After three days culture, there has been very little change in either cell number (Figure 5.14A), or live : dead ratio (Figure 5.14B) for MBG-B5. The hydrogel is not cytotoxic, as the cells are not dying, however they are also not proliferating as seen in the control. The positive control has 2-4 times the number of cells seen at day 3 compared to day 1, And has continued to provide a favourable live : dead ratio. Due to the presence of the IKRG motif in these hydrogles, it is possible the reduced proliferation is caused by activation of the TrkB receptor, leading to differentiation of the cells, and therefore reduced proliferation, however it is not possible to confirm this without further testing, either by immunostaining or performing western blots, to investigate TrkB activation. In serum free conditions, the control wells were nearly empty (Figure 5.15C) and the live : dead cell ratio observed in these wells was reduced relative to at 1 day. MBG-B5 in serum free conditions continues to have more living cells than the serum free control, so despite it's higher ratio of observed dead cells, it is likely providing a better environment for these cells.
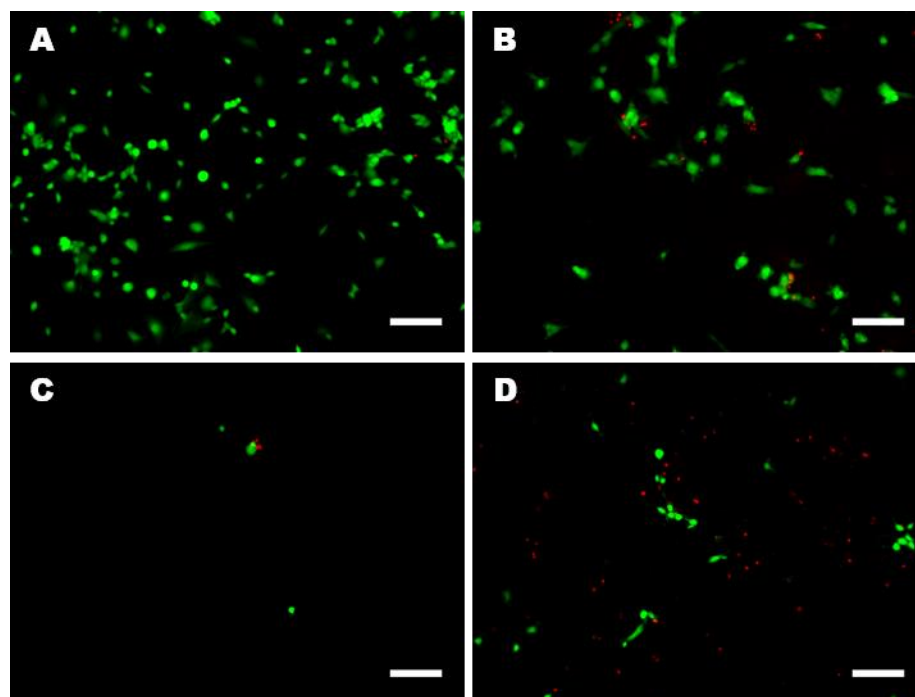
**Figure 5.15: SH-SY5Y cells after 3 days culture. A: Control, B: MBG-B5 hydrogel, C: Cells plated and cultured in serum-free media, and D: Cells growing on MBG-B5 hydrogels plated and cultured in serum-free media. Scale bar: 100 μm.**

5.3.3 Biofunctionality

The ability of MBG-B5 to activate the TrkB receptor was investigated using mouse primary mixed hippocampal/cortical neurons. The cells were grown in 6 well dishes

and once mature, at 7 days *in vitro*, cells were treated according to Table 5.1. Hydrogel/media was removed after 30 minutes of treatment, and cells were lysed. The lysates were analysed by western blot.

The first run of the experiment indicated that MBG-B5 had lower pTrkB than untreated cells, indicating perhaps that in this state, the peptide acts as an antagonist. two further isolations of primary cells were prepared in parallel, and the experiment repeated. This time showing significant activation of the TrkB receptor after 20 min of treatment, which was significantly reduced by the GNF5837 TrkB inhibitor.

Table 5.1 Conditions tested on primary neurons:

Treatment	± GNF5837
Untreated	-
20ng/mL BDNF	-
20ng/mL BDNF	+
MBG-B5	-
MBG-B5	+

These primary cultures, treatments and western blots were all conducted in parallel with those in chapter 4, so the repeated experiment had no significant pTrkB for the +BDNF condition, and no aparent inhibition in the +BDNF +GNF5837 condition. However, the MBG-B5 gel has caused significant phosphorylation, up to 6 times greater than the untreated condition. This is a greater level of pTrkB than was observed in for the soluble IKRG peptide alone[20], and is comprable to +BDNF in the first experiment. As with the chapter 4 work, another repeat of this experiment with fresh reagents would likely confirm the activity of the MBG-B5 hydrogel, but due to time contraints this is not possible at this stage.
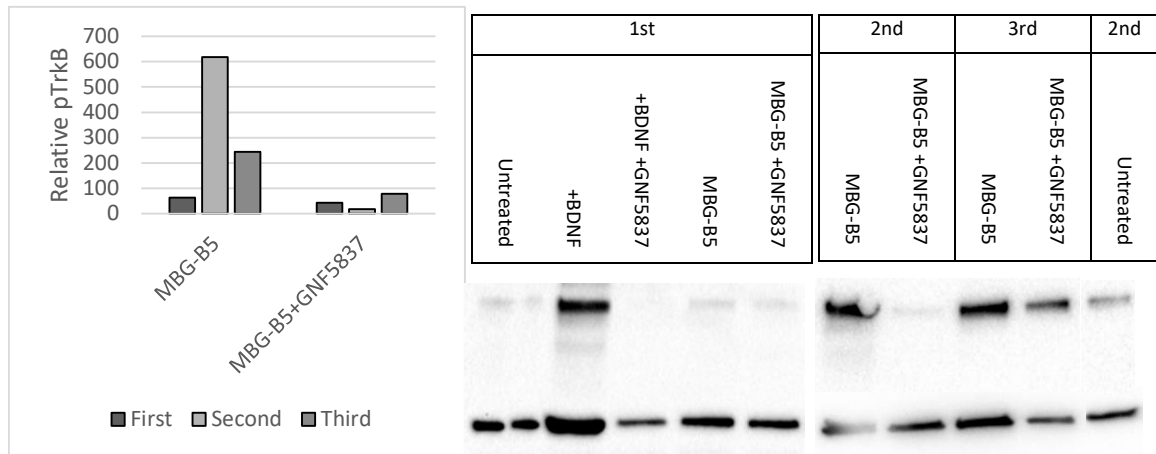
Figure 5.16: pTrkB normalised to untreated cells over 3 biological replicates for primary neurons treated with MBG-B5 and MBG-B5 + pre-treatment with GNF5837. Western blots have been cropped to exclude irrelevant samples which were run in parallel with those presented.

5.4 Conclusion

Modification of the MBG-6 peptide hydrogel system, through the addition of the IKRG motif to form the MBG-B5 peptide hydrogel. MBG-B5 has a lower storage modulus, but is more stable *in vitro* than the original sequence MBG-6, which due to it's rapid degradation in cell culture is not suited to use as a cell scaffold. MBG-B5 is biocompatible, and provides a suitable environment for the growth of neural cells. The IKRG motif is likely functional in this state, as shown by western blot. Although another round of testing would increase confidence in this result.

Further development of this system will involve establishing a protocol for cell encapsulation and 3D culturing of cells. Synthesis of an alternative variant, in which the functional IKRG motif is on the C terminal of the peptide may alter its bioavailability, and be worth investigating. If a successful cell encapsulation protocol can be established, then stem cell culture, and delivery by injection *in vivo* could prove to be very promising.

Developing a version of the MBG-6 peptide with one of RGD, IKVAV or YIGSR, to then co-assemble with MBG-B5, yielding a bi-functional peptide hydrogel would likely result in a biocompatible hydrogel, which is even better suited to the treatment of neurodegenerative diseases.

5.5 References

[1]   C. Martin, E. Oyen, J. Mangelschots, M. Bibian, T. Ben Haddou, J. Andrade, J. Gardiner, B. Van Mele, A. Madder, R. Hoogenboom, M. Spetea, and S. Ballet, "Injectable peptide hydrogels for controlled-release of opioids," *Med. Chem. Commun.*, vol. 7, no. 3, pp. 542–549, 2016.

[2]   C. Martin, E. Oyen, Y. Van Wanseele, T. Ben Haddou, H. Schmidhammer, J. Andrade, L. Waddington, A. Van Eeckhaut, B. Van Mele, J. Gardiner, R. Hoogenboom, A. Madder, M. Spetea, and S. Ballet, "Injectable peptide-based hydrogel formulations for the extended in vivo release of opioids," *Mater. Today Chem.*, vol. 3, pp. 49–59, 2017.

[3]   E. Genové, C. Shen, S. Zhang, and C. E. Semino, "The effect of functionalized self-assembling peptide scaffolds on human aortic endothelial cell function," *Biomaterials*, vol. 26, no. 16, pp. 3341–3351, 2005.

[4]   X. Liu, X. Wang, X. Wang, H. Ren, J. He, L. Qiao, and F. Z. Cui, "Functionalized self-assembling peptide nanofiber hydrogels mimic stem cell niche to control human adipose stem cell behavior in vitro," *Acta Biomater.*, vol. 9, no. 6, pp. 6798–6805, 2013.

[5]   N. Ni, Y. Hu, H. Ren, C. Luo, P. Li, J. B. Wan, and H. Su, "Self-assembling peptide nanofiber scaffolds enhance dopaminergic differentiation of mouse pluripotent stem cells in 3-dimensional culture," *PLoS One*, vol. 8, no. 12, pp. 1–11, 2013.

[6]   A. M. McGrath, L. N. Novikova, L. N. Novikov, and M. Wiberg, "BD™ PuraMatrix™ peptide hydrogel seeded with Schwann cells for peripheral nerve regeneration," *Brain Res. Bull.*, vol. 83, no. 5, pp. 207–213, Oct. 2010.

[7]   F. Moradi, M. Bahktiari, M. T. Joghataei, M. Nobakht, M. Soleimani, G. Hasanzadeh, A. Fallah, S. Zarbakhsh, L. B. Hejazian, M. Shirmohammadi, and F. Maleki, "BD PuraMatrix peptide hydrogel as a culture system for human fetal Schwann cells in spinal cord regeneration," *J. Neurosci. Res.*, vol. 90, no. 12, pp. 2335–2348, Dec. 2012.

[8]   Y. Loo, S. Zhang, and C. A. E. Hauser, "From short peptides to nanofibers to macromolecular assemblies in biomedicine," *Biotechnol. Adv.*, vol. 30, no. 3, pp. 593–603, May 2012.

[9]   A. Kaneko and Y. Sankai, "Long-term culture of rat hippocampal neurons at low density in serum-free medium: Combination of the sandwich culture technique with the three-dimensional nanofibrous hydrogel PuraMatrix," *PLoS One*, vol. 9, no. 7, 2014.

[10]   Y. Kumada, N. A. Hammond, and S. Zhang, "Functionalized scaffolds of shorter self-assembling peptides containing MMP-2 cleavable motif promote fibroblast proliferation and significantly accelerate 3-D cell migration independent of scaffold stiffness," *Soft Matter*, vol. 6, no. 20, p. 5073, 2010.

[11]   J. P. Jung, A. K. Nagaraj, E. K. Fox, J. S. Rudra, J. M. Devgun, and J. H. Collier, "Co-assembling peptides as defined matrices for endothelial cells," *Biomaterials*, vol. 30, no. 12, pp. 2400–2410, 2009.

[12]   J. P. Jung, J. L. Jones, S. A. Cronier, and J. H. Collier, "Modulating the mechanical properties of self-assembled peptide hydrogels via native chemical ligation," 2008.

[13]   S. Koutsopoulos and S. Zhang, "Long-term three-dimensional neural tissue cultures in functionalized self-Assembling peptide hydrogels, Matrigel and Collagen i," *Acta Biomater.*, vol. 9, no. 2, pp. 5162–5169, 2013.

[14]   Z. Zou, T. Liu, J. Li, P. Li, Q. Ding, G. Peng, Q. Zheng, X. Zeng, Y. Wu, and X. Guo, "Biocompatibility of functionalized designer self-assembling nanofiber scaffolds containing FRM motif for neural stem cells," *J. Biomed. Mater. Res. Part A*, vol. 102, no. 5, pp. 1286–1293, May 2014.

[15]   E. Oyen, C. Martin, V. Caveliers, A. Madder, B. Van Mele, R. Hoogenboom, S. Hernot, and S. Ballet, "In Vivo Imaging of the Stability and Sustained Cargo Release of an Injectable Amphipathic Peptide-Based Hydrogel," *Biomacromolecules*, vol. 18, no. 3, pp. 994–1001, Mar. 2017.

[16]   F. Gelain, D. Bottai, A. Vescovi, and S. Zhang, "Designer Self-Assembling Peptide Nanofiber Scaffolds for Adult Mouse Neural Stem Cell 3-Dimensional Cultures," no. 1, 2006.

[17]   S. Cheng, E. C. Clarke, and L. E. Bilston, "Rheological properties of the tissues of the central nervous system: A review," *Med. Eng. Phys.*, vol. 30, no. 10, pp. 1318–1337, Dec. 2008.

[18]   S. Das, K. Zhou, D. Ghosh, N. N. Jha, P. K. Singh, R. S. Jacob, C. C. Bernard, D. I. Finkelstein, J. S. Forsythe, and S. K. Maji, "Implantable amyloid hydrogels for promoting stem cell differentiation to neurons," *Nat. Publ. Gr.*, vol. 8, 2016.

[19]   J. Mangelschots, M. Bibian, J. Gardiner, L. Waddington, Y. Van Wanseele, A. Van Eeckhaut, M. M. D. Acevedo, B. Van Mele, A. Madder, R. Hoogenboom, and S. Ballet, "Mixed α/β-Peptides as a Class of Short Amphipathic Peptide Hydrogelators with Enhanced Proteolytic Stability," *Biomacromolecules*, vol. 17, no. 2, pp. 437–445, Feb. 2016.

[20]   M. D. C. Cardenas-Aguayo, S. F. Kazim, I. Grundke-Iqbal, and K. Iqbal, "Neurogenic and Neurotrophic Effects of BDNF Peptides in Mouse Hippocampal Primary Neuronal Cell Cultures," *PLoS One*, vol. 8, no. 1, p. e53596, 2013.

Chapter 6 In-vivo inflammatory response to self-assembled peptides containing neurotrophic signals

6.1 Abstract

Following the first successful western blot in chapter 4, in which the 1:1 blended Fmoc-FDIKRG, Fmoc-FRGDF hydrogel strongly activated the TrkB receptor, an *in vivo* experiment was undertaken to determine the degree of inflammatory response of this material in the central nervous system. The Fmoc-FRGDF/FDIKRG 1:1 blend hydrogel, Fmoc-FRGDF, and a PBS control were all injected into the brains of mice (NesCreER2-Rosa26eYFP), and the inflammatory response was characterised at 7 and 14 days *in vivo* by characterising the astrocyte and microglia density surrounding the injections. The inflammatory response of the materials indicated that Fmoc-FRGDF alone was not significantly different when compared to the PBS control, which is in contradiction to the literature. The blended hydrogel had a less severe inflammatory response than the other conditions tested, likely caused by either the presence of the IKRG sequence, or a moderate RGD density in this hydrogel.

6.2 Introduction

By performing in vivo injections of the most promising hydrogel blend into mouse brains, it is possible to directly observe the body's inflammatory response to the materials. This is a crucial test before further development of the hydrogels, as it is important to understand what effect the implanted material will have on the brain and avoid a negative immune response. As seen in previous publications[1], [2] the astrocyte and microglial response to an injection of hydrogels is easy to follow. Reactive astrocyte activity may be observed through staining for glial fibrillary acidic protein (GFAP), while microglia identified by staining for ionized calcium binding adaptor molecule 1 (Iba1). The expected trend of both astrocytes and microglia to injury is for a large initial response, which degreases rapidly, then tapers off over the course of approximately a month[3].

Astrocytes have many functions in the brain. They help to control the blood brain barrier[4], [5], control the energy supply to neurons, as well as the turnover of

neurotransmitters[6], [7]. Brain insult leads to reactive astrogliosis. Key features of activated astrocytes is the upregulation of glial fibrillary acidic protein (GFAP) which can be immunologically stained and identified and significant hypertrophy in response to injury[8] also assists in identification. The degree of reactive astrogliosis can vary, with more prominent activation often being associated with glial scar formation[9], [10]. In the case of glia scar formation, astrocytes can be found both within the injured tissue, and as a part of the barrier separating injured from healthy tissue[11]. It has been shown that astrocyte activity is important in re-establishing the blood brain barrier, and attenuating acute neurodegeneration following brain or spinal cord injury[12], [13].

Microglia are the other main cell type observed in the inflammatory response of the brain. These cells behave in a similar manner to macrophages, phagocytosing foreign matter and cellular debris[14]. Immediately following in injury, microglia act to repair damaged tissue, by cleaning up damages cells, and removing foreign material. This is later followed by microglia secreting anti-inflammatory cytokines and removing damaged axons, to promote the growth of new axons[15].

In this chapter, two hydrogels were implanted into the brains of mice. The hydrogels investigated were Fmoc-FRGDF and a 1:1 blend of Fmoc-FRGDF and Fmoc-FDIKRG. A PBS injection was used as a control, as this will tell use the response of the brain to injury alone. Degradation of the hydrogels is likely to contribute to the response of the brain to these materials. The mode of degradation has not been investigated in this work. Similar materials have been shown to degrade in the brain within three weeks[1]. Being composed of alpha amino acids, this is likely caused by enzymatic processes[16], [17]. A more aggressive inflammatory response to Fmoc-FRGDF compared to the PBS injection is expected[18]. The blended hydrogel, which demonstrated better compatibility with neural cells in Chapter 4 than Fmoc-FRGDF alone, is expected to induce less inflammation. Activation of astrocytes and microglia is expected for all conditions surrounding the injection site, as this is necessary in order to repair the damage caused by the injection, but an excessive or prolonged response is undesirable.

6.3 Results and discussion

A major obstacle in the development of neural scaffolding materials is the host response after implantation. In order to assess the inflammatory response to these materials, Fmoc-FRGDF and a 1:1 blemd of Fmoc-FRGDF and Fmoc-FDIKRG was implanted into the caudate putamen of the adult mouse brain, as with previous studies our group has conducted[1], [3]. The following coordinates were used: anteroposterior +0.5mm and lateral +1.5mm medial–lateral from the bregma. The caudate putamen was used for this study, as it is a relatively large and homogenous region of the brain, making analysis of the astrocyte and microglial response simpler. The samples were pre-gelled inside a 23G needle. This was inserted to a depth of 4mm, then a plunger inserted into the barrel of the needle. The needle was then withdrawn, leaving behind the hydrogel. Total volume injected was approximately 0.21 µl. This method was used, as it allows for a continuous tract of hydrogel to be injected, with minimal chance of compression of the host tissue. At 7 and 14 days, mice were killed, and the immune response observed.

Following histological processing, the brains were stained for both GFAP and Iba1 to identify astrocytes and microglia surrounding the injection sites. Contrast was developed using 3,3'-diaminobenzidine (DAB), giving a black colour, and the sections were counterstained with neutral red, a Nissl stain for both neurons and glia present in the sections. The procedure for measuring the response is outlined in Figure 6.1.
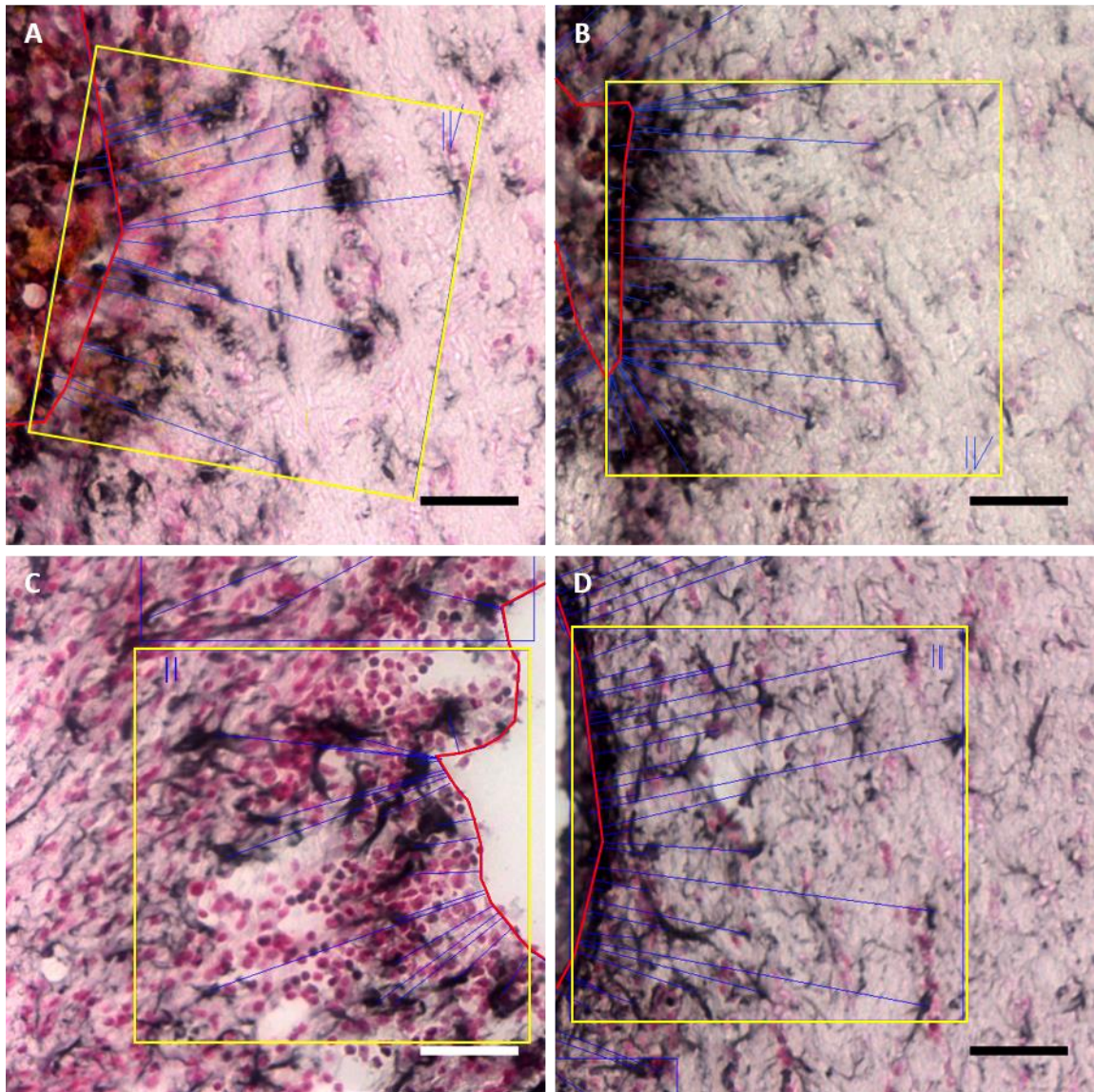
Figure 6.1: High magnification images of Iba1 stained sections at A: 7 days and B: 14 days, and GFAP stained sections at C: 7 days and D: 14 days post injection, to illustrate how micrographs were characterised. First the border of the injection region was outlined(red), then 4 regions measuring 400x400 µm were selected around the injection site(yellow). All positively stained microglia were identified by co-localisation of a red nucleus and DAB staining, or if the DAB stained region was sufficiently large that it likely obscured the nucleus entirely. The distance from each positively identified cell to the nearest edge of the injection site was then measured (blue) and recorded Scale bars: 100µm.

6.3.1 Response of the brain to hydrogel injection

Representative micrographs of stained sections for astrocytes are shown in Figure 6.2. There is an increased density of activated astrocytes surrounding the injections side for all conditions, which decreases to background levels within approximately 200 µm. The overall astrocyte density did not dramatically decrease over the observed time period.
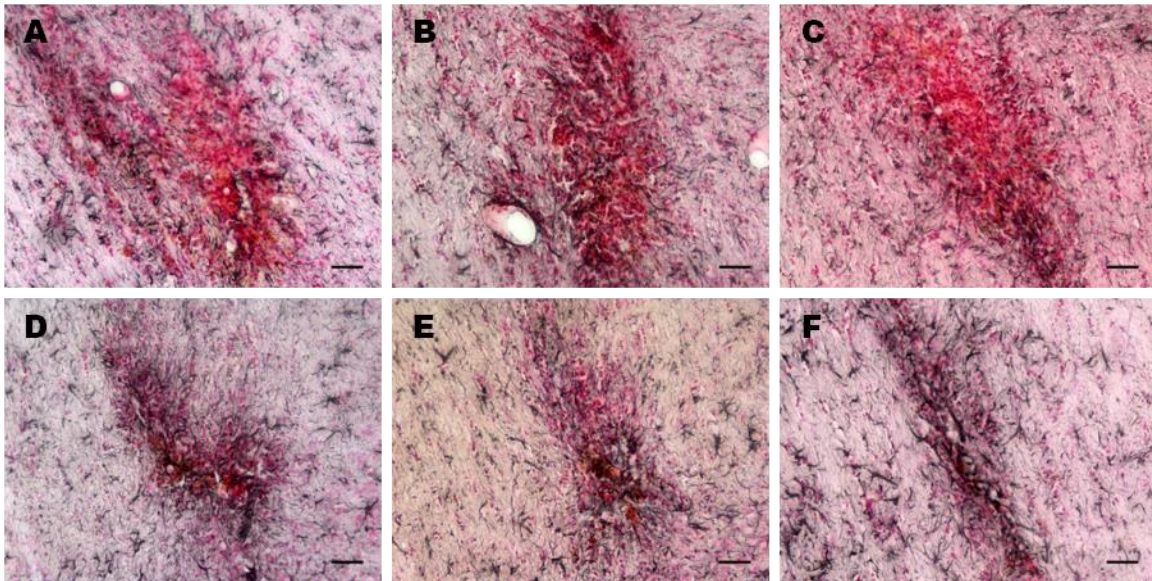
Figure 6.2: Representative micrographs of transverse brain sections stained with anti-GFAP, and DAB substrate, counterstained with Neutral Red. 7 days in vivo, A: PBS control, B: Fmoc-FRGDF and C: Fmoc-FDIKRG/Fmoc-FRGDF blend. And 14 days in vivo, D: PBS Control, E: Fmoc-FRGDF and F: Fmoc-FDIKRG/Fmoc-FRGDF blend. Scale bars 100µm.

A graphical representation of the astrocyte density in the PBS control in shown in Figure 6.3. As can be seen, the injury alone caused a substantial astrocyte response in the immediate area surrounding the wound. Beyond 150 µm, the astrocyte density has reduced to nearly background levels. From 7 to 14 days, there is very little change in astrocyte density immediately adjacent to the injury, but at 50-200 µm, there is a reduction.
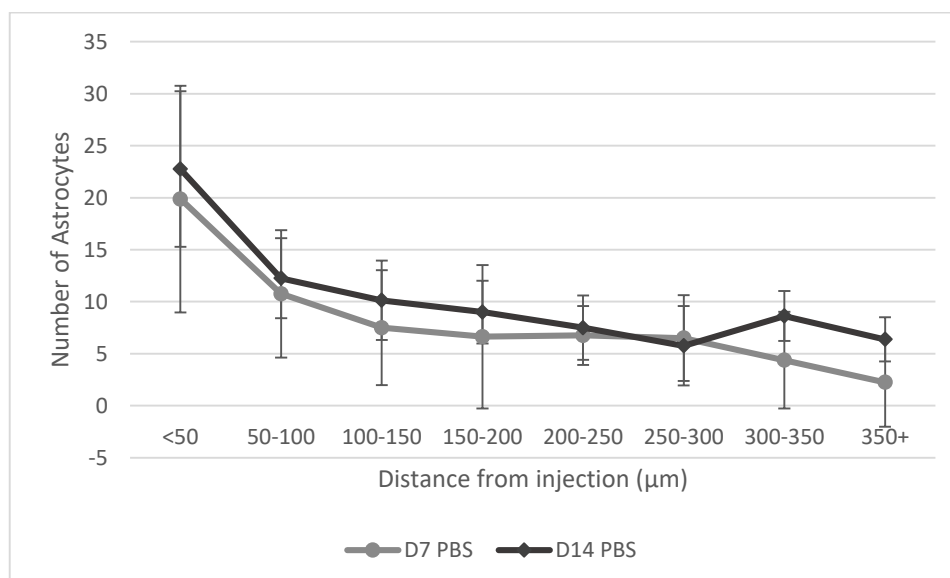

Figure 6.3: Astrocyte density vs distance from injection site at 7 and 14 days post injection for PBS control samples.

From adjacent to the injury, to 150 µm is where the most significant response is seen, therefore this area will be the focus of comparison between the three conditions

under investigation. At 7 days post injection (Figure 6.4A), from adjacent to the injection site to 150 µm, there is no significant (P>0.05) difference between the conditions. This indicates that the hydrogels are not causing any additional inflammatory response than the injury alone. At 14 days (Figure 6.4B), there is still no significant difference (P>0.05) between the conditions, indicating that these materials have a neutral effect on the astrocyte response.
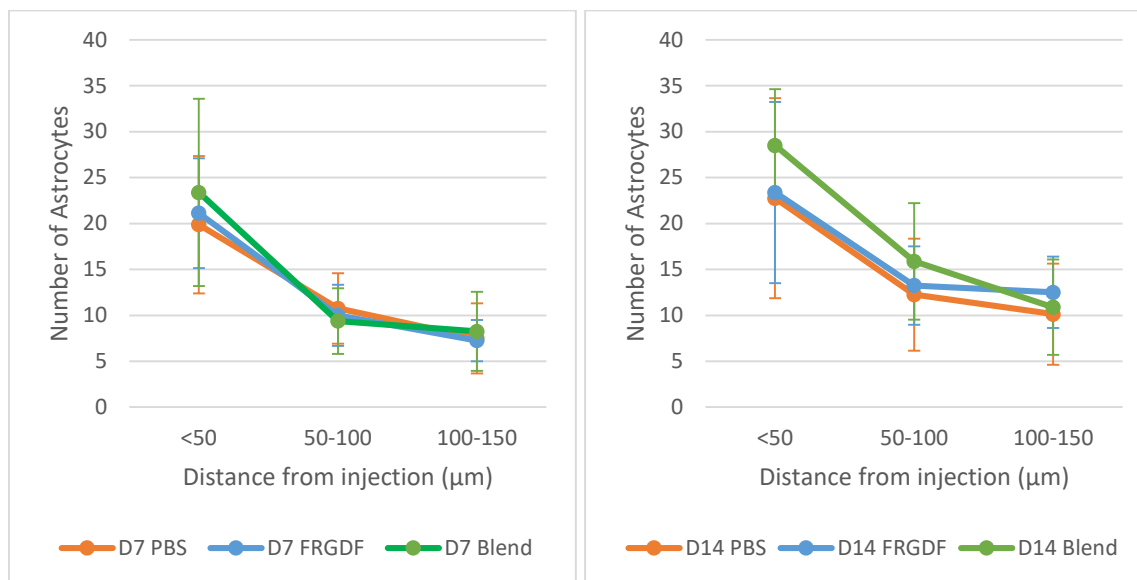

Figure 6.4: Astrocyte density plotted against distance from the injection site for the PBS control, Fmoc-FRGDF and the blended Fmoc hydrogel at A: 7 days and B: 14 days post injection.

Micrographs showing the microglial response to the injections are shown in Figure 6.5. As with the astrocytes, there is a local high density of activated microglia immediately surrounding the injection site. Microglial density has decreased to background levels at approximately 250-300 µm from the injection site. At 7 days *in vivo*, the gel conditions (Figure 6.5B and C) appear to have less Iba1 staining than the control (Figure 6.5A), indicating a less aggressive initial inflammatory response. At 14 days *in vivo*, the control looks to have a similar astrocyte to at day 7, and the hydrogels have increased and now look very similar.
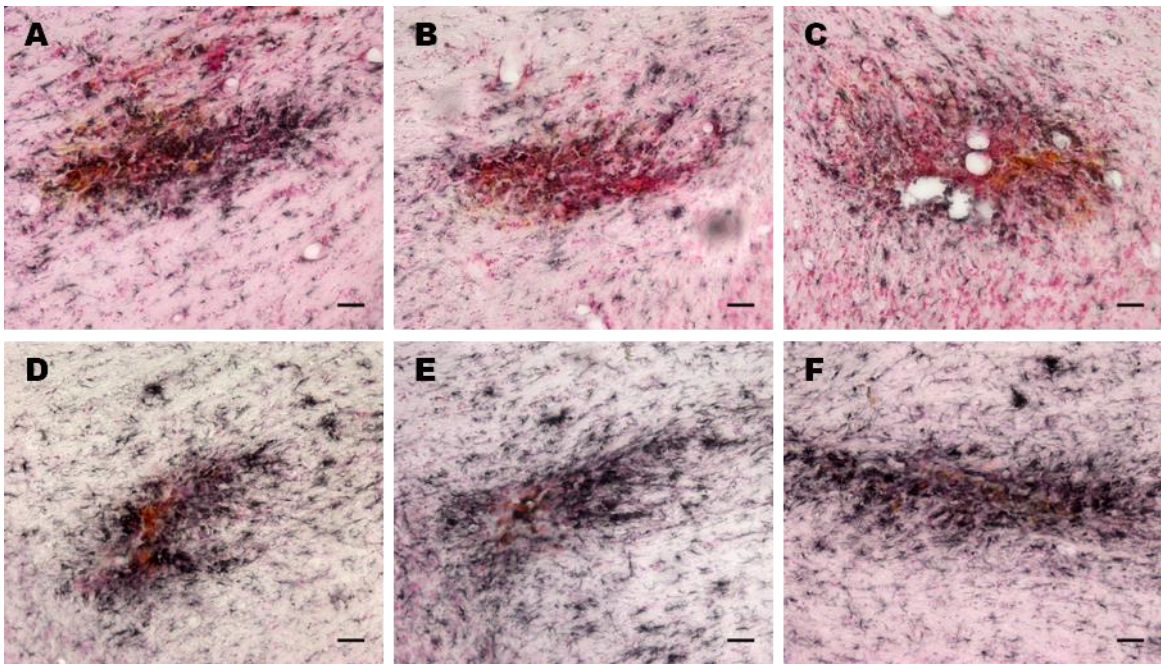
Figure 6.5: Representative micrographs of transverse brain sections stained with anti-Iba1, and DAB substrate, counterstained with Neutral Red. 7 days in vivo, A: PBS control, B: Fmoc-FRGDF and C: Fmoc-FDIKRG/Fmoc-FRGDF blend. And 14 days in vivo D: PBS control, E: Fmoc-FRGDF and F: Fmoc-FDIKRG/Fmoc-FRGDF blend. Scale bars 100μm.

In the PBS control condition, the response of microglia can be seen in Figure 6.6. The microglia density is highest adjacent to the injection, as expected, and tapers off more gradually than the astrocytes did. While the response is still above background levels as far as 250 μm, this is well within the error margin. There is no significant difference in the control condition between 7 and 14 days.
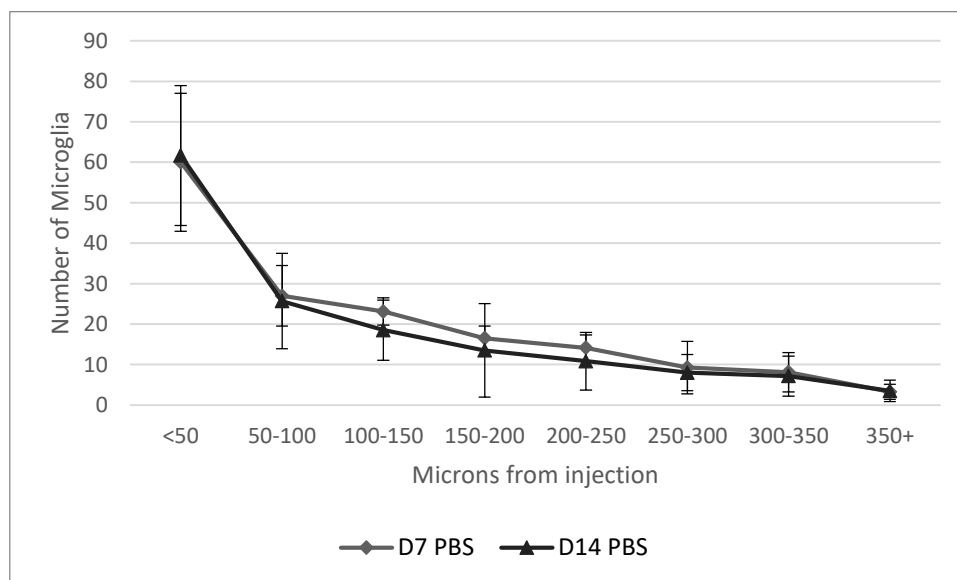

Figure 6.6: Microglia density vs distance from injection site at 7 and 14 days post injection for PBS control samples.

All conditions were examined and compared at distances less than 150 µm from the injection site. Interestingly, at 7 days, the blended hydrogel displays significantly less microglia than the PBS control condition (P<0.05) at <50 µm. While Fmoc-FRGDF is close, but does not quite reach a significant effect (P=0.10). This indicates that the blended hydrogel, containing both the BDNF derived IKRG sequence, and the fibronectin derived RGD sequence in having an anti-inflammatory effect. At day 14, this anti-inflammatory effect has ended, and both hydrogels are not significantly different to the control condition. Typically, the microglial response to an injection is highest immediately following injury, with a rapid decrease over the first week[3].
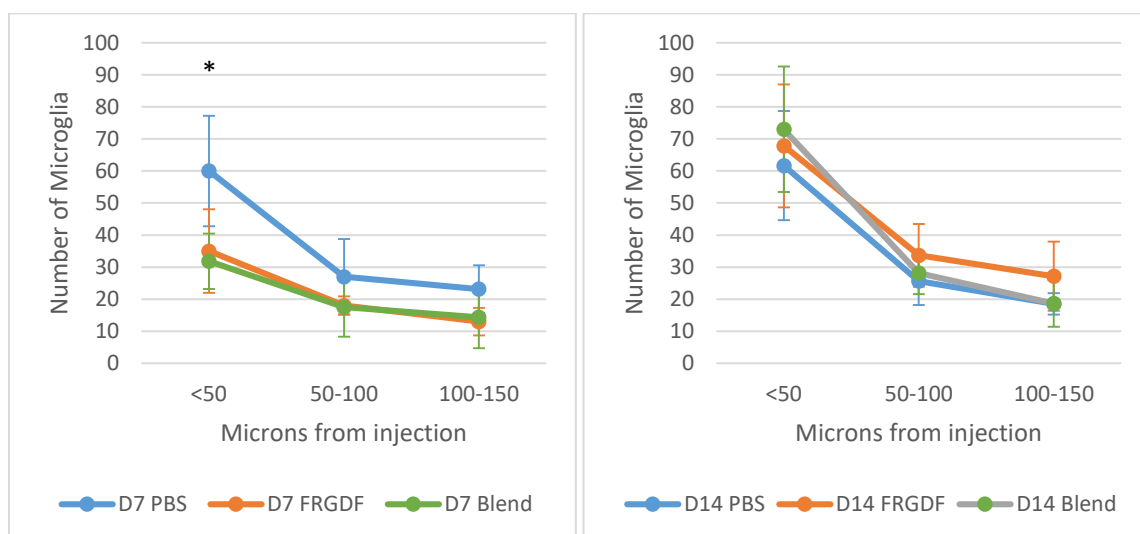

Figure 6.7: Microglia density plotted against distance from the injection site for the PBS control, Fmoc-FRGDF and the blended Fmoc hydrogel at A: 7 days and B: 14 days post injection. *D7 PBS and D7 blend are significantly different (P<0.05) at <50 µm.

The fact that the microglial density surrounding the injury was no longer significantly different at 14 days indicates that these hydrogels were initially reducing the activation of microglia. As the gels degraded, the initial anti-inflammatory effect was reduced, leading to a return to control levels of microglial activity. While degradation rates of these hydrogels were not examined, Fmoc hydrogels have been shown to degrade gradually over time[19], and many alpha peptide hydrogels have demonstrated significant proteolytic degradation [17], [20]. Similar systems have shown minimal gel remaining at 21 days in vivo[1]. Therefore, the biological effect of the materials is expected to be reduced at the later time points, as observed in Figure 6.7.

Microglia are known to be responsive to fibronectin[21], [22], so the presence of the RGD motif in these hydrogels is a likely cause for the this response.

Fmoc-FRGDF has been shown to be suitable for implantation into the central nervous system, having no significant difference in the microglial or astrocytic response when compared to a PBS control. This is in contrast to the published results, which indicated that Fmoc-FRGDF hydrogels caused an increased inflammatory response in the central nervous system[23]. The reason stated in their study for increased inflammation was that fibronectin is not suitable for presentation in the CNS[23] claiming that it is not observed in significant amounts in the brain. However, Fibronectin, from which the RGD sequence is derived is found within the ECM of the CNS, particularly following an injury[24], with fibronectin playing important regulatory roles in microglial function and activation[22].

The blended hydrogel at 7 days *in vivo* reduced microglial activation, and had comparable astrocyte activation as the PBS control, indicating that, unlike some other Fmoc hydrogels[1] this blended hydrogel initially has an anti- inflammatory effect. At 14 days *in vivo*, the microglial activity was not significantly different from the PBS control. The blended hydrogel contains a reduced amount of the RGD motif, as well as the IKRG motif. The surface density of integrin ligands has been demonstrated to have significant effects on cell behaviour[25]–[27], too high a signal density has been shown to inhibit cell migration[28], with moderate signal density being superior for encouraging neurite extension[29]. The reduced RGD density in this hydrogel is one possible explanation for the significant reduction microglia density. Another likely cause being that the IKRG motif is active *in vivo*, resulting in an anti-inflammatory effect.

6.4 Conclusion

This work has confirmed that the peptide hydrogel composed of a 1:1 blend Fmoc-FDIKRG and Fmoc-FRGDF is appropriate for use in the CNS. The astrocyte response to this hydrogel was comparable to a PBS control, while the microglial response was significantly reduced at day 7. The inflammatory response observed was no worse than that observed in the PBS control. We have also shown that Fmoc-FRGDF alone under the tested conditions is not pro-inflammatory in the central nervous system, contradicting previously published experiments.

Further analysis of the remaining tissue sections will involve staining for neurofilaments, so that penetration of neurites into the injection area may be characterised. If the IKRG motif in the blended hydrogel is functional, we would expect increased neurite activity around the injection site.

6.5 References

[1]	S. Das, K. Zhou, D. Ghosh, N. N. Jha, P. K. Singh, R. S. Jacob, C. C. Bernard, D. I. Finkelstein, J. S. Forsythe, and S. K. Maji, "Implantable amyloid hydrogels for promoting stem cell differentiation to neurons," *Nat. Publ. Gr.*, vol. 8, 2016.

[2]	K. Zhou, S. Motamed, G. A. Thouas, C. C. Bernard, D. Li, H. C. Parkington, H. A. Coleman, D. I. Finkelstein, and J. S. Forsythe, "Graphene functionalized scaffolds reduce the inflammatory response and supports endogenous neuroblast migration when implanted in the Adult Brain," *PLoS One*, vol. 11, no. 3, pp. 1–15, 2016.

[3]	D. R. Nisbet, A. E. Rodda, M. K. Horne, J. S. Forsythe, and D. I. Finkelstein, "Neurite infiltration and cellular response to electrospun polycaprolactone scaffolds implanted into the brain," *Biomaterials*, vol. 30, no. 27, pp. 4573–4580, Sep. 2009.

[4]	S. Liebner, C. J. Czupalla, and H. Wolburg, "Current concepts of blood-brain barrier development," *Int. J. Dev. Biol.*, vol. 55, no. 4–5, pp. 467–476, 2011.

[5]	B. A. Barres, "The Mystery and Magic of Glia: A Perspective on Their Roles in Health and Disease," *Neuron*, vol. 60, no. 3, pp. 430–440, Nov. 2008.

[6]	L. Pellerin, A.-K. Bouzier-Sore, A. Aubert, S. Serres, M. Merle, R. Costalat, and P. J. Magistretti, "Activity-dependent regulation of energy metabolism by astrocytes: An update," *Glia*, vol. 55, no. 12, pp. 1251–1262, Sep. 2007.

[7]	A. Suzuki, S. A. Stern, O. Bozdagi, G. W. Huntley, R. H. Walker, P. J. Magistretti, and C. M. Alberini, "Astrocyte-Neuron Lactate Transport Is Required for Long-Term Memory Formation," *Cell*, vol. 144, no. 5, pp. 810–823, Mar. 2011.

[8]	U. Wilhelmsson, E. A. Bushong, D. L. Price, B. L. Smarr, V. Phung, M. Terada, M. H. Ellisman, and M. Pekny, "Redefining the concept of reactive astrocytes as cells that remain within their unique domains upon reaction to injury," *Proc. Natl. Acad. Sci.*, vol. 103, no. 46, pp. 17513–17518, Nov. 2006.

[9]	C. Goritz, D. O. Dias, N. Tomilin, M. Barbacid, O. Shupliakov, and J. Frisen, "A Pericyte Origin of Spinal Cord Scar Tissue," *Science (80-.).*, vol. 333, no. 6039, pp. 238–242, Jul. 2011.

[10]   M. V Sofroniew, "Molecular dissection of reactive astrogliosis and glial scar formation," *Trends Neurosci.*, vol. 32, no. 12, pp. 638–647, Dec. 2009.

[11]   M. Pekny and M. Nilsson, "Astrocyte activation and reactive gliosis," *Glia*, vol. 50, no. 4, pp. 427–434, Jun. 2005.

[12]   J. R. Faulkner, "Reactive Astrocytes Protect Tissue and Preserve Function after Spinal Cord Injury," *J. Neurosci.*, vol. 24, no. 9, pp. 2143–2155, Mar. 2004.

[13]   M. V Sofroniew, T. G. Bush, N. Blumauer, Lawrence Kruger, L. Mucke, and M. H. Johnson, "Genetically-targeted and conditionally-regulated ablation of astroglial cells in the central, enteric and peripheral nervous systems in adult transgenic mice1Published on the World Wide Web on 7 June 1999.1," *Brain Res.*, vol. 835, no. 1, pp. 91–95, Jul. 1999.

[14]   F. Aloisi, "Immune function of microglia," *Glia*, vol. 36, no. 2, pp. 165–179, Nov. 2001.

[15]   M. R. Ritter, E. Banin, S. K. Moreno, E. Aguilar, M. I. Dorrell, and M. Friedlander, "Myeloid progenitors differentiate into microglia and promote vascular repair in a model of ischemic retinopathy," *J. Clin. Invest.*, vol. 116, no. 12, pp. 3266–3276, Dec. 2006.

[16]   E. Beniash, J. D. Hartgerink, H. Storrie, J. C. Stendahl, and S. I. Stupp, "Self-assembling peptide amphiphile nanofiber matrices for cell entrapment," *Acta Biomater.*, vol. 1, no. 4, pp. 387–397, 2005.

[17]   C. Martin, E. Oyen, Y. Van Wanseele, T. Ben Haddou, H. Schmidhammer, J. Andrade, L. Waddington, A. Van Eeckhaut, B. Van Mele, J. Gardiner, R. Hoogenboom, A. Madder, M. Spetea, and S. Ballet, "Injectable peptide-based hydrogel formulations for the extended in vivo release of opioids," *Mater. Today Chem.*, vol. 3, pp. 49–59, 2017.

[18]   X. Du, J. Zhou, J. Shi, and B. Xu, "Supramolecular Hydrogelators and Hydrogels: From Soft Matter to Molecular Biomaterials," *Chem. Rev.*, vol. 115, no. 24, pp. 13165–13307, Dec. 2015.

[19]   K. M. Eckes, K. Baek, and L. J. Suggs, "Design and Evaluation of Short Self-Assembling Depsipeptides as Bioactive and Biodegradable Hydrogels," *ACS Omega*, vol. 3, no. 2, pp. 1635–1644, Feb. 2018.

[20]   J. Mangelschots, M. Bibian, J. Gardiner, L. Waddington, Y. Van Wanseele, A. Van Eeckhaut, M. M. D. Acevedo, B. Van Mele, A. Madder, R. Hoogenboom, and S. Ballet, "Mixed α/β-Peptides as a Class of Short Amphipathic Peptide Hydrogelators with Enhanced Proteolytic Stability," *Biomacromolecules*, vol. 17, no. 2, pp. 437–445, Feb. 2016.

[21]   B. Chamak and M. Mallat, "Fibronectin and laminin regulate thein vitro differentiation of microglial cells," *Neuroscience*, vol. 45, no. 3, pp. 513–527, Jan. 1991.

[22]   R. Milner and I. L. Campbell, "The Extracellular Matrix and Cytokines Regulate Microglial Integrin Expression and Activation," *J. Immunol.*, vol. 170, no. 7, pp. 3850–3858, Apr. 2003.

[23]   A. L. Rodriguez, T. Y. Wang, K. F. Bruggeman, C. C. Horgan, R. Li, R. J. Williams, C. L. Parish, and D. R. Nisbet, "In vivo assessment of grafted cortical neural progenitor cells and host response to functionalized self-assembling peptide hydrogels and the implications for tissue repair," *J. Mater. Chem. B*, vol. 2, no. 44, pp. 7771–7778, 2014.

[24]   M. N. Meland, M. E. Herndon, and C. S. Stipp, "Expression of α5 integrin rescues fibronectin responsiveness in NT2N CNS neuronal cells," *J. Neurosci. Res.*, vol. 88, no. 1, pp. 222–232, Jan. 2010.

[25]   J. T. Connelly, A. J. García, and M. E. Levenston, "Interactions between integrin ligand density and cytoskeletal integrity regulate BMSC chondrogenesis," *J. Cell. Physiol.*, vol. 217, no. 1, pp. 145–154, Oct. 2008.

[26]   E. Schuh, S. Hofmann, K. Stok, H. Notbohm, R. Müller, and N. Rotter, "Chondrocyte redifferentiation in 3D: The effect of adhesion site density and substrate elasticity," *J. Biomed. Mater. Res. Part A*, vol. 100A, no. 1, pp. 38–47, Jan. 2012.

[27]   J. T. Connelly, T. A. Petrie, A. J. García, and M. E. Levenston, "Fibronectin- and collagen-mimetic ligands regulate bone marrow stromal cell chondrogenesis in three-dimensional hydrogels.," *Eur. Cell. Mater.*, vol. 22, no. 2, pp. 168-76; discussion 176–7, Sep. 2011.

[28]   P. X. Ma, "Biomimetic materials for tissue engineering," *Adv. Drug Deliv. Rev.*, vol. 60, no. 2, pp. 184–198, 2008.

[29]   J. C. Schense and J. A. Hubbell, "Three-dimensional Migration of Neurites Is Mediated by Adhesion Site Density and Affinity," *J. Biol. Chem.*, vol. 275, no. 10, pp. 6813–6818, Mar. 2000.

Chapter 7 Conclusions and further work

7.1 Conclusions

This project focused on the development of self-assembling hydrogels for the delivery of neurotrophic signals to the central nervous system. The two categories of hydrogel investigated are Fmoc peptide hydrogels, and self-complementary peptide hydrogels.

7.1.1 Fmoc peptide hydrogels

From the literature, the functional short peptide IKRG was identified. This was modified with additional amino acids and the Fmoc N-terminal functionalisation, resulting in the Fmoc-FDIKRG peptide, which could for a hydrogel at pH 7.4, but was not stable long term. Co-assembly of this new peptide with Fmoc-LLY resulted in stable hydrogels. The morphology of these co-assembled hydrogels was investigated using a combination of negative stain and CryoTEM, which enabled comparison between the unblended and blended systems. The macromolecular structure of Fmoc-FDIKRG compared to the blended peptide hydrogels revealed a relationship between thinner (<10 nm), homogenous nanofiber assemblies and hydrogel stability, where Fmoc-FDIKRG alone had a significantly greater fibre diameter (32 ±19 nm). Fmoc-LLY was found to be cytotoxic to neural cell lines, given the direction of this project, it was decided to discontinue work with Fmoc-LLY.

Moving away from the Fmoc-LLY peptide provided the opportunity to introduce a second bifunctional motif into the system. Three functional Fmoc hydrogels from the literature, Fmoc-FRGDF, Fmoc-DYGSRF and Fmoc-DIKVAV had all previously been shown to be biocompatible, and had been used in neural applications[1]. Blends of these peptides at various concentrations were made, with only Fmoc-FRGDF forming a hydrogel. The resulting hydrogel contained two peptide motifs, which independently have been shown to be biofunctional. The resulting hydrogels when blended 1:1 were biocompatible, and supported the growth of neural cell lines.

Investigations into whether the Fmoc-FDIKRG motif was able to activate the TrkB receptor have been inconclusive. Once a working protocol had been established, our initial experiment using primary mixed cortical-hippocampal neurons indicated that

the hydrogel formed of a 1:1 blend of Fmoc-FDIKRG and Fmoc-FRGDF was capable of strongly activating the TrkB receptor. However subsequent experiments have not been able to replicate this result.

In vivo analysis of the inflammatory response of the brain to Fmoc-FRGDF and a 1:1 blend of Fmoc-FDIKRG and Fmoc-FRGDF showed that, contrary to published results, Fmoc-FRGDF caused no significant difference in inflammation when compared to control PBS injection at 7 and 14 days post injection. The blended hydrogel caused a significant reduction in the density of microglia adjacent to the injection site at 7 days *in vivo* and in all other regards was not significantly different to a control. Both hydrogels therefore do not provoke an aggressive immune response in the central nervous system.

A new method of preparing bulk hydrogels was developed in this project. The use of carbon dioxide to trigger gelation of Fmoc hydrogels has resulted in more consistent hydrogels, compared to the hydrochloric acid method, which often resulted in opaque aggregates forming in the hydrogels. The new CO_2 diffusion method had the additional benefit of greatly simplifying preparation of tissue culture substrates, as the basic peptide solution could be simply pipetted as required, and then gelled *in situ*.

7.1.2 Self-complementary peptide hydrogels

The self-complementary hydrogel system, MBG-6 (Ac-FEFQFK-NH$_2$) was investigated for use in neural applications. A functionalised version, MBG-B5 (Ac-FEFQFKGGIKRG-NH$_2$) was synthesised, containing the BDNF derived IKRG sequence separated by a di-glycine spacer. MBG-B5 formed stable hydrogels, which were not as rigid as MBG-6, with a storage modulus of 175 kPa versus 1,640 kPa respectively at 10mg/ml. MBG-6 was found to rapidly degrade in culture conditions despite its high storage modulus. MBG-B5 persisted in cell culture conditions for several days without significant degradation, and was capable of supporting neural cell growth for several days. Blends of the two peptides formed hydrogels, but all degraded just as rapidly as MBG-6 in cell culture conditions.

As with the Fmoc hydrogels, investigations into whether MBG-B5 is capable of activating the TrkB receptor have been inconclusive. The initial primary cell isolation when treated with MBG-B5 showed no pTrkB above background levels, but the two repeated experiments both indicated high levels of TrkB activation. This hydrogel is a promising candidate for further development in neural scaffolding and drug delivery applications, due to its biocompatibility, mild gelation conditions and indicated neurotrophic function.

7.2 Future directions

This project has developed two peptide hydrogels capable of supporting the growth of neural cells. There are many additional research directions highlighted by this project.

7.2.1 Repeats of western blots

One of the main challenges in this project was testing the biofunctionality of the IKRG containing peptide hydrogels. Many problems were encountered early on, caused by a combination of cell lines not expressing the protein as expected, and antibodies not recognising pTrkB. Once the problems had been resolved, the project was already reaching its later stages, and there was not sufficient time for the replicates required to verify biological function of either hydrogel system. Additional issues were potentially caused by the dynamics of the system. Activation of TrkB is a time dependent process[2], it is possible detection of phosphorylation was unsuccessful due to 'missing' the event.

Additional biological replicates of the primary cell experiments, conducted with fresh reagents, including BDNF full protein, GNF5837 Trk inhibitor, and freshly prepared peptides would give the greatest chance of verifying the ability of these hydrogels to activate the TrkB receptor. A preliminary time-dependent assay to ensure maximal TrkB phosphorylation is captured would increase the chances of successfully verifying the function of these gels.

7.2.2 Variations of Fmoc-FDIKRG

The peptide Fmoc-FDIKRG was able to form clear hydrogels, but these were not stable, with the fibres which form the gel growing over time, and within a day, forming thick aggregates, leading to the collapse of the hydrogel. Interactions of the Fmoc planar aromatic group and the sidechains all influence the self-assembly of these materials. A variant of this peptide which is capable of solitary self-assembly into a temporally stable hydrogel would enable greater flexibility in application of the system. In order to make a biofunctional peptide into a self-assembling hydrogel, many examples utilise phenylalanine residues to increase hydrophobicity of the peptide, and increase hydrophobic interactions[3], [4], while aspartic acid is also frequently used to alter the pK_a of the peptide and therefore shift the pH at which self-assembly occurs[5]. It may therefore be possible to achieve a more stable hydrogel through the addition of extra aspartic acid resides to the peptide, making it more stable at pH 7.4. It has also been shown that the specific order of amino acids in these systems has a significant effect on the properties of the resulting hydrogel[3]. Re-ordering, or relocating the current Asp and Phe amino acids in the Fmoc-FDIKRG peptide may yield different assembly behaviour, and therefore a more stable hydrogel. A selection of proposed alternative sequences is outlined in Table 7.1.

Table 7.1: Alternative formulations for IKRG containing Fmoc peptides

Modification	Example Sequences
Re-order modifying peptides	Fmoc-D<u>IKRG</u>F-OH
	Fmoc-F<u>IKRG</u>D-OH
	Fmoc-DF<u>IKRG</u>-OH
	Fmoc-<u>IKRG</u>FD-OH
	Fmoc-<u>IKRG</u>DF-OH
Insert additional aspartic acid residues	Fmoc-FDD<u>IKRG</u>-OH
	Fmoc-FDDD<u>IKRG</u>-OH
Combined approach	Fmoc-DD<u>IKRG</u>F-OH
	Fmoc-F<u>IKRG</u>DD-OH

Once a successful candidate has been identified, it may be possible for this to be co-assembled with a different range of other peptides compared to Fmoc-FDIKRG. Different combinations of bioactive Fmoc peptides would result in a variety of possible responses from a diverse range of cell types.

7.2.3 New functional self-complementary peptides

The MBG system of peptide, like the RADA system offers a great deal of flexibility in how it may be functionalised. As demonstrated with the synthesis of MBG-B5, doubling the length of the peptide, with additional residues not optimised for self-assembly still resulted in a stable self-supporting hydrogel. Developing another version of MBG-6, this time containing one of the common integrin binding peptides, RGD, IKVAV or YIGSR would result in a hydrogel capable of better supporting adherent cells in culture. Co-assembly of one of these new peptides with MBG-B5 would further improve the response of neural cells to these materials.

7.2.4 In vivo testing of materials – inflammation, neural ingrowth and

In order to achieve the desired outcome of this project, to successfully treat neurodegenerative diseases, it is necessary to thoroughly test these materials both *in vivo* and *in vitro*. Initially it will be necessary to investigate the inflammatory response of the brain for any new hydrogels developed, and the MBG-B5 hydrogel. Moving beyond this, investigating the infiltration of neurites into the injection site would give further insight into the brain's response to these materials. As neural stem cells, such as those found in the subventricular zone in the adult brain have been shown to migrate towards high BDNF concentrations[6]. Implanting these materials so that they intercept the subventricular zone will enable the evaluation of whether these materials can guide resident neuroblasts.

7.2.5 Modelling of co-assembled gels

The co-assembly of these peptide systems has not been heavily investigated. Combining what was learned through TEM analysis with additional characterisation techniques would enable a greater understanding of the interactions in these multicomponent systems.

7.2.6 Cell encapsulation

MBG-B5 forms a hydrogel at physiological pH at physiologically relevant temperatures. For this reason, encapsulation and 3D growth and culture of cells in this material should be possible. Through encapsulation of cells in this hydrogel, delivery of cells to the CNS would be possible, with the hydrogel protecting the encapsulated cells from shear stress during the injection process, as well as protecting the cells from the initial inflammatory response to the injection. Depending on the choice of cells, this would enable neural stem cells to an injured area, which could differentiate and help repair damage, or encapsulation of cells which would release beneficial growth factors, leading to enhanced recovery.

7.3 References

[1]   A. L. Rodriguez, T. Y. Wang, K. F. Bruggeman, C. C. Horgan, R. Li, R. J. Williams, C. L. Parish, and D. R. Nisbet, "In vivo assessment of grafted cortical neural progenitor cells and host response to functionalized self-assembling peptide hydrogels and the implications for tissue repair," *J. Mater. Chem. B*, vol. 2, no. 44, pp. 7771–7778, 2014.

[2]   S.-W. Jang, X. Liu, S. Pradoldej, G. Tosini, Q. Chang, P. M. Iuvone, and K. Ye, "N-acetylserotonin activates TrkB receptor in a circadian rhythm," *Proc. Natl. Acad. Sci.*, vol. 107, no. 8, pp. 3876–3881, Feb. 2010.

[3]   V. N. Modepalli, A. L. Rodriguez, R. Li, S. Pavuluri, K. R. Nicholas, C. J. Barrow, D. R. Nisbet, and R. J. Williams, "In vitro response to functionalized self-assembled peptide scaffolds for three-dimensional cell culture," *Biopolymers*, vol. 102, no. 2, pp. 197–205, Mar. 2014.

[4]   X.-D. Xu, L. Liang, C.-S. Chen, B. Lu, N. Wang, F.-G. Jiang, X.-Z. Zhang, and R.-X. Zhuo, "Peptide Hydrogel as an Intraocular Drug Delivery System for Inhibition of Postoperative Scarring Formation," *ACS Appl. Mater. Interfaces*, vol. 2, no. 9, pp. 2663–2671, Sep. 2010.

[5]   A. L. Rodriguez, C. L. Parish, D. R. Nisbet, and R. J. Williams, "Tuning the amino acid sequence of minimalist peptides to present biological signals via charge neutralised self assembly," *Soft Matter*, vol. 9, no. 15, p. 3915, 2013.

[6]   D. Fon, K. Zhou, F. Ercole, F. Fehr, S. Marchesan, M. R. Minter, P. J. Crack, D. I. Finkelstein, and J. S. Forsythe, "Nanofibrous scaffolds releasing a small molecule BDNF-mimetic for the re-direction of endogenous neuroblast migration in the brain," *Biomaterials*, vol. 35, no. 9, pp. 2692–2712, 2014.